INHIBITION OF MONOAMINE OXIDASE B BY SUBSTITUTED BENZAMIDAZOLE ANALOGUES.

Deidré van den Berg

B.Pharm.

Dissertation submitted in partial fulfillment of the requirements for the degree Magister Scientiae in Pharmaceutical Chemistry at the North-West University, Potchefstroom Campus

Supervisor: Dr. J.P. Petzer
Co-supervisor: Prof.J.J. Bergh

2006

Potchefstroom

ABSTRACT

Both monoamine oxidase A and B (MAO-A and B) play an important role in the metabolism of monoamine neurotransmitters in the central nervous system (CNS) and are therefore of considerable pharmacological interest for the development of new drug therapies. Inhibitors of MAO are of therapeutic interest for both the treatment of psychiatric and neurological diseases. Selective inhibitors of MAO-B are in use and are under investigation for the treatment of the symptoms and underlying neurodegeneration of Parkinson's disease (PD).

PD is one of the most common neurological diseases of the elderly and is an idiopathic, slowly progressive, degenerative CNS disorder. At present the treatment of PD is mainly based on dopamine replacement therapy. The current treatment strategies for PD are believed to lack selectivity and may lead to severe side effects. These therapeutic strategies ameliorate the symptoms of the disease but do not prevent further progression of the disease. For this reason there are currently several studies underway to develop drugs that can delay or even halt the progression of the disease. Besides providing relief of the symptoms of PD, inhibition of MAO-B is also reported to exert a neuroprotective effect. Therefore, MAO-B may be an attractive alternative target for the development of drugs for the treatment of PD.

Currently, the only MAO-B inhibitors that are used clinically are irreversible inactivators of the enzyme. Because of safety considerations it may be desirable to develop potent inhibitors of MAO-B that are reversible. A recent report of a small series of benzimidazole inhibitors of MAO-B has prompted us to study additional benzimidazole analogues in an attempt to develop compounds with improved potency. The principal objective of this study was to examine the MAO-B inhibition properties of a series of synthetic benzimidazole analogues in an effort to explore the possibility of designing inhibitors that are reversible while retaining their selectivity towards MAO-B. The study included the synthesis and characterization of a series of (E)-2-styryl-1-methylbenzimidazole analogues containing different substituents in the four position of the styryl ring. Also included in this study is 1-methylbenzimidazole. This compound was included in the study to investigate the importance of styryl substitution for MAO-B inhibition activity. This research forms part of a collaborative effort to discover new inhibitors of MAO-B that are reversible while retaining their selectivity towards MAO-B.

Following the preparation of the target compounds, they were evaluated as MAO-B inhibitors *in vitro* using a spectrophotometric assay. The inhibition potencies were expressed as the enzyme-inhibitor dissociation constants (K_i values). The K_i values for the competitive inhibition

of MAO-B by the test compounds were estimated by measuring the extent by which various concentrations of the test inhibitors slowed the rate of the oxidation of 1-methyl-4-(1-methylpyrrol-2-yl)-1,2,3,6-tetrahydropyridine (MMTP) to the corresponding dihydropyridinium metabolite ($MMDP^+$). Lineweaver-Burke plots with increasing concentrations of the test inhibitors were constructed and the K_i values were determined. A Hansch type structure-activity relationship study indicated that the enzyme inhibition activity correlated with both the Taft steric parameter and the lipophylicity of the substituent attached to the four position of the styryl ring. (E)-2-styryl-1-methylbenzimidazole analogues containing styryl ring substituents with a large degree of steric hindrance were found to be the most potent inhibitors.

All of the benzimidazole analogues synthesized were found to be moderately potent reversible inhibitors of MAO-B. The modes of inhibition were found to be competitive with enzyme-inhibitor dissociation constants (K_i values) in the low micro-molar range. The most potent compound was found to be (E)-2-(4-trifluoromethylstyryl)-1-methylbenzimidazole with a K_i value of 0.56 μM. In accordance with the SAR study the trifluoromethyl substituent also had the highest degree of steric hindrance. 1-Methylbenzimidazole was found to be the least potent inhibitor of MAO-B. This suggests that the styryl functional group plays an important role in the interaction between the inhibitors and the active site of the enzyme.

OPSOMMING

Beide monoamienoksidase A en B (MAO-A en B) speel 'n belangrike rol in die metabolisme van monoamien neurotransmitters in die sentrale senuweestelsel. As gevolg hiervan het monoamienoksidase 'n fokuspunt geword vir die ontwikkeling van nuwe geneesmiddels. Die inhibeerders van monoamienoksidase is veral van terapeutiese belang in die behandeling van psigologiese en neurologiese siektetoestande. Selektiewe inhibeerders van monoamienoksidase word reeds gebruik terwyl sommige in 'n eksperimentele fase vir die behandeling van die onderliggende simptome van Parkinson se siekte (PD) is.

Parkinson se siekte is een van die bekendste neurologiese siektes van bejaardes in die wêreld. PD is 'n idiopatiese, stadig progressiewe siekte wat gekenmerk word deur die degenerasie van die sentrale senuweestelsel. Die bestaande terapie vir PD is meestal gebaseer op die vervanging van die uitgeputte dopamien in die substantia nigra. Die huidige terapie is nie baie selektief nie en veroorsaak ernstige newe-effekte. Alhoewel die terapie die simptome van die siekte verlig, behandel dit nie die onderliggende oorsaak van die siekte nie. Dit het daartoe gelei dat talle studies tans onderweg is om nuwe geneesmidels te ontwikkel wat moontlik die ontwikkeling van PD kan vertraag of selfs stop. MAO-B inhibeerders is tans van groot belang vir die ontwikkeling van nuwe medikasie vir die behandeling van PD. MAO-B-inhibeerders verskaf verligting van die simptome van PD en oefen ook 'n neurobeskermende effek uit. As gevolg hiervan is MAO-B inhibeerders 'n aantreklike teiken vir die onwikkeling van geneesmiddelterapie.

Die MAO-B-inhibeerders wat tans gebruik word is onomkeerbare inaktiveerders van die ensiem. Vir veiligheidsredes kan dit van groot waarde wees om potente inhibeerders van MAO te ontwikkel wat omkeerbaar is. Onlangs is 'n studie op klein groep bensimidasoolverbindings gedoen en daar is gevind dat hulle matige MAO-B-inhibeerders is. Op grond van hierdie bevindings het ons besluit om die groep bensimidasole verder te ondersoek in 'n poging om verbindings te sintetiseer met verhoogde aktiwiteit. Die sentrale doel van die studie was om die MAO-B inhiberende aktiwiteit van 'n nuwe groep (E)-2-stiriel-1-metielbensimidasoolverbindings te evalueer in 'n poging om inhibeerders te onwikkel wat selektief is vir die ensiem en wat omkeerbaar optree. 'n Reeks bensimidasoolverbindings met verskillende substituente op die 4-posisie van die stirielring is gesintetiseer, gekarakteriseer en *in vitro* getoets vir MAO-B inhibisie. Die studie het ook die sintese van 1-metielbensimidasool ingesluit. Die rede waarom hierdie verbinding ingesluit is was om die noodsaaklikheid van 'n stirielsubstituent vir MAO-B inhibisie aktiwiteit te bepaal.

Na afloop van die sintese is die verbindings *in vitro* getoets vir MAO-B-inhibisie deur middel van 'n spektrofotometriese metode. Die inhibeerderpotensie is uitgedruk as die dissosiasie konstante (K_i-waarde) van die ensieminhibeerder. Die K_i-waarde vir kompeterende inhibisie is bepaal deur die mate waartoe verskillende konsentrasies van die toetsverbindings die oksidasie van 1-metiel-4-(1-metielpirrool-2-iel)-1,2,3,6-tetrahidropiridien (MMTP) na die ooreenstemmende dihidropiridinium vertraag, te meet. Lineweaver-Burkegrafieke, in die teenwoordigheid van toenemde konsentrasies inhibeerder, is gebruik om die K_i waardes te bepaal. Na afloop van die studie is die struktuuraktiwiteitverwantskappe van die reeks met behulp van 'n Hanschtipe studie ondersoek. Daar is gevind dat die inhibisieaktiwiteit korreleer met die Taft-steriese-parameter asook die lipofilisiteit van die substituente in die vier posisie van die stirielring. (E)-2-stiriel-1-metielbensimidasoolanaloë, wat substituente in die vier posisie van die stiriel ring bevat met 'n hoë mate van steriese hindernis, het die hoogste inhibisie-aktiwiteit getoon.

Al die bensimidasoolverbindings het omkeerbare inhibiese-aktiwiteit van MAO-B getoon met matige potensie. Die tipe inhibisie is as kompeterend geïdentifiseer. Die mees potente verbinding, (E)-2-(4-trifluorostiriel)-1-metielbenzimidasool, het 'n Ki-waarde van 0.56 μM gehad. Hierdie bevinding is in ooreenstemming met die struktuuraktiwiteitsverwantskap studie wat aangetoon het dat substituente soos die trifluorometielgroep, wat 'n groot mate van steriese hindernis het, 'n goeie MAO-B inhibeerder behoort te wees. 1-Metielbensimidasool was die swakste inhibeerder in die reeks. Hierdie resultate dui daarop dat die stiriel syketting 'n belangrike rol speel in die interaksie tussen die inhibeerders en die aktiewe setel van die ensiem.

TABLE OF CONTENTS

ABBREVIATIONS

^{13}C-NMR	– Carbon thirteen nuclear magnetic resonance
^{1}H-NMR	– Proton nuclear magnetic resonance
5-HT	– Serotonin
Ach	– Acetyl choline
AD	– Alzheimer's disease
CNS	– Central nervous system
CSC	– (E)-8-(3-Chlorostyryl)caffeine
DA	– Dopamine
DMAP	– 4-(N,N-dimethylamino)pyridine
DMF	– Dimethylformamide
DMSO	– Dimethylsulphoxide
DSC	– Differential scanning calorimetry
EDAC	– 1-Ethyl-3-[3-(dimethylamino)-propyl]carbodiimide
EI-MS	– Electron ionization mass spectroscopy
FAD	– Flavin-adenine dinucleotide
GPO	– Glutathione peroxidase
HCl	– Hydrochloric acid
MAO-A	– Monoamine oxidase A
MAO-B	– Monoamine oxidase B
$MMDP^{+}$	– 1-Methyl-4-(1-methylpyrrol-2-yl)-2,3-dihydropyridinium.
MMP^{+}	– 1-Methyl-4-(1-methylpyrrol-2-yl)pyridinium.
MMTP	– 1-Methyl 4-(1-methylpyrrol-2-yl)-1,2,3,6-tetrahydropyridine
Mp	– Melting point

MPTP	– 1-Methyl-4 phenyl-1,2,3,6-tetrahydropyridine
PD	– Parkinson's disease
SAR	– Structure-activity relationship
SN	– Substantia nigra
SNPC	– Substantia nigra pars compacta
TLC	– Thin layer chromatography

Chapter 1

INTRODUCTION AND OBJECTIVES

1.1 Parkinson's disease

Neurodegenerative diseases are a growing concern for the world population. This has lead to an enhanced interest in the science of neuroprotection. Parkinson's disease (PD) is one of the most common neurological diseases of the elderly and is an idiopathic, slowly progressive, degenerative central nervous system (CNS) disorder. The disease is characterized by slow and decreased movement, muscular rigidity, resting tremor and postural instability. During primary PD the neurons of the substantia nigra, locus caeruleus, and other dopaminergic cell groups of the brain stem is lost. The loss of the neurons of the substantia nigra results in the depletion of dopamine, an important neurotransmitter in this area. Although the etiology of PD has not yet been established it is proposed to be the result of other idiopathic degenerative diseases, genetic factors and exogenous or endogenous toxins such as hydrogen peroxide. An illicit and very toxic drug, 1-methyl-4-phenyl-1,2,3,6-tetrahydropyridine (MPTP), has been found to induce the motor symptoms seen in PD in humans and animals (Langston *et al.*, 1983). This is a result of MPTP's ability to cause degeneration of the nigro-striatal neuronal pathway which leads to depletion of dopamine in the striatum.

At present the treatment of the disease is mainly based on dopamine replacement therapy which is achieved with levodopa (**1**) in combination with a peripheral aromatic L-amino acid decarboxylase inhibitor such as carbidopa or benserazid (Jankovic & Marsden, 1993). Levodopa is a metabolic precursor of dopamine, which crosses the blood-brain barrier and replaces the depleted neurotransmitter, dopamine. However, the continued use of levodopa results in a loss of drug efficacy and the onset of unwanted side-effects such as dyskinesia, hallucinations, delirium and orthostatic hypertension (Volz & Gleiter, 1998). The early symptoms of PD can also be treated with dopamine agonists such as pergolide. Similar to levodopa, dopamine agonists are also associated with motor side effects (Arnold *et al.*, 2005).

The mechanism based inactivator of monoamine oxidase B (MAO-B), (R)-deprenyl (**2**), is currently used in combination with levodopa as dopamine replacement therapy (Rabey *et al.*, 2000). The beneficial effects of (R)-deprenyl may be attributed to the conservation of the depleted supply of dopamine via the inhibition of the MAO-B catalyzed oxidation of dopamine in the CNS, therefore delaying the need for levodopa therapy in patients diagnosed with early

PD (Rabey *et al.*, 2000). In contrast to the reversible inhibitors, following treatment with an inactivator such as (R)-deprenyl, *de novo* synthesis of the MAO-B protein is required in order for the enzyme activity to return to normal levels. This leads to increased safety considerations especially since enzyme activity may take up to two weeks to normalize again (Riederer *et al.*, 2004).

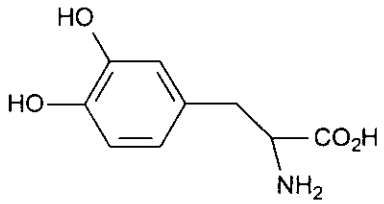

(1)

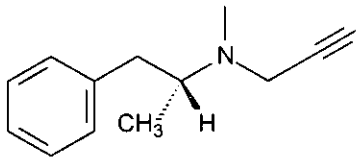

(2)

Figure 1: The structures of the metabolic precursor of dopamine, levodopa (**1**) and the MAO-B inactivator (R)-deprenyl (**2**).

The current treatment strategies for PD are believed to lack selectivity and may lead to severe side effects. These therapeutic strategies ameliorate the symptoms of the disease temporarily but the approach is not capable of preventing further progression of the disease. For this reason there are currently several studies underway to develop drugs that can delay or even halt the progression of the disease. This concept is known as neuroprotection and is a subject of intense research. Besides providing relief from the symptoms of PD, MAO-B inhibitors are also believed to be neuroprotective. For this reason MAO-B may be an attractive alternative target for the development of drugs for the treatment of PD.

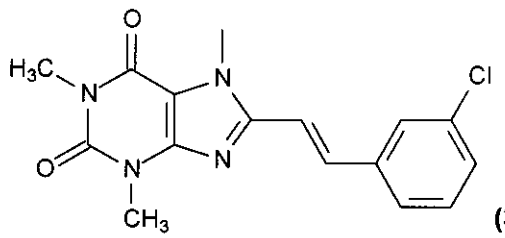

(3)

Figure 2: (*E*)-8-(3-chlorostyryl)caffeine, an adenosine A_{2A} receptor antagonist that was recently found to be a very potent inhibitor of MAO-B (**3**).

One reversible MAO-B inhibitor of particular interest is (*E*)-8-(3-chlorostyryl)caffeine (CSC) an adenosine A_{2A} receptor antagonist (figure 2). CSC was recently found to be a very potent inhibitor of MAO-B (Chen *et al.*, 2002) with a K_i value of 70 nM. Selected analogues of the

compound were prepared in an effort to determine the relative importance of the caffeine moiety for MAO-B inhibition. Among these analogues (figure 3) was a series of (E)-2-styrylbenzamidazolyl derivatives (Petzer *et al.*, 2003). Both the caffeinyl and benzimidazolyl aromatic rings are planar and literature supports the idea that planarity is important in MAO-B inhibition. (Gnerre *et al.*, 2000). This series of (E)-2-styrylbenzimidazole analogues showed moderate to potent inhibition of MAO-B and the mode of inhibition was observed to be competitive (Petzer *et al.*, 2003). In this study we prepared additional (E)-2-styrylbenzimidazole analogues in an attempt to further characterize the binding interactions between the enzyme and the benzimidazole inhibitors. The results obtained may be used to design inhibitors of MAO-B that are both reversible and potent.

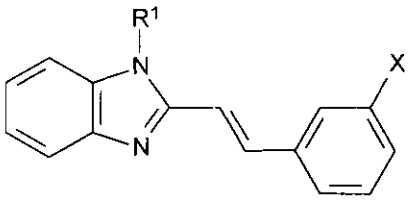

(4)

R^1 = H, CH_3

X = H, Cl, F

Figure 3. The series of (E)-2-styrylbenzimidazole derivatives that were previously synthesized and found to be MAO-B inhibitors.

1.2 Biological importance of Monoamine Oxidase

Both monoamine oxidase A and B play an important role in the metabolism of monoamine transmitters and are therefore of considerable pharmacological interest. Inhibitors of MAO are of therapeutic interest for the treatment of psychiatric and neurological disease. The reversible inhibitors of MAO-A are currently used as anti-anxiety and antidepressant drugs (Volz & Gleiter, 1998), while selective inhibitors of MAO-B are in use and are under investigation for the treatment of the symptoms and underlying neurodegeneration of Parkinson's disease (Youdim & Riederer, 2004; Riederer *et al.*, 2004) and Alzheimer's disease (Saura *et al.*, 1994). The primary goal of MAO-B inhibitors is to increase the availability of the neurotransmitters at the nerve terminals. MAO-B inhibitors increase the basal dopamine levels in the dopaminergic input pathway. Inhibition of MAO-B may also have a neuroprotective effect because it results in the reduction of hydrogen peroxide production, which is believed to play an important role in the etiology of PD.

Metabolism of monoamines by MAO is a major source of hydrogen peroxide (H_2O_2) in the brain. Normally H_2O_2 is inactivated by glutathione peroxidase (GPO) but when GPO activity is

decreased it can be converted chemically by Fe^{2+} ions (Fenton reaction, figure 4) into the highly reactive hydroxyl radical (Riederer *et al.*, 1989). This radical has widespread deleterious effects which can lead to neuronal damage and death. Inhibition of MAO therefore decreases the formation of H_2O_2, resulting in decreased formation of hydroxyl radicals and oxidative stress.

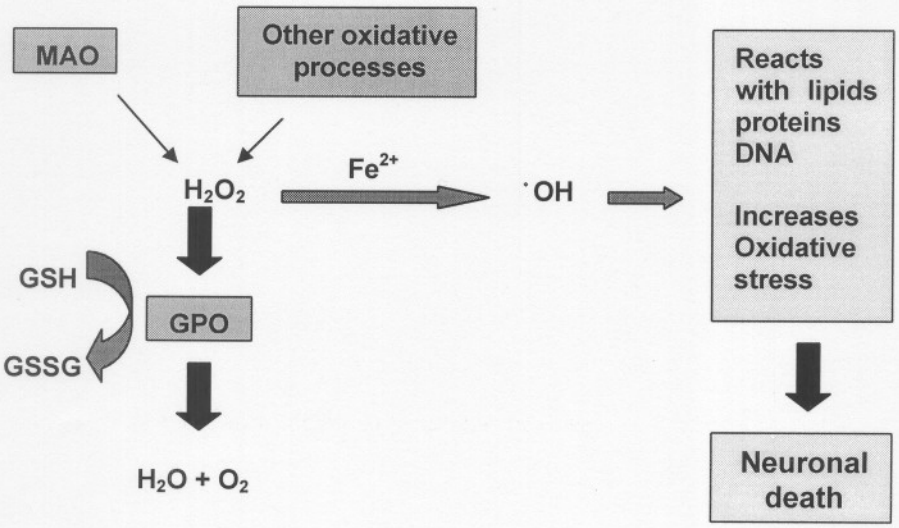

Figure 4: The mechanism of neurotoxicity induced by iron and hydrogen peroxide, *via* the Fenton reaction (Youdim & Bakhle, 2006) which can be partly prevented by MAO-B inhibition.

Furthermore, MAO-B is of considerable pharmacological interest due its role as the catalyst that mediates the bio-activation of the pro-neurotoxin, MPTP (1-methyl-4-phenyl-1,2,3,6-tetrahydropyridine) (**5**). MPTP causes movement disorders in animals and humans similar to that observed in idiopathic Parkinson's disease (Langston *et al.*, 1983). Critical to the mode of action of MPTP is the MAO-B catalyzed α-carbon oxidation of the starting compound, yielding the corresponding dihydropyridinium metabolite ($MPDP^+$) (**6**) (figure 5). A second two electron oxidation yields the ultimate neurotoxin MPP^+ (**7**) (Chiba *et al.*, 1984). MPTP has made it possible to create experimental models reproducing the human disease in several animal species and represents one of the most investigated models for studying the pathogenesis of PD (Gerlach & Riederer, 1996).

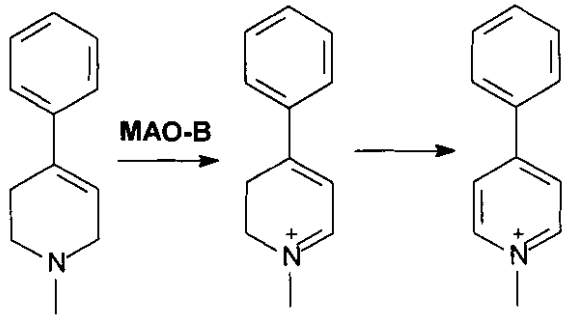

MPTP **MPDP$^+$** **MPP$^+$**

5 **6** **7**

Figure 5: The MAO-catalyzed oxidation of the 1-methyl-4-phenyl-1,2,3,6-tetrahydropyridine (MPTP (**5**)).

1.2.1 MAO-B Inhibitors

MAO-B inhibition in the brain primarily reduces the catabolism of dopamine and β-phenylethylamine and has therefore found its greatest application in the therapy of neurodegenerative disorders including PD. Inhibition of dopamine oxidation also results in the stoichiometric reduction of hydrogen peroxide production which is thought to play a significant role in the etiology of neurodegenerative diseases such as PD. MAO-B inhibitors also prevents MPTP toxicity by blocking MAO-B catalyzed oxidation of MPTP to the very toxic MPP$^+$. Two classes of MAO-B inhibitors can be identified based on their kinetics of MAO inhibition (Tipton & Fowler, 1984; Gaal & Hermecz, 1993).

Reversible, competitive inhibitors. These compounds are structurally similar to MAO substrates, and can, as a result, bind the active site of the enzyme. Reversible competitive inhibitors are not metabolized by the enzyme.

Irreversible, K_{cat} or "suicide" inhibitors. These inhibitors primarily bind MAO in a reversible, competitive manner, but are then oxidized by the enzyme to the active inactivator, which covalently binds the enzyme active site via the FAD co-factor, thus rendering it permanently unavailable for amine metabolism. The inhibition is more persistent than that achieved by reversible inhibitors (weeks rather than hours), as its effects can only be overcome by *de novo* synthesis of the enzyme.

As mentioned previously, the interest in MAO-B inhibition is mostly stimulated by the desire to elevate the depleted DA concentrations in the striatum during PD. Because of the safety

considerations associated with irreversible MAO-B inhibitors, there are at present several studies underway to develop reversible, competitive inhibitors that may offer a safer alternative for the treatment of neurodegenerative disease.

1.3 Summary

Because of the important role of MAO-B in the CNS, it is an attractive drug target for the development of antiparkinsonian agents. Inhibition of MAO-B not only conserves central dopamine levels, but is also reported to exert a neuroprotective effect (Tatton & Greenwod, 1991; Tatton, 1993). The current MAO-B inhibitors used clinically are irreversible inactivators of the enzyme. For safety reasons it may be desirable to develop potent inhibitors MAO-B that are reversible. A recent report of a small series of benzimidazole inhibitors of MAO-B (Petzer *et al.*, 2003) has prompted us to study additional benzimidazole analogues in an attempt to develop compounds with improved potency. Structural features of the chosen compounds are a benzimidazolyl aromatic ring which is planar and a styryl double bond with trans configuration. Literature supports the idea that planarity and the trans configuration is important in MAO-B inhibition. (Gnerre *et al.*, 2000)

1.4 Objective

The aim of this study was to synthesize analogues of the (E)-2-styryl-1-methylbenzamidazole series, which has recently been reported to possess MAO-B inhibition (Petzer *et al.*, 2003). The series chosen for this study was monosubstituted in the 4 position of the phenyl ring with both electron withdrawing and electron donating substituents to form an inclusive series. This research will form part of a collaborative effort to discover new inhibitors of MAO-B that are reversible while retaining their selectivity towards MAO-B. The structures that were selected are illustrated in Figure 6.

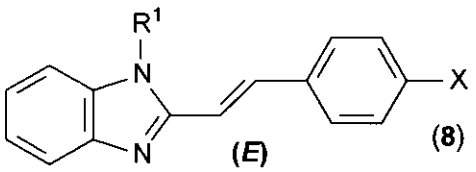

R^1 = H, CH_3

X = H, Cl, F, Br, CH_3, CF_3, OCH_3

Figure 6: Structures of compounds that were synthesized and investigated in this study.

Following the preparation of the target compounds, they were evaluated for their ability to act as MAO-B inhibitors *in vitro* using a spectrophotometric assay. Using a Hansch type

structureactivity relationship study, we attempted to determine whether correlations exist between the inhibition activity and descriptors of the substituents at the 4-position of the styryl ring.

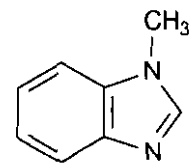

(9)

Figure 7: The structure of 1-methylbenzimidazole.

We also investigated 1-methylbenzimidazole (figure 7) as a possible inhibitor of MAO-B. Since this compound lacks the styryl side chain, it may be possible to determine the importance of this functional group in the interaction between the (E)-2-styryl-1-methylbenzimidazole analogues and the active site of MAO-B.

Chapter 2

PREPARATION OF THE SYNTHETIC TARGETS

2.1 Objectives of this chapter

The objective was to prepare a series of E-(2)-styryl-1-methylbenzimidazole analogues in an effort to explore the possibility of designing antiparkinsonian drugs that will be reversible inhibitors of MAO-B, while retaining their selectivity towards MAO-B. The motivation behind the research was the discovery of a small series of (E)-2-styryl-1-methylbenzimidazole analogues which were found to be competitive inhibitors of MAO-B (Petzer *et al.*, 2003). This chapter will discuss the preparation of the series of benzimidazole analogues according to adapted literature procedures. Also included in this chapter is the synthesis of 1-methylbenzimidazole which does not have a styryl functional group.

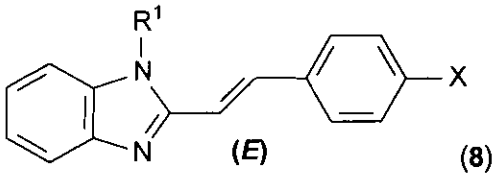

(8)

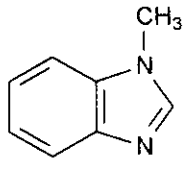

(9)

R^1 = H, CH_3
X = H, Cl, F, Br, CH_3, CF_3, OCH_3

Figure 8: Structures of the (E)-2-styryl-1-methylbenzimidazole analogues (**8**) and the 1-methylbenzimidazole (**9**) that were synthesized and investigated in this study.

2.2 Materials and instrumentation

All of the starting materials used, including chemicals and reagents not described elsewhere, were obtained from Sigma-Aldrich. Proton and carbon NMR spectra were recorded on a Varian Gemini 300 spectrometer. Proton (^1H) spectra were recorded at a frequency of 300 MHz and carbon (^{13}C) spectra at 75 MHz. Chemical shifts are reported in parts per millon (δ) downfield from the signal of tetramethylsilane dissolved in deuterated chloroform ($CDCl_3$) or DMSO (DMSO-D_6). Spin multiplicities are indicated as s (singlet), d (doublet), t (triplet), q (quartet) or m (multiplet) and the coupling constants (J) are given in hertz (Hz). Direct insertion electron ionization mass spectra (EIMS) and high resolution mass spectra (HRMS) were obtained on a VG 7070E mass spectrometer.

Melting points (mp) were obtained on a Gallenkamp melting point apparatus and by differential scanning calorimetry (DSC) on a Shimadzu DSC-50 instrument.

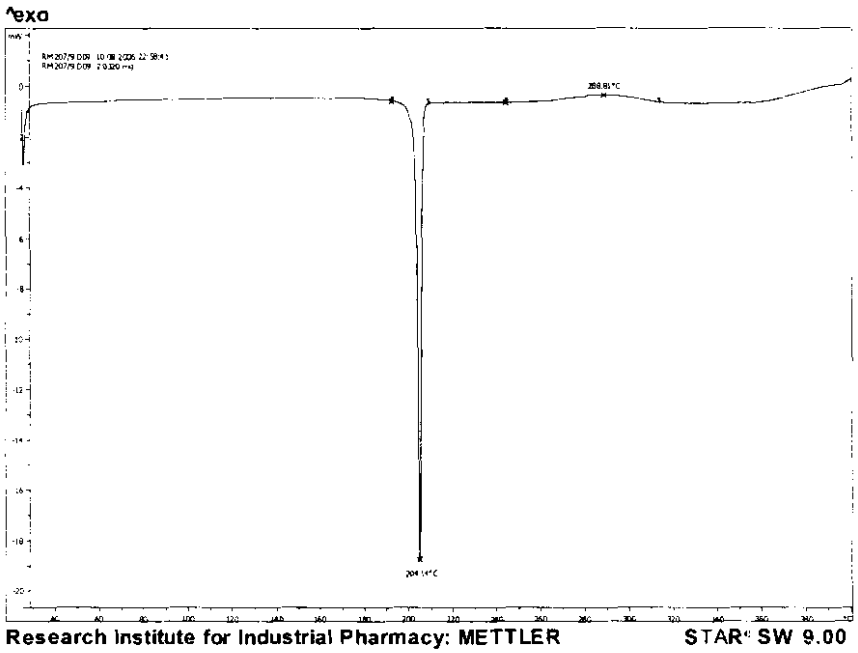

Figure 9: An example of the melting point of (E)-2-(4-methylstyryl)-1-methylbenzimidazole determined by differential scanning calorimetry (DSC).

2.3 Preparation of (E)-2-styryl-1-methylbenzimidazole derivatives

2.3.1 General synthetic approaches of (E)-2-styryl-1-methylbenzimidazole derivatives

The recent discovery that (E)-2-styryl-1-methylbenzimidazole analogues act as MAO-B inhibitors prompted us to examine additional analogues containing various substituents at the 4 position of the styryl ring. Literature suggests that the styryl moiety is essential for inhibition and that trans geometry is required (Petzer *et al.*, 2003). Recent studies have also shown that a large electron withdrawing substituent on the styryl moiety might be important for potent inhibition (Vlok *et al.*, 2006). Following standard literature procedures and altering the procedure via experimentation, eight differently substituted (E)-2-styryl-1-methylbenzimidazole derivatives were prepared.

The (E)-2-styryl-1-methylbenzimidazoles may be prepared following a similar procedure as the procedure reported for the preparation of (E)-8-styrylcaffeines (Jacobson *et al.*, 1993) (figure 10). In order to prepare (E)-8-styrylcaffeines, cinnamic acid (**11**) was reacted with 5,6-

diamino-1,3-dimethyluracil (**10**) to yield the intermediate amide. A commercial carbodimide reagent, 1-ethyl-3-(3-(dimethylamino)-propyl)carbodiimide (EDAC), was used to convert the carboxylic acid to an active acylating agent. In this reaction 4-(N,N-dimethylamino)pyridine (DMAP) and imidazole acted as catalysts for the condensation reaction. The resulting amides underwent cyclization when heated in the presence of a base to give the corresponding (E)-8-styrylcaffeine derivatives (**12**) (Suzuki *et al.*, 1993; Jacobson *et al.*, 1993). Treatment with iodomethane led to the desired 7-N-methylated analogues (**13**).

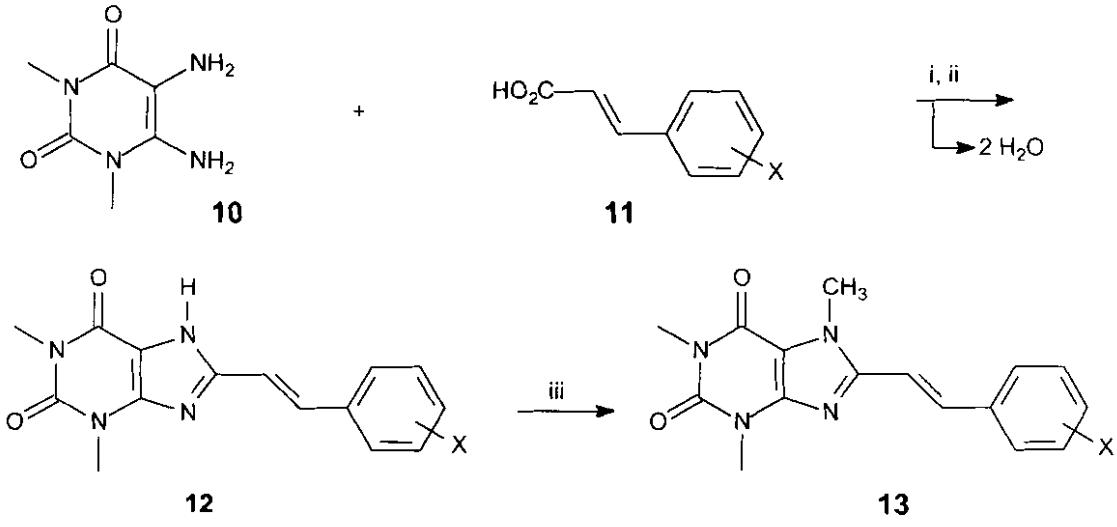

Figure 10: Synthetic pathway to substituted (E)-8-styrylcaffeine derivatives (i) EDAC, DMF, DMAP and Imidazole (ii) NaOH, reflux (iii) CH_3I, K_2CO_3, and DMF.

A possible method to synthesize (E)-2-styryl-1-methylbenzimidazole analogues is illustrated in figure 11 (Dubey *et al.*, 1998). The key intermediate, 2-methyl-1H-benzimidazole (**16**), was prepared by condensing o-phenylenediamine (**14**) with acetic acid (Dubey *et al.*, 1998) (**15**). 2-Methylbenzimidazole was then reacted with commercially available benzaldehyde at high temperatures to yield the substituted (E)-2-styryl-1H-benzimidazoles (**17**). Treatment of **17** with an equivalent of iodomethane resulted in the desired (E)-2-styryl-1-methylbenzimidazole (**18**).

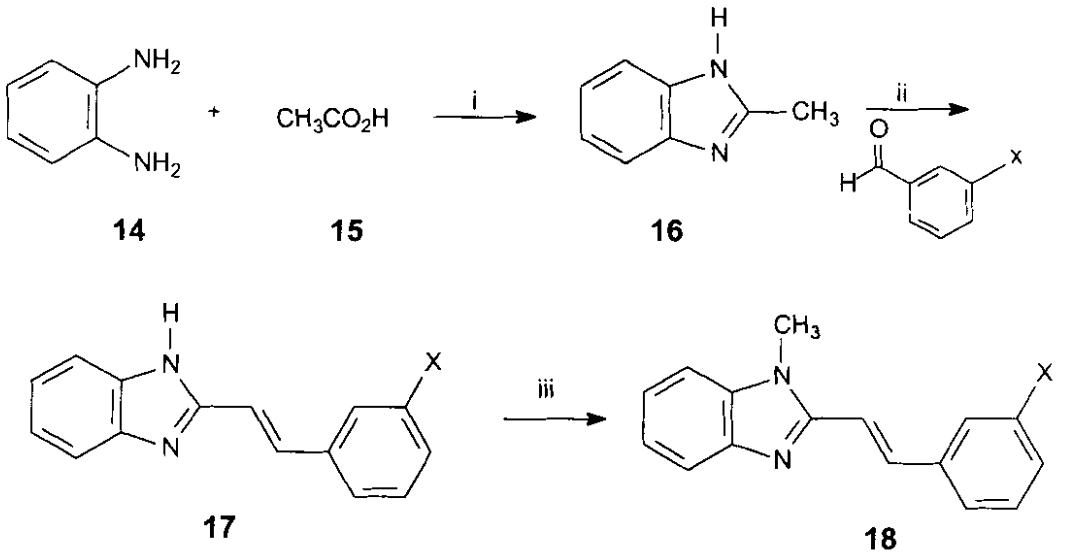

Figure 11: Synthetic pathway to substituted (E)-2-styryl-1-methylbenzimidazole analogues. (i) 4N HCl, reflux 1hr. (ii) 180 °C, 24 hrs. (iii) CH_3I (1 equiv.), K_2CO_3, DMF.

2.3.2 Synthesis and characterization

In this study the synthetic targets were prepared as illustrated in figure 12. o-Phenylenediamine (**19**) was condensed with an appropriately substituted cinnamic acid (**20**) in the presence of a carbodimide reagent, EDAC, to afford the amide intermediate. The intermediate amides underwent cyclization when heated in the presence of hydrochloric acid to yield the corresponding (E)-2-styrylbenzimidazole HCl-salt (**22a-g**). The cyclization of the intermediates (**21**) in the presence of base was replaced by refluxing the intermediate amide in the presence of acid since treatment of the intermediate amide with base resulted in hydrolysis of the amide. The target compounds were produced by treating the (E)-2-styryl-benzimidazoles with iodomethane. The methylation yielded the (E)-2-styryl-1-methylbenzimidazole analogues (**23a-g**) which were purified through crystallization and column chromatography.

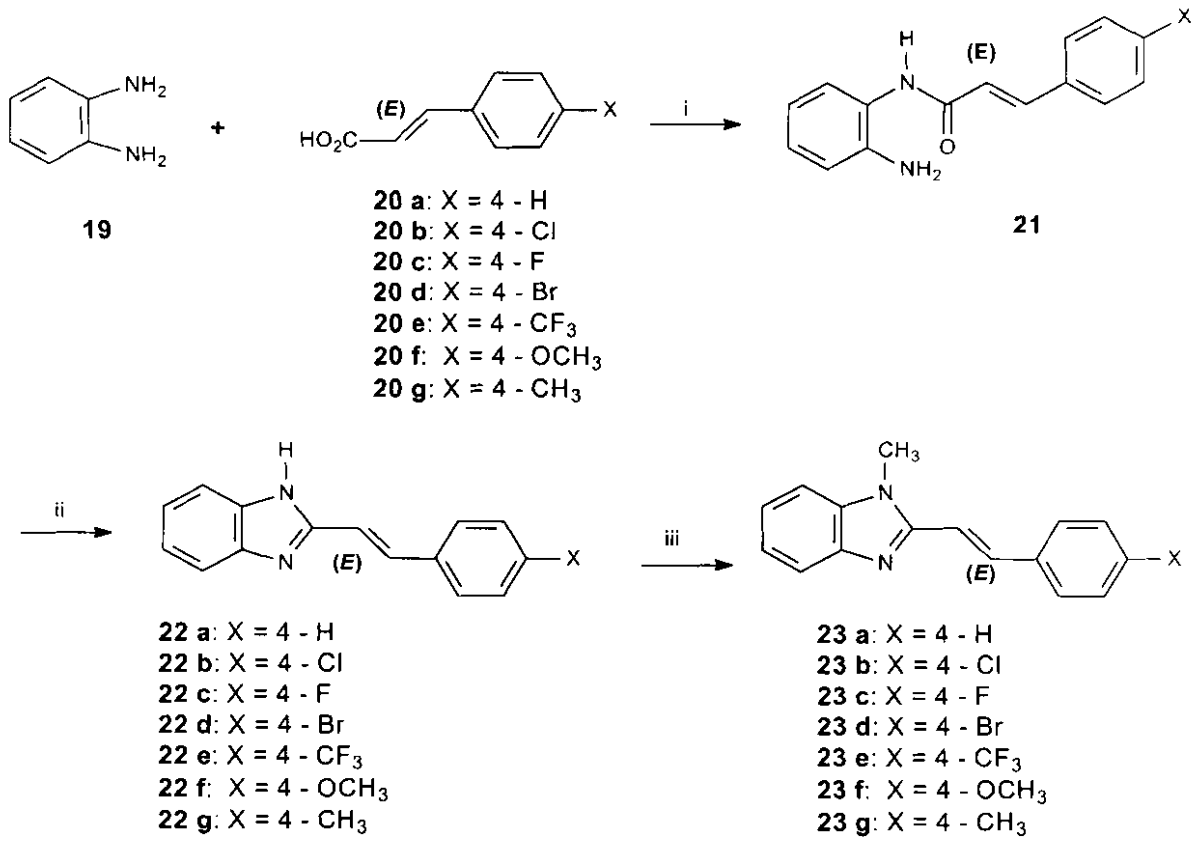

Figure 12: Synthetic pathway to substituted (E)-2-styryl-1-methylbenzimidazole analogues. (i) EDAC, DMF, DMAP and imidazole (ii) HCl, reflux (iii) CH_3I, K_2CO_3, DMF.

2.3.3 General Method A (22a-22g)

o-Phenylenediamine (**19**) (9.25 mmmol) was reacted with an appropriately substituted cinnamic acid (1 eq) (**20**) in the presence of EDAC (1.5 eq) dissolved in a minimum amount of DMF. DMAP (0.05 eq) and imidazole (0.05 eq) was added as catalysts. The reaction was stirred at room temperature for 4 hours. An excess amount of water was added to the mixture and the precipitate that was formed was collected via filtration. The intermediate amide (**21**) was subsequently cyclisized by refluxing at 90-100 °C in the presence of a sufficient amount of 6 N hydrochloric acid (HCl). Sufficient ethanol was added to the reaction to keep the intermediate amide in solution. The reaction was monitored using silica gel thin layer chromatography with ethylacetate:petroleum ether (1:1) as mobile phase. The reaction was cooled and the precipitate which formed was collected by filtration and washed with water. The product intermediate (**22a-g**) was recrystallized from a suitable solvent as the HCl salt. The structures were confirmed by MS, ^{1}H-NMR and ^{13}C-NMR. The trans geometry of the

styryl moiety was confirmed by proton-proton coupling constants (J ≥ 15 Hz) of the olefinic protons.

2.3.3.1 (E)-2-styryl-1H-benzimidazole hydrochloride (22a)

Compound **22a** was synthesized from o-phenylenediamine (**19**) and cinnamic acid (**20a**) according to general method A and was recrystallized from boiling ethanol to yield dirty white fine crystals. **Yield** 71.4%; **mp** 208 °C, lit. 203-205 °C (Dubey et al., 1998; Petzer et al., 2003); **^{1}H-NMR** (DMSO-D_6) δ 8.32 (d, 1H J=16.72 Hz). 7.82 (m, 2H), 7.69 (m, 2H), 7.51 (m, 5H), 7.32 (d, 1H, J=16.62 Hz); **^{13}C-NMR** (DMSO-D_6) δ 147.99, 142.81, 133.98, 131.36, 130.91, 129.25, 128.00, 125.81, 113.64, 109.83; **EIMS** *m/z* 221 (M^{+}).

2.3.3.2 (E)-2-(4-Chlorostyryl)-1H-benzimidazole hydrochloride (22b)

Compound **22b** was synthesized from o-phenylenediamine (**19**) and 4-chlorocinnamic acid (**20b**) according to general method A and was recrystallized from boiling ethanol to yield light yellow crystals. **Yield** 82.1%; **mp** 286 °C; **^{1}H-NMR** (DMSO-D_6) δ 8.19 (d, 1H, J=16.62 Hz), 7.78 (m, 4H), 7.55 (m, 4H), 7.34 (d, 1H, J=16.62 Hz); **^{13}C-NMR** (DMSO-D_6) δ 149.33, 143.58, 138.26, 133.97, 132.63, 130.84, 130.51, 127.01, 114.67, 110.48; **EIMS** *m/z* 255 (M^{+}).

2.3.3.3 (E)-2-(4-Fluorostyryl)-1H-benzimidazole hydrochloride (22c)

Compound **22c** was synthesized from o-phenylenediamine (**19**) and 4-fluorocinnamic acid (**20c**) according to general method A and was recrystallized from boiling ethanol to yield white crystals. **Yield** 62.4%; **mp** 171 °C; **^{1}H-NMR** (DMSO-D_6) δ 8.15 (d, 1H, J=16.61 Hz), 7.81 (m, 4H), 7.52 (m, 2H), 7.38 (m, 2H), 7.24 (d, 1H, J=16.62 Hz); **^{13}C-NMR** (DMSO-D_6) δ 167.52, 164.19, 149.51, 143.85, 132.55, 131.82, 127.71, 117.47, 114.62, 109.55; **EIMS** *m/z* 239 (M^{+}).

2.3.3.4 (E)-2-(4-Bromostyryl)-1H-benzimidazole hydrochloride (22d)

Compound **22d** was synthesized from o-phenylenediamine (**19**) and 4-bromocinnamic acid (**20d**) according to general method A and was recrystallized from boiling ethanol to yield yellow crystals. **Yield** 76.7%; **mp** 156 °C; **^{1}H-NMR** (DMSO-D_6) δ 8.19 (d, 1H, J=16.62 Hz), 7.80 (m, 2H), 7.67 (m, 4H), 7.51 (m, 2H), 7.35 (d, 1H, J=16.62 Hz); **^{13}C-NMR** (DMSO-D_6) δ 147.66, 141.26, 133.17, 132.10, 131.40, 129.69, 125.70, 124.06, 113.58, 110.67; **EIMS** *m/z* 300 (M^{+}).

2.3.3.5 (E)-2-(4-Trifluoromethylstyryl)-1H-benzimidazole hydrochloride (22e)

Compound **22e** was synthesized from o-phenylenediamine (**19**) and 4-trifluorocinnamic acid (**20e**) according to general method A and was recrystallized from boiling ethanol to yield white crystals. **Yield** 23.7%; **mp** 188 °C; **^{1}H-NMR** (DMSO-D_6) δ 8.35 (d, 1H, J=16.65 Hz), 7.89 (m, 4H), 7.77 (m, 2H), 7.53 (m, 2H), 7.46 (d, 1H, J=16.79); **^{13}C-NMR** (DMSO-D_6) δ 147.33, 140.69, 137.88, 131.47, 128.56, 126.10, 125.68, 122.07, 113.78, 112.79; **EIMS** *m/z* 289 (M^+).

2.3.3.6 (E)-2-(4-Methoxystyryl)-1H-benzimidazole hydrochloride (22f)

Compound **22f** was synthesized from o-phenylenediamine (**19**) and 4-methoxycinnamic acid (**20f**) according to general method A and was recrystallized from boiling ethanol to yield yellow crystals. **Yield** 71.0%; **mp** 155 °C; **^{1}H-NMR** (DMSO-D_6)δ 8.26 (d, 1H, J=16.62 Hz), 7.75 (m, 2H), 7.63 (m, 2H), 7.47 (m, 2H), 7.17 (d, 1H, J=16.51 Hz), 7.03 (m, 2H) 3.81 (s, 3H); **^{13}C-NMR** (DMSO-D_6) δ 161.55, 148.43, 142.85, 131.20, 129.91, 126.57, 125.59, 114.73, 113.41, 106.75, 55.41; **EIMS** *m/z* 251 (M^+).

2.3.3.7 (E)-2-(4-Methylstyryl)-1H-benzimidazole hydrochloride (22g)

Compound **22g** was synthesized from o-phenylenediamine (**19**) and 4-methylcinnamic acid (**20g**) according to general method A and was recrystallized from boiling ethanol to yield dirty white crystals. **Yield** 42.9%; **mp** 266 °C; **^{1}H-NMR** (DMSO-D_6) δ 8.21 (d, 1H, J=16.62 Hz), 7.77 (m, 2H), 7.61 (d, 2H, J=8.21 Hz), 7.50 (m, 2H), 7.34 (m, 2H), 7.24 (d, 1H, J=16.59 Hz), 2.35 (s, 3H); **^{13}C-NMR** (DMSO-D_6)δ 148.16, 142.85, 141.07, 131.32, 131.27, 129.81, 127.99, 125.67, 113.54, 108.59, 21.04; **EIMS** *m/z* 235 (M^+).

2.3.4 General Method B (23a-23h)

To a stirred suspension of 1 eq (E)-2-styryl-1H-benzimidazole (**22 a-g**), dissolved in a minimum amount of DMF, was added 2.53 eq potassium carbonate. The mixture was cooled in an ice bath while being stirred. While on ice, 1 eq iodomethane was added and the suspension was allowed to slowly return to room temperature. The reaction was monitored with silica gel thin layer chromatography using ethyl acetate:dichloromethane (1:1) as mobile phase. Except in the case of compounds (**23a and 23 f-g**) the final product was isolated by adding an excess amount of water to the reaction. The precipitate that formed was collected via filtration and crystallized from an appropriate solvent. In the cases of **23a and 23 f-g**, the remaining DMF solvent was removed by vacuum distillation. The residue was either extracted

with chloroform (3×30 ml) or directly crystallized using an appropriate solvent. The target compounds were isolated and purified through either crystallization or column chromatography. The structures of the synthetic targets were confirmed by MS, ^{1}H-NMR and ^{13}C-NMR. The trans geometry of the styryl moiety was confirmed by proton-proton coupling constants (J) in the range of 15 Hz of the olefinic protons.

2.3.4.1 (E)-2-styryl-1-methylbenzimidazole (23a)

Compound **23a** was synthesized according to general method B starting with 1.93 mmol of **22a** and adding 4.89 mmol K_2CO_3 and 1.93 mmol CH_3I. The product was recovered after removal of the DMF solvent via vacuum distillation and crystallized from boiling toluene to yield light yellow crystals. **Yield** 9.53%; **mp** 121-122 °C, lit. 119-121 °C (Petzer *et al.*, 2003); **HRMS** calcd. 234.11569, found. 234.11259.

2.3.4.2 (E)-2-(4-Chlorostyryl)-1-methylbenzimidazole (23b)

Compound **23b** was synthesized according to general method B using 1.25 mmol of **22b** and adding 3.17 mmol K_2CO_3 and 1.25 mmol CH_3I. The product was isolated after adding distilled water to the reaction and the collected precipitate was crystallized from boiling ethyl acetate:dichloromethane (1:1) to yield light yellow crystals. **Yield** 15.96%; **mp** 155 °C; **^{1}H-NMR** (DMSO-D_6) δ 7.82 (m, 3H), 7.61 (m, 1H), 7.50 (d, 1H, J=15.93 Hz), 7.49 (m, 3H), 7.20 (m, 2H), 3.91 (s, 3H);**^{13}C-NMR** (DMSO-D_6) δ 29.50, 110.07, 115.20, 118.45, 122.03, 128.70, 129.03, 133.16, 134.31, 134.91, 136.00, 142.75, 150.50; **HRMS** calcd. 268.07672, found. 268.07431.

2.3.4.3 (E)-2-(4-Fluorostyryl)-1-methylbenzimidazole (23c)

Compound **23c** was synthesized according to general method B using 4.68 mmol of **22c** and adding 11.85 mmol K_2CO_3 and 74.88 mmol CH_3I. The product was recovered after adding enough distilled water to obtain a precipitate. The product was crystallized from boiling ethyl acetate:dichloromethane (1:1) to yield beige crystals. **Yield** 10.07%; **mp** 113 °C; **^{1}H-NMR** (DMSO-D_6) δ 7.86 (m, 3H), 7.57 (m, 2H), 7.44 (d, 1H, J=15.79 Hz), 7.21 (m, 4H), 3.90 (s, 3H); **^{13}C-NMR** (DMSO-D_6) δ 163.96, 160.69, 150.82, 142.74, 135.99, 134.56, 132.57, 129.51, 121.96, 118.37, 115.49, 114.28, 110.02, 29.49. **HRMS** calcd. 252.10627, found. 252.10458.

2.3.4.4 (E)-2-(4-Bromostyryl)-1-methylbenzimidazole (23d)

Compound **23d** was synthesized according to general method B using 6.61 mmol of **22d** and adding 16.71 mmol K_2CO_3 and 6.61 mmol CH_3I. The product was recovered after adding enough distilled water to obtain a precipitate. The product was crystallized three times from boiling ethyl acetate:dichloromethane (1:1) to yield yellow crystals. **Yield** 15.47%; **mp** 161 °C; **^{1}H-NMR** (DMSO-D_6) δ 7.79 (d, 1H, J=15.93Hz), 7.74 (m, 2H), 7.56 (m, 4H), 7.53 (d, 1H),7.21 (m, 2H), 3.92 (s, 3H).; **^{13}C-NMR** (DMSO-D_6) δ 150.62, 142.75, 136.00, 135.26, 134.38, 131.63, 129.33, 122.04, 121.86, 118.45, 115.28, 110.10, 29.52. **HRMS** calcd. 312.02621, found. 312.02495.

2.3.3.5 (E)-2-(4-Trifluoromethylstyryl)-1-methylbenzimidazole (23e)

Compound **23e** was synthesized according to general method B using 1.73 mmol of **22e** and adding 4.38 mmol K_2CO_3 and 1.73 mmol CH_3I. The product was recovered after adding enough distilled water to obtain a precipitate. The product was crystallized from boiling ethyl acetate:dichloromethane (1:1) to yield light yellow crystals. **Yield** 42.76%; **mp** 127 °C; **^{1}H-NMR** (DMSO-D_6) δ 8.02 (d, 2H, J=8.21 Hz), 7.89 (d, 1H, J=15.8 Hz), 7.76 (d, 2H, J=8.18 Hz), 7.66 (d, 1H, J=15.8 Hz), 7.62 (m, 1H), 7.52 (m, 1H), 7.22 (m, 2H), 3.94 (s, 3H); **^{13}C-NMR** (DMSO-D_6) δ 150.25, 142.73, 140.01, 139.99, 136.05, 133.90, 127.931, 125.55, 122.24, 118.61, 117.27, 110.21, 29.58; **HRMS** calcd. 302.10308, found. 302.10426.

2.3.3.6 (E)-2-(4-Methoxystyryl)-1-methylbenzimidazole (23f)

Compound **23f** was synthesized according to general method B using 5.01 mmol of **22f** and adding 12.68 mmol K_2CO_3 and 5.01 mmol CH_3I. The product was recovered after vacuum distillation at 130 °C and was crystallized from boiling acetonitrile to yield light yellow crystals. **Yield** 18.04%; **mp** 133 °C; **^{1}H-NMR** (DMSO-D_6) δ 7.80 (d, 1H, J=15.79 Hz), 7.71 (m, 2H), 7.58 (m, 1H), 7.48 (m, 1H), 7.32 (d, 1H, J=15.79 Hz), 7.19 (m, 2H), 6.99 (m, 2H), 3.90 (s, 3H), 3.79 (s, 3H); **^{13}C-NMR** (DMSO-D_6) δ 159.90, 151.30, 142.81, 135.97, 135.62, 128.89, 128.62, 121.80, 121.60, 117.18, 114.19, 111.83, 109.84, 55.18, 29.42; **HRMS** calcd. 264.1262, found. 264.12127.

2.3.3.7 (E)-2-(4-Methylstyryl)-1-methylbenzimidazole (23g)

Compound **23g** was synthesized according to general method B using 1.02 mmol of **22g** and adding 2.58 mmol K_2CO_3 and 1.52 mmol CH_3I. The product was recovered after vacuum

distillation at 130 °C and was crystallized from boiling acetonitrile to yield fine white crystals. **Yield** 9.37%; **mp** 108 °C; **^{1}H-NMR** (DMSO-D_6) δ 7.81 (d, 1H, J=15.9 Hz), 7.68 (m, 2H), 7.55 (m, 2H), 7.41 (d, 1H, J=15.8 Hz), 7.18 (m, 4H), 3.88 (s, 3H), 2.33 (s, 3H); **^{13}C-NMR** (DMSO-D_6) δ 151.05, 142.79, 138.48, 135.99, 133.20, 129.47, 129.32, 127.33, 126.86, 121.89, 118.30, 113.24, 109.94, 39.46, 20.88; **HRMS** calcd. 248.13134, found. 248.13505.

2.4 Preparation of 1-methylbenzimidazole

2.4.1 General synthetic approaches of 1-methylbenzimidazole

The procedure followed for the synthesis of 1-methylbenzimidazole was that described by Gazit et al. (2003) (figure 13). Starting material **24** was methylated with methyl iodide in the presence of crushed KOH in acetone. Water was added and the reaction product was extracted with CH_2Cl_2 and chromatographed on silica gel.

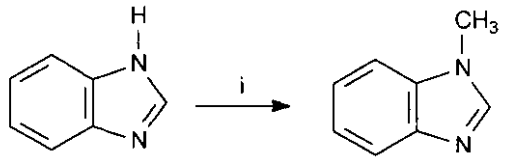

24 **25**

Figure 13: Synthetic pathway to 1-methylbenzimidazole (i) CH_3I, KOH, acetone.

2.4.2 General Method C (25)

Compound **25** was synthesized by dissolving 37.5 mmol benzimidazole (**24**) and 225 mmol potassium hydroxide in 150 ml of acetone to obtain a clear solution. After addition of 105 mmol methyl iodide, the solution became turbid and stiring was continued at room temperature for one hour. An excess amount of distilled water was added, to obtain a clear yellow solution. The product was extracted to dichloromethane (3 × 50 ml), and the solvent was removed by vacuum distillation. A yellow oily residue remained. The reaction progress was followed on silica gel TLC-plates using dichloromethane:ethylacetate:methanol (10:10:2) as mobile phase. In order to purify the product, silica gel column chromatography was performed on the residue using dichloromethane:ethylacetate:methanol (10:10:2) as mobile phase.

2.4.2.1 1-methyl benzimidazole

Compound **25** was synthesized according to general method C. **Yield** 26%; **^{1}H-NMR** (DMSO-D_6) δ 8.16 (s, 1H), 7.67 (m, 1H), 7.53 (m, 1H), 7.23 (m, 2H), 3.80 (s, 3H); **^{13}C-NMR** (DMSO-D_6) δ 30.53, 110.04, 119.23, 121.34, 122.15, 134.53, 143.31, 144.46; **HRMS** calcd. 132.06874 , found. 132.06905.

2.5 Summary

In this chapter the synthesis of seven (E)-2-styryl-1-methylbenzimidazole analogues substituted at the 4 position of the styryl ring was discussed. The series were monosubstituted in the 4 position of the phenyl ring with both electron withdrawing and electron donating substituents to form an inclusive series. These compounds will be tested as MAO-B inhibitors in *vitro* and a Hansch type structural activity relationship (SAR) study will be carried out to determine whether any correlations exist between descriptors of the substituents at the 4-position of the styryl ring and the inhibition activity of the compounds. Also described in this chapter is the synthesis of 1-methylbenzimidazole. This compound will be used to determine the relative importance of the styryl functional group in the interaction between (E)-2-styryl-1-methylbenzimidazoles and the active site of the MAO-B enzyme.

Chapter 3

ENZYMOLOGY AND BIOLOGICAL ACTIVITY

3.1 Objective of this chapter

In this chapter the enzyme, MAO and its therapeutic potential is discussed. The (E)-2-styryl-1-methylbenzimidazole analogues prepared in the previous chapter are evaluated as reversible MAO-B inhibitors in an attempt to examine specific structural features of the inhibitors that may be important for potent MAO-B inhibition. The applicable enzyme kinetics are discussed and the results of the enzyme analyses are presented. The relationship between the structures of the inhibitors and their MAO-B inhibition activity is determined via a Hansch type SAR study and are discussed.

3.2 Monoamine oxidase

Monoamine oxidase is an integral protein believed to be located in the outer mitochondrial membranes of neuronal, glial and other cells. MAO has been characterized as a flavin-adenine dinucleotide (FAD) containing enzyme, which consists of approximately 520 amino acids. The most prominent function of MAO is that it acts as a catalyst for the oxidative deamination of biogenic and xenobiotic amines (Bach *et al.*, 1988) in the periphery as well as in the CNS (Weyler *et al.*, 1990). Two types of MAO (A and B) have been described. Although the amino acid sequence of the two isoforms is 71% identical, they exhibit different substrate and inhibitor selectivities. MAO-A is sensitive to inhibition by the selective MAO-A inhibitor clorgyline, preferentially deaminates serotonin, norepinephrine and epinephrine (Waldmeier, 1987) and is also responsible for the oxidation of tyramine in the intestine. The selective and irreversible MAO-B inhibitor (R)-deprenyl, is responsible for MAO-B inhibition at very low concentrations (Grimsby *et al.*, 1990). MAO-B preferentially deaminates β-phenylethylamine (PE) and benzylamine. Both of the isoforms utilize dopamine as a substrate with MAO-B exhibiting a higher catalytical turnover. The amines are deaminated to the corresponding aldehyde and ammonia in the periphery as well as in the central nervous system (CNS) (Weyler *et al.*, 1990).

The mechanism of action of MAO forms part of the vast research field for this very interesting enzyme. MAO catalyses α-carbon oxidation of amines to imines and iminiums with simultaneous reduction of the covalently bound FAD cofactor. The primary product of MAO

acting on a monoamine is the corresponding aldehyde, usually rapidly further oxidized by aldehyde dehydrogenase (ADH) to a carboxylic acid, which is the final excreted product. The enzyme is regenerated by oxidation of the reduced FAD with synchronized reduction of molecular oxygen to hydrogen peroxide. For each mole of substrate oxidized one mole of hydrogen peroxide is produced (figure 14).

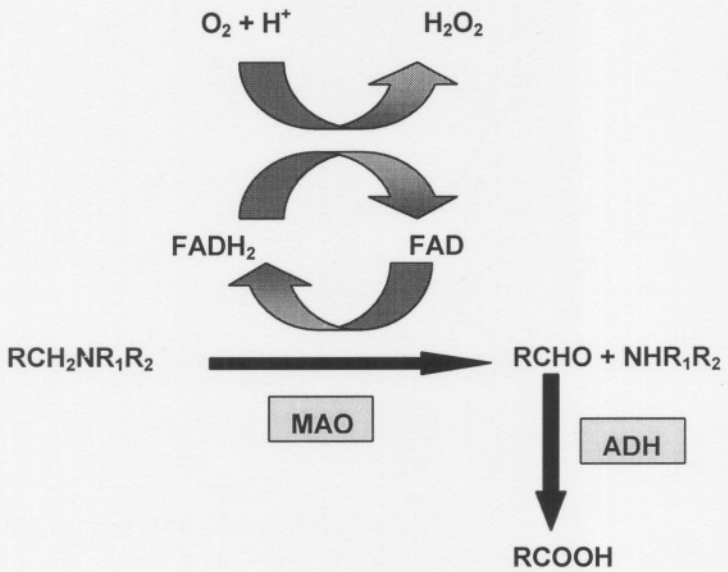

Figure 14: The reaction pathway for mitochondrial monoamine metabolism of amines by oxidative deamination (Youdim & Bakhle, 2006).

Both monoamine oxidase A and B play an important role in the metabolism of monoamine transmitters and are therefore of considerable pharmacological interest. Inhibitors of MAO are of therapeutic interest for the treatment of psychiatric and neurological disease. Reversible inhibitors of MAO-A are currently used as anti-anxiety and antidepressant drugs (Volz & Gleiter, 1998), while selective inhibitors of MAO-B are in use and are under investigation for the treatment of the symptoms and underlying neurodegeneration of Parkinson's disease (PD) (Youdim & Riederer, 2004; Riederer *et al.*, 2004) and Alzheimer's disease (Saura, 1994). Furthermore, MAO-B is of considerable pharmacological interest due its role as the catalyst that mediates the bio-activation of the pro-neurotoxin MPTP.

3.2.1 Pharmacological actions of Monoamine Oxidase B inhibitors

The primary goal of MAO-B inhibitors is to increase the availability of the neurotransmitters at the nerve terminals. MAO-B inhibitors increase the basal dopamine levels in the dopaminergic input pathway. Because MAO-B metabolizes dopamine, inhibition of the enzyme in the brain can help conserve the depleted supply of dopamine in PD. In patients with advanced PD,

MAO-B inhibition can prolong the effects of levodopa and allow for a lower dosage. Inhibition of MAO-B also results in the reduction of hydrogen peroxide production, which is believed to play an important role in the etiology of PD. Pharmacological analyses have generated the concept of neuroprotection which is concerned with the possibility of slowing, halting or even reversing the neurodegeneration in PD. MAO inhibitors are believed to play an important role in neuroprotection since they appear to decrease the oxidative stress in dopaminergic neurons by decreasing hydrogen peroxide (H_2O_2) production (Cano *et al.*, 1996). Since H_2O_2 is a possible neurotoxin, MAO-B inhibitors can therefore also act as neuroprotective agents.

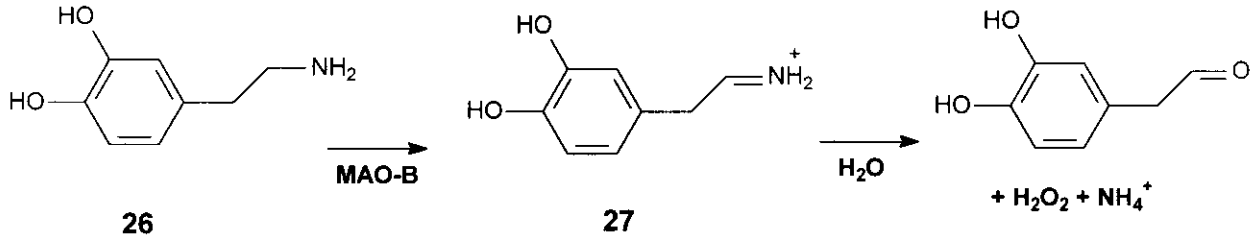

Figure 15: MAO-B catalyzed oxidative deamination of dopamine (**26**) to the corresponding aldehyde (**27**), ammonium and hydrogen peroxide by MOA-B.

MAO-B inhibitors are also important since they prevent MAO-B from oxidizing MPTP to the very toxic compound MPP^+ (Nicora & Parvez, 2000).

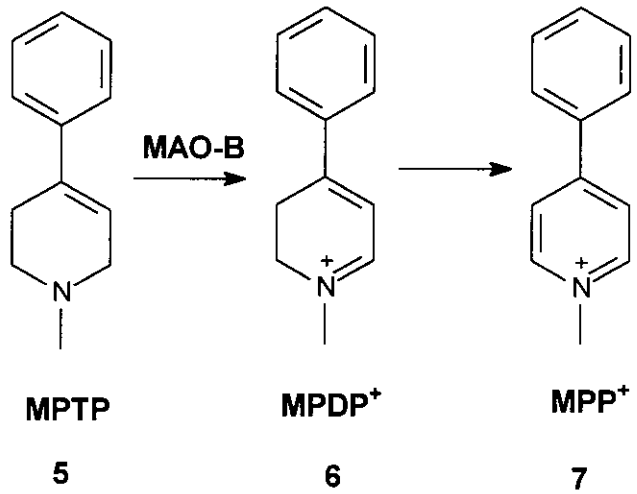

Figure 16: The MAO-catalyzed oxidation of the 1-methyl-4-phenyl-1,2,3,6-tetrahydropyridine (MPTP) (**5**).

Current trends in research clearly show that monoamine oxidase inhibitors play an important role in various physiological and pathological processes, designating MAO-B as an important drug target.

3.2.2 Known inhibitors

Inhibitors of MAO-B that have been demonstrated to be of clinical value are irreversible inhibitors such as (*R*)-deprenyl (**1**) (The Parkinson Study Group, 1989) and rasagiline (**28**) (Rabey *et al.*, 2000) as well as reversible inhibitors such as lazabemide (**29**) (The Parkinson Study Group, 1996) and safinamide (**30**) (Figure 17).

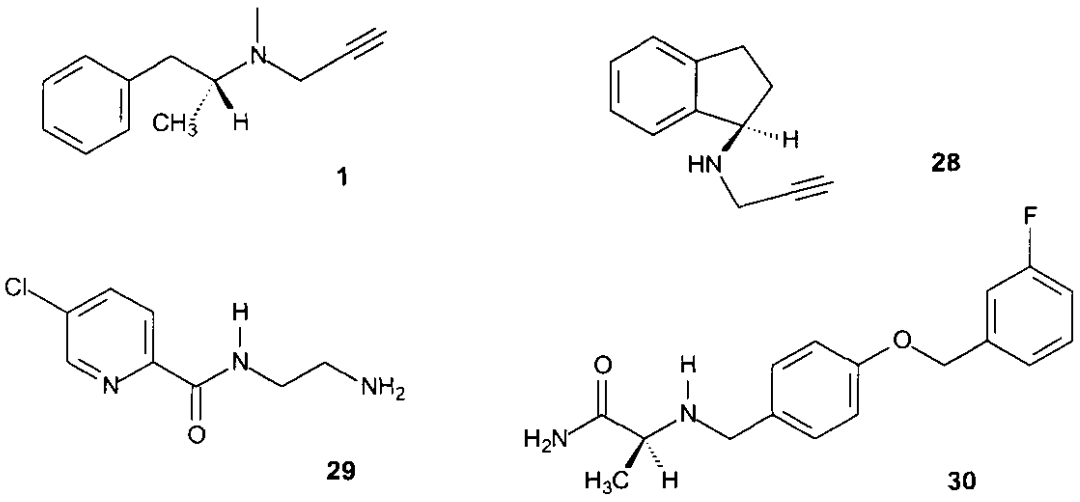

Figure 17: Structures of MAO-B inhibitors (R)-deprenyl (**1**), rasagiline (**28**), lazabemide (**29**) and safinamide (**30**).

(R)-deprenyl is at present the best known irreversible inhibitor of MAO-B and has been found to be neuroprotective in MPTP treated animals (Heikkila *et al.*, 1984). Lazabemide, a selective reversible inhibitor of MAO-B is currently under clinical evaluation for the treatment of PD and AD. These inhibitors were developed for the treatment of PD, based on the hypothesis that MAO-B inhibition increases the basal central dopamine levels in PD. (Knoll, 2000). A rise in the levodopa induced dopamine levels is also expected to be prolonged and enhanced in patients receiving MAO-B inhibitors.

Although the current inhibitors used in the treatment of PD ameliorate the symptoms temporarily, clinical studies of these inhibitors have reported them to cause anorexia/nausea,

dry mouth, dyskinesia and orthostatic hypotension in patients with PD, especially when used in combination with levodopa. An overdose of irreversible MAO-B inhibitors could lead to serious side-effects because the inhibitor is irreversibly bound to the FAD co-factor of the enzyme. The enzyme activity can only be regained via *de novo* synthesis of new MAO-B proteins, a process that may require several days. Apart from being irreversible, (R)-deprenyl is metabolized to L-amphetamine and L-metamphetamine (Heinonen *et al.*, 1994) which are neurotoxic to the brain and may cause cell damage (OH *et al*, 1994.) This may antagonise the neuroprotective effect of (R)-deprenyl. For this reason several research groups are currently attempting to identify new MAO-B inhibitors that are reversible while retaining selectivity for MAO-B.

3.2.3 Substrates of MAO-B

Since it was discovered that the two isomers of MAO differ in their substrate selectivity, a wide range of selective substrates for MAO-A and B have been identified.

Table 1: Known substrates of MAO-A and MAO-B.

MAO-A	**MAO-B**	**MAO-A/B**
Serotonin	Benzylamine	Tyramine
Octopamine	Phenylethylamine	Dopamine
Adrenaline	Methylhistamine	Tryptamine
Noradrenaline	*N*-acetylputrescine	Kynuramine
	MPTP	3-Methoxytyramine
	n-Phenylamine	
	Octylamine	
	Milacemide	

(Fowler *et al.*, 1980; Kalir *et al.*, 1981 ; Shih *et al.*, 1998)

A well known MAO substrate, MPTP, was discovered when a drug addict, preparing meperidine, inadvertently synthesized it as an impurity. After injection of the drug the person, still in his twenties, rapidly developed PD-like symptoms. MPTP was found to be selectively toxic to the dopaminergic neurons in the substantia nigra of animals and induced PD-like neurodegeneration. MAO inhibitors protected the nigrostriatal neurons in mice against damage caused by MPTP, but only (R)-deprenyl and not clorgyline was protective when used as pre-treatment (Heikkila *et al.*, 1984). This indicated that the neurotoxin was selectively being metabolized by MAO-B to the active toxin MPP^+. This discovery led to MPTP and other

tetrahydropyridinyl substrates becoming popular agents for neuroprotective studies in the field of PD.

MAO-B has been identified as the principal enzyme responsible for the metabolic activation of the proneurotoxin MPTP (**28**) in the brains of mammals including humans (Figure 17) (Chiba et al., 1984; Heikkila *et al.*, 1984). The molecular mechanisms by which MPTP selectively damages nigrostriatal neurons and induces a parkinsonian syndrome in mammals, including humans, has been the subject of extensive research (Heikkila *et al.*, 1984)

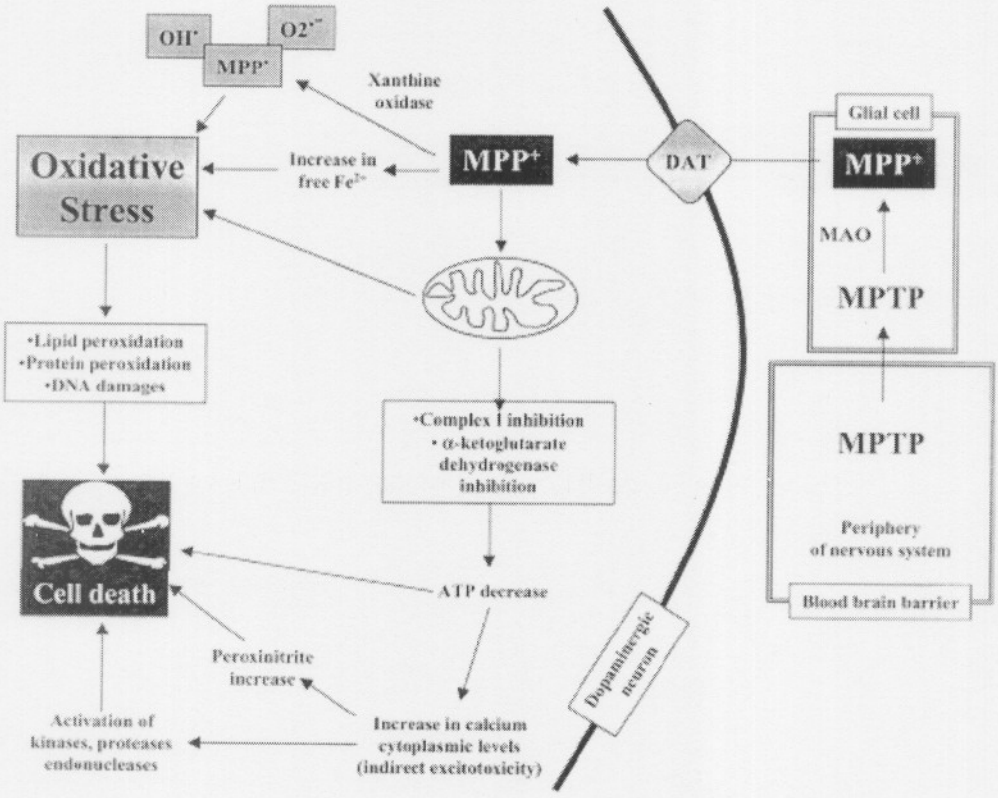

Figure 18: An illustration of the mechanism of MPTP toxicity. MPTP, injected peripherally, crosses the blood-brain barrier and is transformed by glial MAO into the active compound MPP^+, as illustarted by Blum *et al.* (2001).

Critical to its mode of action is the MAO-B catalyzed α-carbon oxidation of the parent compound yielding the corresponding 1-methyl-4-phenyl-2,3-dihydropyridinium species $MPDP^+$ (**29**). This metabolic intermediate undergoes a second two-electron oxidation to generate the 1-methyl-4-phenylpyridinium metabolite MPP^+ (**30**), the ultimate neurotoxin (Chiba *et al.*, 1984a). This process appears to take place mainly in glial cells where MAO-B is

located (Takada et al., 1990). MPP^+ is believed to be transported into the nigrostriatal dopaminergic nerve terminals, possibly via the plasma membrane dopamine transporter (DAT) (figure 18) where it is localized within the inner mitochondrial membrane. Inhibition of complex I of the mitochondrial respiratory chain by MPP^+ leads to downstream events such as ATP depletion and oxidative stress which eventually result in degeneration of nigrostriatal dopaminergic neurons. The remarkable selectivity of MPP^+ as a nigrostriatal toxin can presumably be explained by the ability of the DAT system to actively concentrate MPP^+ in the dopaminergic neuron (Chiba *et al.*, 1985b; Javitch *et al.*, 1985). MPTP has been studied extensively as an experimental model of neurodegeneration due to its selective destruction of dopaminergic neurons and the production of behavioural and pathological symptoms resembling PD. The cyclic tertiary amine is an excellent substrate for MAO-B that catalyses an initial bioactivation event, leading to the corresponding dihydropyridinium intermediate $MPDP^+$ (figure 16). Autoxidation of $MPDP^+$ to the pyridinium species MPP^+ is accompanied with the generation of superoxide radicals (Zang & Misra, 1992). MPP^+ is actively transported into the striatal nerve terminals and localized in the mitochondrial matrix where it inhibits complex I of the electron transport system, resulting in depletion of ATP (Wu *et al.*, 1992). MPP^+ has also been shown to induce apoptosis via cytochrome c release and caspase activation, properties that may contribute further to its neurotoxicity (Yoshinaga *et al.*, 2000).

3.3 Determining MAO-B inhibition activity

The most convenient method for the measurement of MAO activity is a spectrophotometric technique (Houslay *et al.*, 1974; Kalgutkar et *al.*, 1994). The discovery that MAO catalyzes the allylic ring α-carbon oxidation of tetrahydropyridinyl substrates such as MPTP, is the basis of the assay used in this study. (Figure 16).

The first documented tetrahydropyridinyl substrate was the pro-neurotoxin MPTP (**5**) (figure 16), which proved to be an excellent MAO-B selective substrate (Chiba *et al.*, 1984). As discussed previously [see 2.3.3], the neurotoxic properties of MPTP are reliant on its MAO-B catalyzed oxidation to the corresponding dihydropyridinium intermediate ($MPDP^+$ (**6**); λ_{max} = 345 nm) which undergoes a second two-electron oxidation to generate the toxic pyridinium species (MPP^+ (**7**); λ_{max} = 295 nm). When measuring MAO-B catalytic activity through quantitative estimations of $MPDP^+$ and MPP^+ it is necessary to employ chromatographic techniques for accurate kinetic measurements (Castagnoli *et al.*, 1997). Because of its ease and speed of operation, most laboratories prefer spectrophotometry above chromatography.

Because the metabolites of MPTP absorbs light at a relative low wavelength it is a less suitable substrate for exploratory studies of MAO-B inhibition.

It has been found that other tetrahydropyridinyl analogues can also serve as substrates for MAO. Of interest to us is 1-methyl-4-(1-methylpyrrol-2-yl)-1,2,3,6-tetrahyropyridine (MMTP (**31**)) which is both an MAO-A and -B substrate. MAO catalyzes the oxidation of MMTP to the corresponding dihydropyridinium species ($MMDP^+$ (**32**); λ_{max} = 420 nm) which, unlike $MPDP^+$, is stable to further oxidation to the pyridinium species (**33**) (Figure 19). MMTP is, therefore, an excellent substrate for screening MAO-A and -B activity spectrophotometrically (Inoue *et al.*, 1999; Nimkar *et al.*, 1996). For preparations that contain both MAO-A and –B, it is required to inactivate one of the isoforms by preincubation in the presence of a selective inactivator. Clorgyline is used to inactivate MAO-A and (*R*)-deprenyl is used to inactivate MAO-B. During our study we utilized MMTP as our substrate because it's conversion to $MMDP^+$ can easily be measured spectophotometrically. Baboon liver MAO was used as enzyme source because it closely resembles that of human MAO and it is free of MAO-A which makes pre-treatment with clorgyline unnecessary.

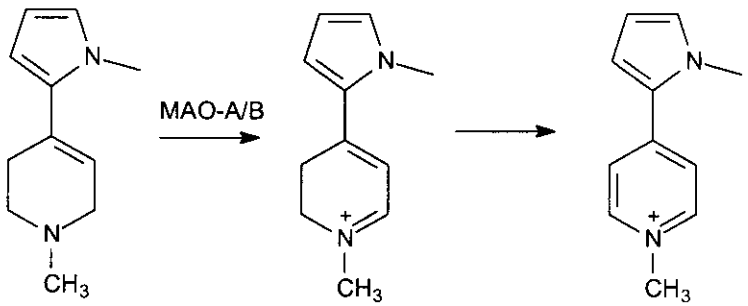

31 **32** **33**

Figure 19: The MAO-catalyzed oxidation of the 1-methyl-4-(1-methylpyrrol-2-yl)-1,2,3,6-tetrahydropyride MMTP (**31**) to the dihydropyridinium intermediate $MMDP^+$ (**32**) and the toxic pyridinium species MMP^+ (**33**) which is not observed in *in vitro* studies (Petzer *et al.*, 2003).

The technique used to study the enzymology can be summarized as a spectophotometrical assay, based on measuring the extent to which the synthesized MAO-B inhibitor slows the rate of oxidation of MMTP to $MMDP^+$. The determination can be carried out spectrophotometrically because $MMDP^+$ has a maximal radiation absorbance at a wavelength

of 420 nm, which is distant from the maximal absorbance wavelengths of the species being incubated (eg. MMTP).

3.4 Enzyme kinetics

3.4.1. K_m determination

If the concentration of the enzyme substrate [S] is increased while all other conditions are kept constant, the initial velocity (V_i) of an enzymatic reaction will increase to a maximum value, V_{max}. V_i is the velocity when a very small amount of the substrate has been consumed. At V_{max} the enzyme is saturated with substrate and V_i is unchanged by further increases in substrate concentration. The substrate concentration [S] that produces half-maximal velocity ($V_{max}/2$), termed the K_m value or Michaelis constant, is determined experimentally by graphing V_i vs. [S] (Figure 20). The K_m value may approximate, with certain assumptions, the binding constant (K_d) for the enzyme-substrate complex. Because the affinity of an enzyme for its substrate is equal to the inverse of K_d, a numerically small K_m indicates a high affinity of the substrate for the enzyme (Rodwell, 1993). The Michaelis-Menten equation expresses the behaviour of various enzymes under the influence of different substrate concentrations (Equation 3.1).

$$V_i = \frac{V_{\max} \times [S]}{K_m + [S]} \qquad \textbf{Equation 3.1}$$

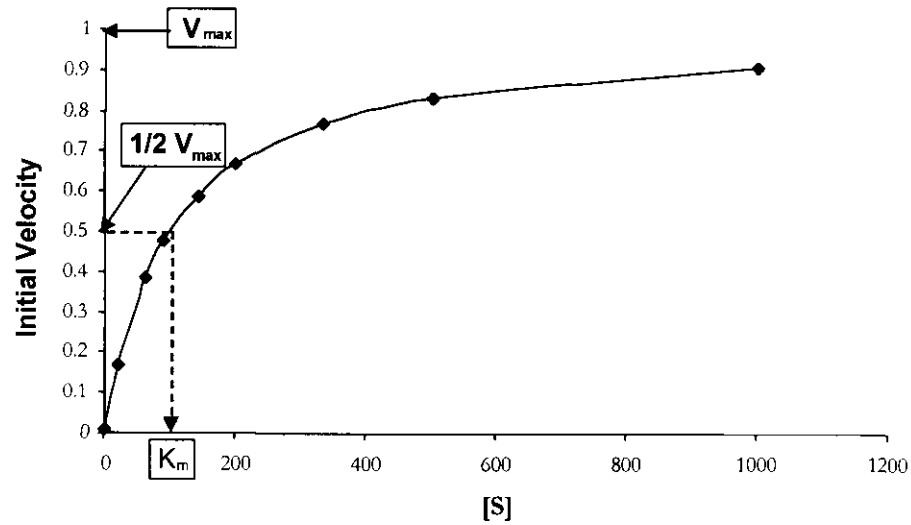

Figure 20: The Michaelis-Menten equation 3.1 illustrated graphically (V_i versus [S]).

Numerous enzymes give saturation curves that do not permit exact measurement of V_{max} (and therefore K_m) when V_i is plotted against [S]. By inversion of the Michaelis-Menten equation (Equation 3.2) and graphing the inverse of the initial velocity ($1/V_i$) as a function of the inverse of substrate concentration (1/[S]), a straight line is obtained. The resulting plot is called a double reciprocal plot or Lineweaver-Burke plot (Figure 21). The K_m and V_{max} values can easily be obtained from this plot since the y-axis intercept is equal to $1/V_{max}$ and the slope is K_m/V_{max}. The x-axis intercept is equivalent to $-1/K_m$ (Segel, 1993).

$$\frac{1}{V} = \left(\frac{K_m}{V_{\max}}\right) \times \left(\frac{1}{[S]}\right) + \frac{1}{V_{\max}} \qquad \textbf{Equation 3.2}$$

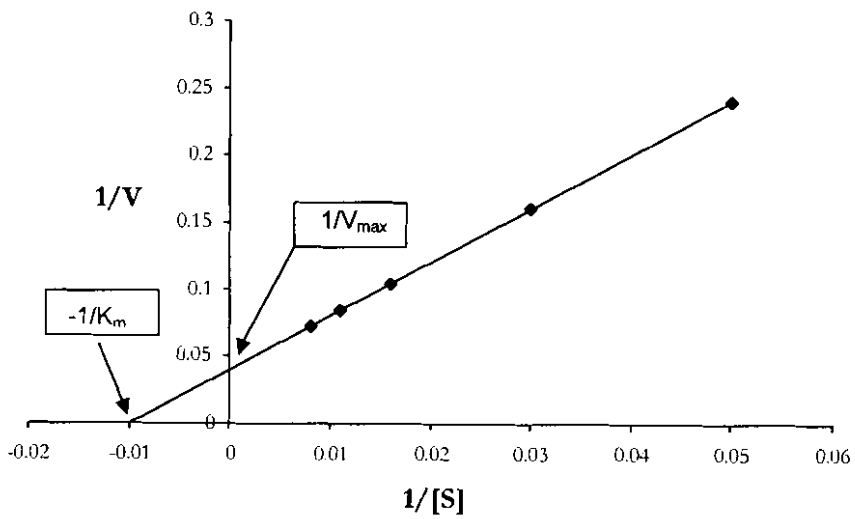

Figure 21: An illustrated example of the Lineweaver-Burke plot ($1/V_i$ versus 1/[S]).

When [S] is approximately equivalent to K_m, V_i is very receptive to changes in substrate concentrations and the presence of inhibitors. For that reason, when examining the MAO-B catalytic rate the substrate concentrations that bracket the apparent K_m value are used.

3.4.2 K_i determination

Classic competitive inhibition takes place at the substrate-binding site of an enzyme in a mode that prevents the substrate from binding. The inhibitor and substrate are mutually exclusive, this means that they compete for binding at the identical site and that the association of the inhibitor and enzyme is reversible. Competitive inhibition is represented graphically by the Lineweaver-Burke plot (Figure 22). The addition of a competitive inhibitor to an enzyme-substrate reaction increases the slope of the straight line while the y-axis intercept remains unchanged. The intercept on the x-axis increases and becomes less negative. Therefore a competitive inhibitor raises the apparent K_m value of a substrate while V_{max} remains unchanged. The form of the Michaelis-Menten equation describing the inhibitor-substrate-enzyme relationship for many enzymes is illustrated in equation 3.3:

$$V_i = \frac{V_{\max} \times \frac{[S]}{K_m}}{1 + \frac{[S]}{K_m} + \frac{[I]}{K_i}} \qquad \textbf{Equation 3.3}$$

The inverse of this equation expresses the double reciprocal plot in the presence of a competitive inhibitor as described in equation 3.4:

$$\frac{1}{V_i} = \frac{K_m}{V_{\max}}\left(1 + \frac{[I]}{K_i}\right) \times \frac{1}{[S]} + \frac{1}{V_{\max}} \qquad \textbf{Equation 3.4}$$

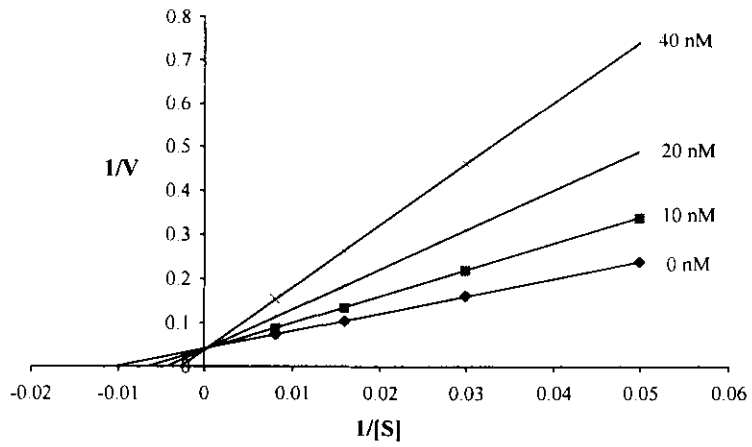

Figure 22: The double reciprocal plot in the presence of different preset concentrations of a competitive inhibitor.

The K_i value of a competitive inhibitor is used to describe the affinity of the inhibitor for the active site of the enzyme. In a series of competitive inhibitors, those with the lowest K_i values will cause the highest level of inhibition at a fixed concentration of inhibitor [I]. The K_i value for an inhibitor can be determined from the secondary plot in which the slope of each reciprocal plot is graphed vs. the corresponding inhibitor concentration (Figure 23). The x-axis value is equal to $-K_i$. In the presence of a concentration of inhibitor [I] that is approximately equal to K_i, the substrate concentration has to double to maintain the same original velocity as in the absence of the inhibitor. Generally it is believed that if plasma or tissue concentrations of a competitive inhibitor are larger than K_i, an interaction with the enzyme is expected to lead to a physiological effect. On the contrary, if the plasma or tissue concentrations are lower than K_i, an interaction between the inhibitor and enzyme is unlikely to lead to a physiological significant effect (Kakkar *et al.*, 1999).

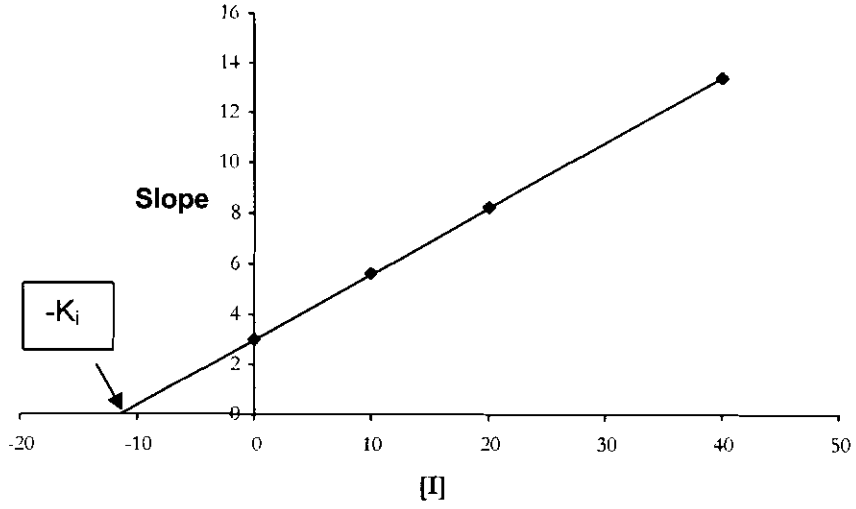

Figure 23: Secondary plot of the slopes from the double reciprocal plot versus inhibitor concentration.

3.5 Experimentation and results

3.5.1 Materials and instrumentation

Prof. Neal Castagnoli Jr., Virginia Tech, Blacksbury, USA, generously supplied us with the oxalate salt of MMTP. UV-Vis spectra were recorded on a Milton-Roy Spectronic 1202 spectrophotometer. The mitochondria were isolated from baboon liver tissue as described by

Salach and Weyler (1987) and stored at -70 °C. The mitochondrial isolate was suspended in sodium phosphate buffer (100 mM, pH 7.4 containing 50% glycerol, w/v). The protein concentration was determined by the Bradford method (Bradford, 1976). For the inhibition studies with MAO-B we utilized the MAO-A and –B substrate MMTP (K_m = 60.9 μM for baboon liver MAO-B) (Inoue *et al.*, 1999). Baboon liver mitochondria do not have measurable MAO-A activity and therefore the inactivation of this enzyme was unnecessary when MMTP was used as the substrate. Each incubation consisted of MMTP (30-120 μM), the mitochondrial isolate (0.15 mg protein/ml) and different concentrations of the test inhibitor. The final volumes of the incubations were 500 μl in the 100 μM sodium phosphate buffer, pH 7.4. The inhibitor solutions were prepared in DMSO and were added to the incubation at a constant volume of 20 μL. The samples were incubated for 15 min at 37 °C. The MAO-B catalyzed production of $MMDP^+$ is reported to be linear for this time period (Inoue *et al.*, 1999). The reaction was terminated by adding 10 μL 70% perchloric acid to the incubations and the samples were placed on ice and centrifuged at 16 000g for 10 min. The supernatant fractions were used to determine the concentration of MAO-B generated products. The $MMDP^+$ concentration was measured spectrophotometrically at a wavelength of 420 nm (Inoue *et al.*, 1999). Initial rates were expressed as nmoles of product formed per mg mitochondrial protein per minute. Competitive K_i values were determined by calculating the initial rates of substrate oxidation in the absence and presence of different concentrations of the inhibitor. Lineweaver–Burke plots with increasing concentrations of the inhibitor were constructed. The slopes of the Lineweaver–Burke plots were plotted as a function of the inhibitor concentration and the K_i was determined from the intercept (intercept = $-K_i$) (Segel, 1993). The regression analysis was performed with the SigmaPlot software package (Systat Software Inc.)

3.5.2 Calculations

The initial velocity (V_i) for MAO-B catalytic oxidation of MMTP was calculated using equation 3.5. For spectrophotometric determination of MAO-B activity, the equation was substituted with the measured absorbance (Abs) of the dihydropyridinium metabolite $MMDP^+$, the reported molar absorptivity (ε) for $MMDP^+$ (24 000 M^{-1}) together with the mitochondrial concentration [E] (0.15 mg protein/ml) and incubation time (15 minutes). The dimension of V_i in this equation is mol.mg $protein^{-1}$.$min.^{-1}$of the dihydropyridinium ($MMDP^+$) formed.

$$V_i = \frac{Abs}{\varepsilon} \times \frac{1}{[E]} \times \frac{1}{Time}$$ **Equation 3.5**

3.5.3 Determination of K_i values.

The enzyme inhibitor dissociation constants (K_i values) were measured by spectrophotometry. The assay is based on measuring the extent to which the synthesized inhibitors slow down the rate of the MAO-B catalyzed oxidation of MMTP to $MMDP^+$. The $MMDP^+$ concentration was measured at a relatively long wavelength of 420 nm. This wavelength is particularly convenient since it is distant from the wavelength at which the substrate and other constituents of the incubation absorb UV and visible radiation.

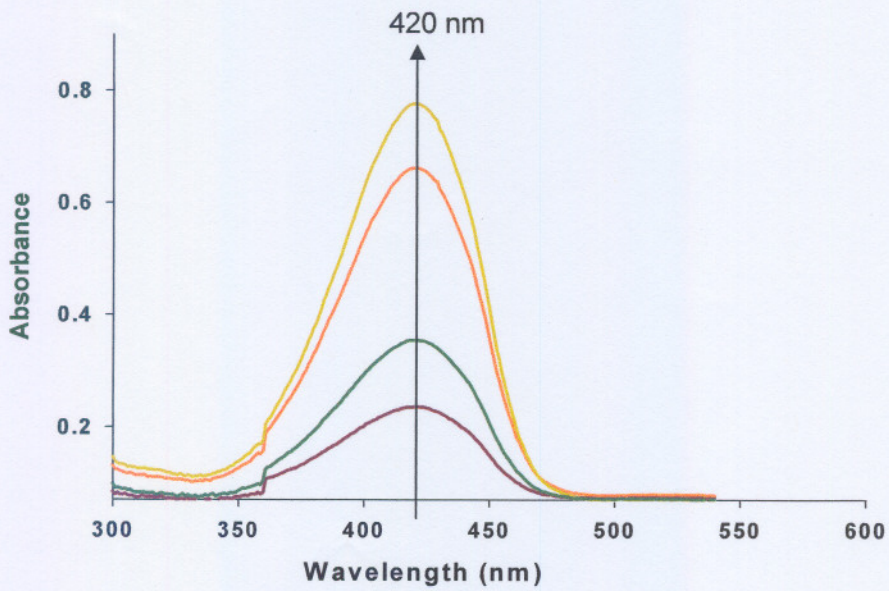

Figure 24: An example of UV scans of $MMDP^+$ formed in incubations of MMTP and baboon liver mitochondria. The incubations were carried out in the absence (yellow plot) and in the presence of various concentrations of **23c** (orange plot, 5 μM; green plot, 10 μM; red plot, 20 μM).

All of the benzimidazole analogues synthesized were found to be inhibitors of MAO-B. As illustrated by the graphs (Figure 25-32), the lines of the Lineweaver-Burke plots intersect, which indicate that the mode of inhibition is competitive.

3.5.3.1 (E)-2-styryl-1-methylbenzimidazole (23a)

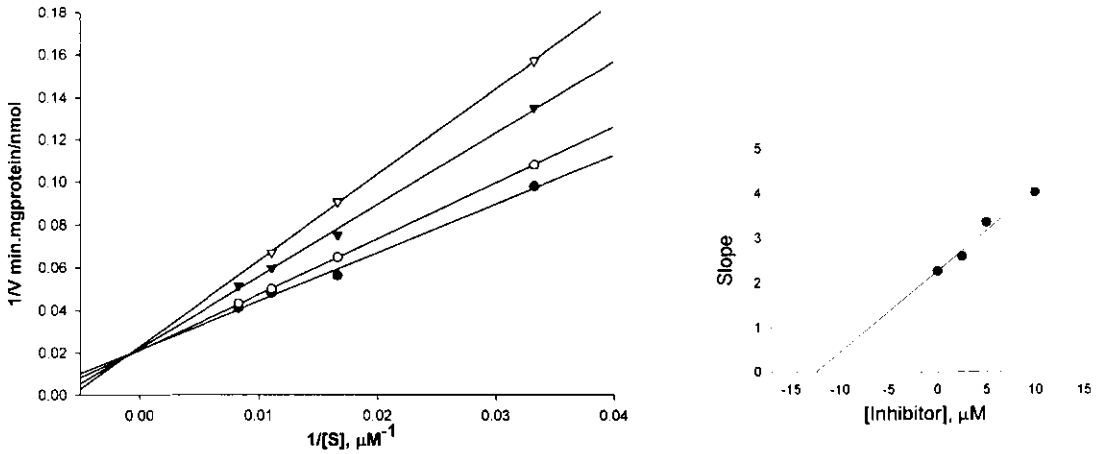

Figure 25: Lineweaver-Burke plots of the oxidation of MMTP by baboon liver MAO-B in the absence (filled circles) and the presence of various concentrations of **23a** (open circles, 3 μM; filled triangles, 6 μM; open triangles, 12 μM). The concentration of the baboon liver mitochondrial preparation was 0.15 mg/ml and the rates are expressed as nmol/min.mg protein of $MMDP^+$ formed. The secondary plot is that of of the slopes of the double reciprocal plot versus the inhibitor concentration.

3.5.3.2 (E)-2-(4-Chlorostyryl)-1-methylbenzimidazole (23b)

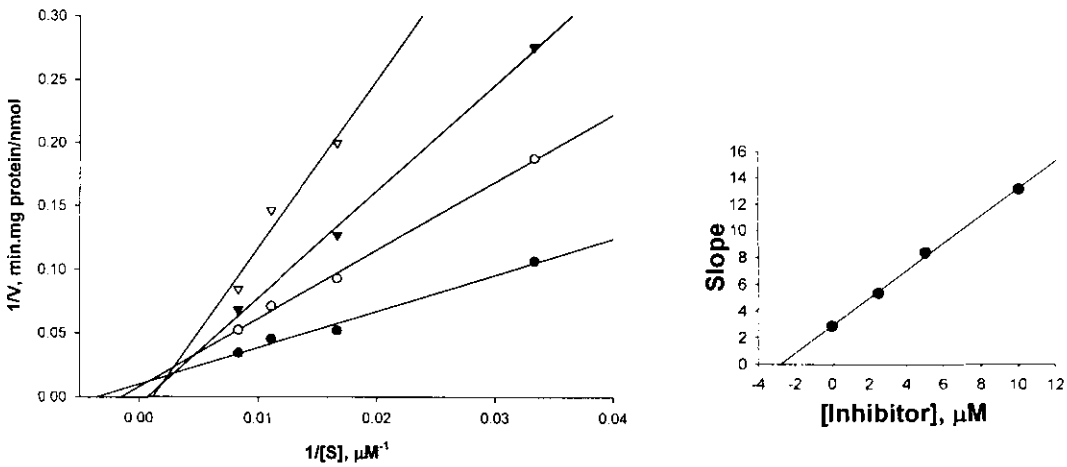

Figure 26: Lineweaver-Burke plots of the oxidation of MMTP by baboon liver MAO-B in the absence (filled circles) and the presence of various concentrations of **23b** (open circles, 3 μM; filled triangles, 6 μM; open triangles, 12 μM). The concentration of the baboon liver

mitochondrial preparation was 0.15 mg/ml and the rates are expressed as nmol/min.mg protein of $MMDP^+$ formed. The secondary plot is that of the slopes of the double reciprocal plot versus the inhibitor concentration.

3.5.3.3 (E)-2-(4-Fluorostyryl)-1-methylbenzimidazole (23c)

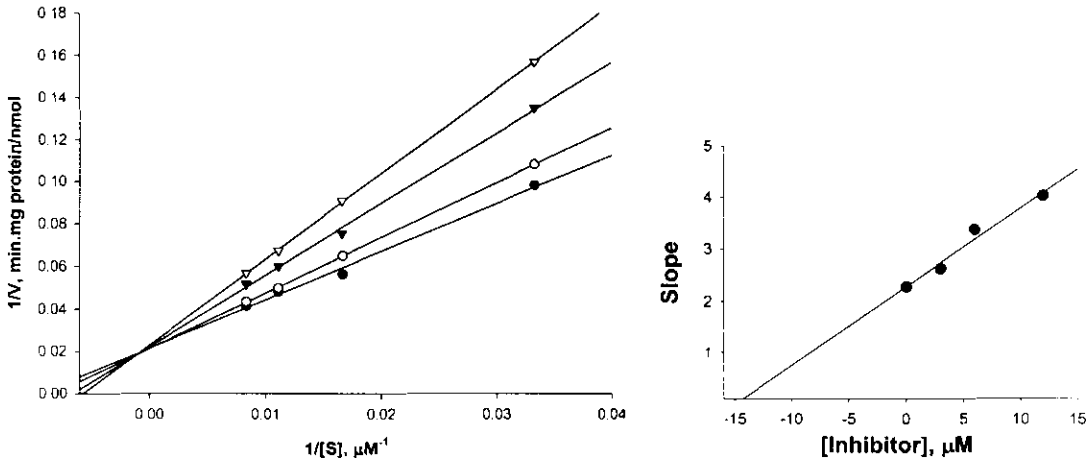

Figure 27: Lineweaver-Burke plots of the oxidation of MMTP by baboon liver MAO-B in the absence (filled circles) and the presence of various concentrations of **23c** (open circles, 3 μM; filled triangles, 6 μM; open triangles, 12 μM). The concentration of the baboon liver mitochondrial preparation was 0.15 mg/ml and the rates are expressed as nmol/min.mg protein of $MMDP^+$ formed. The secondary plot is that of the slopes of the double reciprocal plot versus the inhibitor concentration.

3.5.3.4 (E)-2-(4-Bromostyryl)-1-methylbenzimidazole (23d)

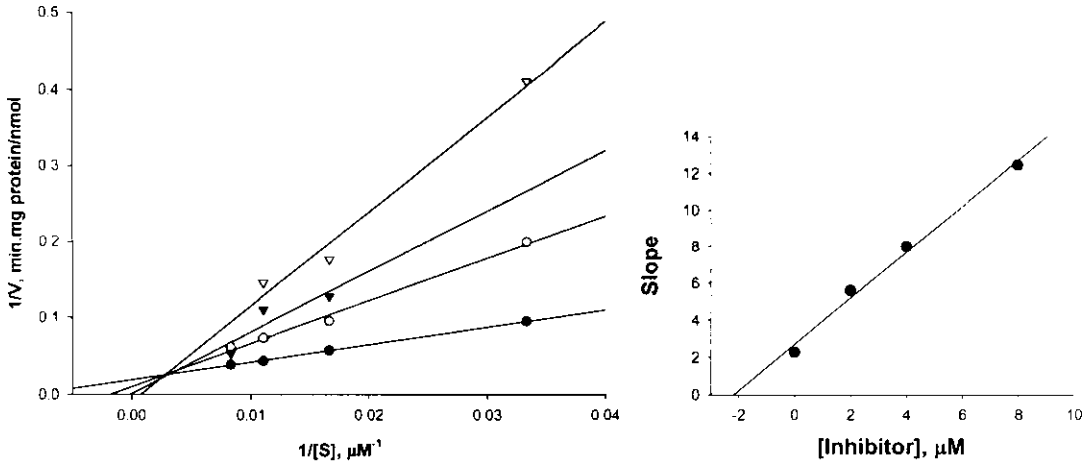

Figure 28: Lineweaver-Burke plots of the oxidation of MMTP by baboon liver MAO-B in the absence (filled circles) and the presence of various concentrations of **23d** (open circles, 2 μM; filled triangles, 4 μM; open triangles, 8 μM). The concentration of the baboon liver mitochondrial preparation was 0.15 mg/ml and the rates are expressed as nmol/min.mg protein of $MMDP^+$ formed. The secondary plot is that of the slopes of the double reciprocal plot versus the inhibitor concentration.

3.5.3.5 (E)-2-(4-Trifluoromethylstyryl)-1-methylbenzimidazole (23e)

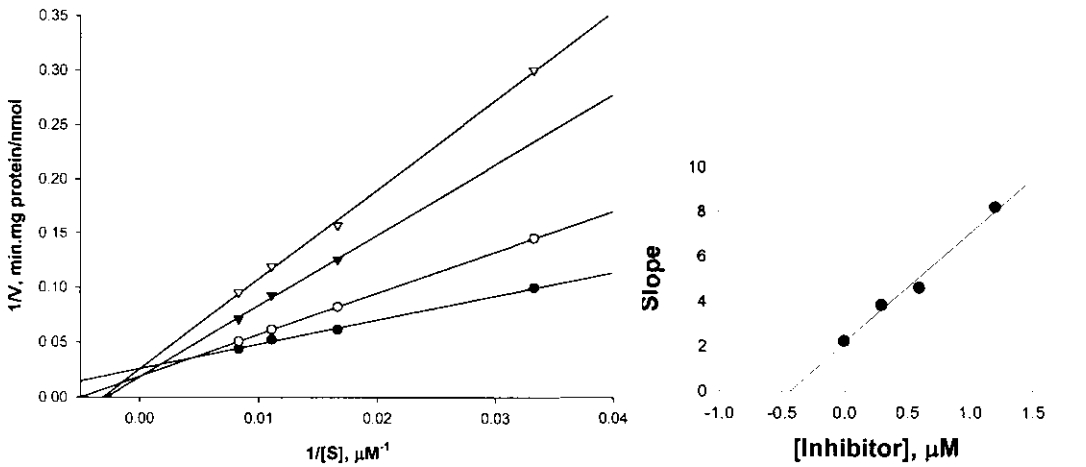

Figure 29: Lineweaver-Burke plots of the oxidation of MMTP by baboon liver MAO-B in the absence (filled circles) and the presence of various concentrations of **23e** (open circles, 0.3

μM; filled triangles, 0.6 μM; open triangles, 1.2 μM). The concentration of the baboon liver mitochondrial preparation was 0.15 mg/ml and the rates are expressed as nmol/min.mg protein of $MMDP^+$ formed. The secondary plot is that of the slopes of the double reciprocal plot versus the inhibitor concentration.

3.5.3.6 (E)-2-(4-Methoxystyryl)-1-methylbenzimidazole (23f)

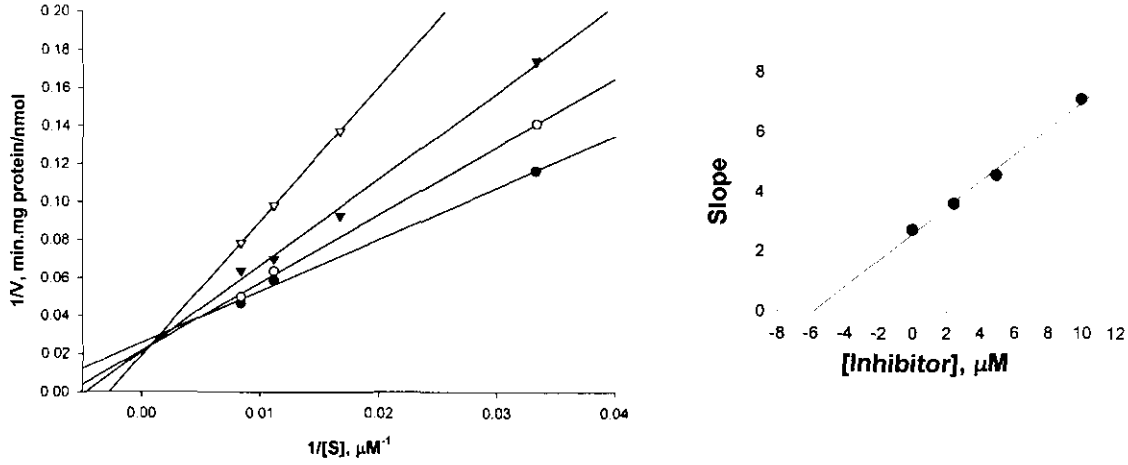

Figure 30: Lineweaver-Burke plots of the oxidation of MMTP by baboon liver MAO-B in the *absence (filled circles) and the presence of various concentrations of* **23f** *(open circles,* 2.5 μM; filled triangles, 5 μM; open triangles, 10 μM). The concentration of the baboon liver mitochondrial preparation was 0.15 mg/ml and the rates are expressed as nmol/min.mg protein of $MMDP^+$ formed. The secondary plot of the slopes of the double reciprocal plot versus the inhibitor concentration.

3.5.3.7 (E)-2-(4-Methylstyryl)-1-methylbenzimidazole (23g)

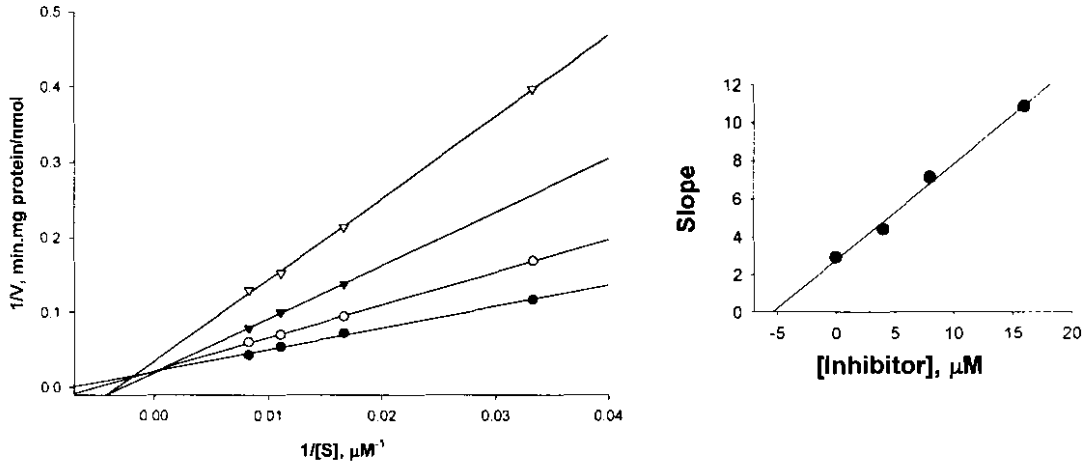

Figure 31: Lineweaver-Burke plots of the oxidation of MMTP by baboon liver MAO-B in the absence (filled circles) and the presence of various concentrations of **23g** (open circles, 4 μM; filled triangles, 8 μM; open triangles, 16 μM). The concentration of the baboon liver mitochondrial preparation was 0.15 mg/ml and the rates are expressed as nmol/min.mg protein of $MMDP^+$ formed. The secondary plot is that of the slopes of the double reciprocal plot versus the inhibitor concentration

3.5.3.8. 1-Methylbenzimidazole

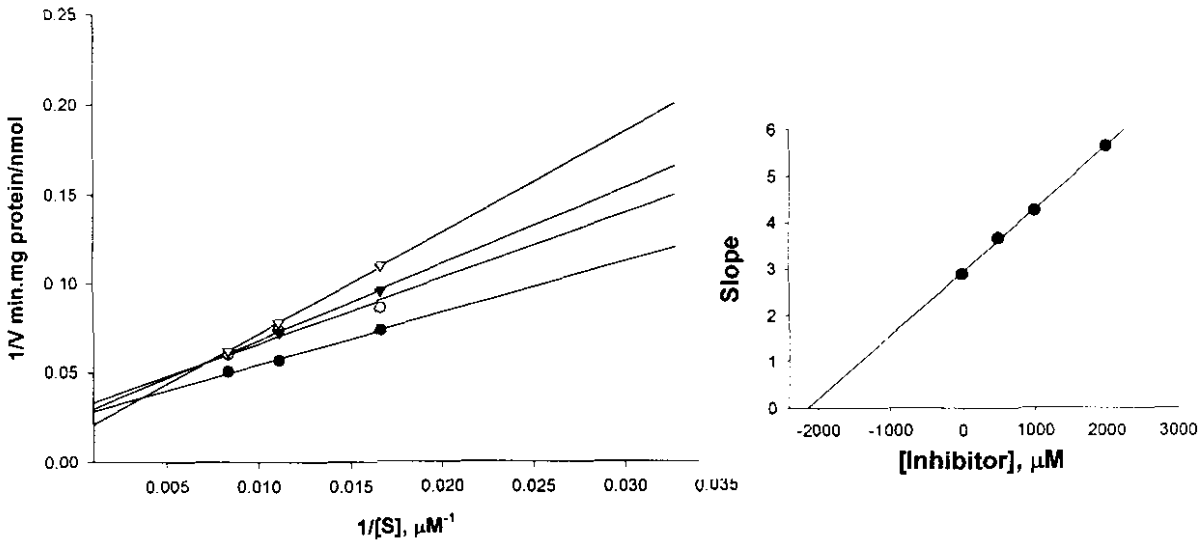

Figure 31: Lineweaver-Burke plots of the oxidation of MMTP by baboon liver MAO-B in the absence (filled circles) and the presence of various concentrations of **23a** (open circles, 500 μM; filled triangles, 1000 μM; open triangles, 2000 μM). The concentration of the baboon liver mitochondrial preparation was 0.15 mg/ml and the rates are expressed as nmol/min.mg protein of $MMDP^+$ formed. The secondary plot is that of the slopes of the double reciprocal plot versus the inhibitor concentration.

3.5.4 Results

All of the (E)-2-styryl-1-methylbenzimidazole analogues (**23a-g**) that were tested were found to be inhibitors of MAO-B. As demonstrated by the common intercept of the Lineweaver-Burke plots, the mode of inhibition was competitive. The K_i values determined for the series are presented in Table 2. All of the K_i values were found to be in the low μM range. (E)-2-(4-trifluoromethylstyryl)-1-methylbenzimidazole (**23e**) proved to be the most potent inhibitor with a K_i value of 560 nM.

Table 2: The K_i values for the inhibition of MAO-B by (E)-2-styryl-1-methylbenzimidazole analogues.

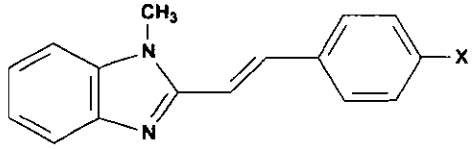

Compound	X	K_i value (μM)[a]
23a	H	12.43
23b	Cl	2.83
23c	Br	2.54
23d	F	14.95
23e	CF_3	0.43
23f	CH_3	5.52
23g	OCH_3	5.82

[a]The enzyme source used was MAO-B from baboon liver mitochondria and MMTP served as enzyme substrate.

Table 3: The K_i value for the inhibition of MAO-B by 1-methylbenzimidazole.

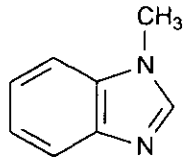

Compound	K_i value (μM)[a]
24	2084

The large K_i value of the 1-methylbenzimidazole, which lacks the styryl functional group, is an indication of the importance of the styryl moiety for MAO-B inhibition. This could be explained by the binding mode of the inhibitor in the enzyme active site. We believe that the styrylbenzimidazole analogues binds to both the entrance and the substrate cavities simultaneously. In contrast, 1-methylbenzimidazole can bind to only the substrate or the entrance cavity leaving the other cavity unoccupied. The styryl functional group assists with

dual binding which leads to increased inhibition potency. This dual mode of binding has also been reported for other inhibitors of MAO-B. Hubalek *et al*, (2005) reported that 1,4-diphenyl-2-butene (**34**) and trans,trans-farnesol (**35**) binds in both cavities according to high resolution crystal structures.

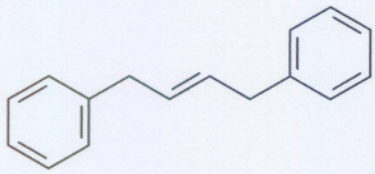

34

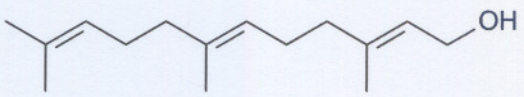

35

Figure 33: The structure of the reversible MAO-B inhibitors 1,4-diphenyl-2-butene (**34**) and trans,trans-farnesol (**35**).

Using the published crystal structures of MAO-B with trans,trans-farnesol bound too the enzyme (2BK3.pdb) and the molecular docking software Arguslab, we have docked (E)-2-styryl-1-methylbenzimidazole into the active site of the enzyme. The simple model generated showed that the inhibitor possibly binds to MAO-B with the benzimidazole ring in the substrate cavity (figure 34) while the styryl ring extends to the entrance cavity. In contrast similar models obtained with 1-methylbenzimidazole as inhibitor showed that the inhibitor binds only to the substrate or the entrance cavity (for example figure 35).

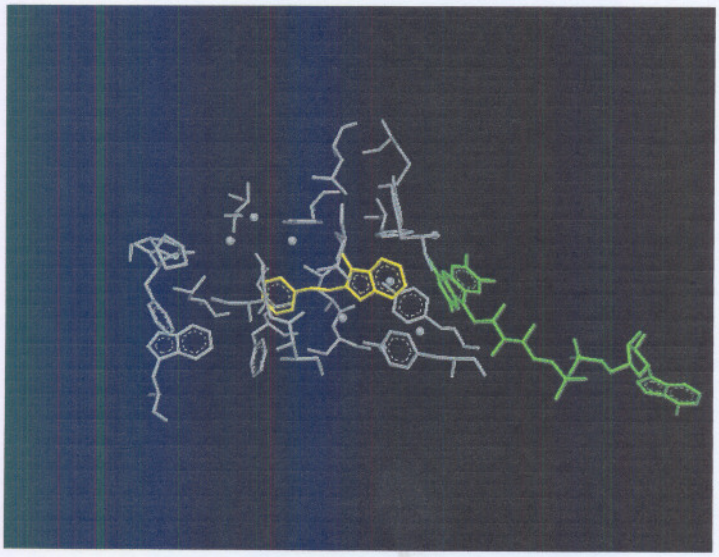

Figure 34: A simple model of (E)-2-styryl-1-methylbenzimidazole bound to both the substrate and the entrance cavity of the active site of MAO-B. The green structure represents the FAD-

cofactor, the grey structures are the amino acids lining the active site and the yellow structure is the inhibitor.

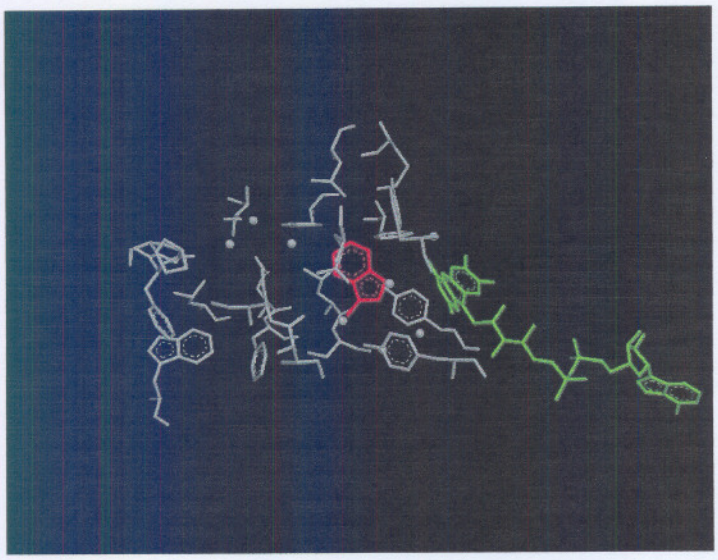

Figure 35: A simple model of 1-methylbenzimidazole bound to only the substrate cavity of the enzyme active site leaving the entrance cavity unoccupied. The green structure illustrates the FAD-cofactor, the grey structures are the amino acids lining the active site and the red structure is 1-methylbenzimidazole bound in the substrate cavity.

3.6 SAR studies.

Inspection of the K_i values suggests that the potency of inhibition is influenced by the size and electronic characteristics of the substituents. For example, (E)-2-styryl-1-methylbenzimidazole analogues with electron withdrawing groups (**23b-c and 23e**) are significantly more potent than the unsubstituted analogue (**23a**) and the analogues substituted with electron donating functional groups (**23f and g**). The bulkiness of the substituent on the 4-position also seems to play a role since analogues with bulky substituents (**23b-c, e-g**) are more potent than the unsubstituted analogue (**23a**) and the analogue bearing a fluorine at C-4 of the styryl ring (**23d**). These apparent correlations between inhibitor activity and physiochemical properties are similar to previous findings (Vlok *et al.*, 2006), which demonstrated a positive correlation between the Van der Waals volume of substituents at the 4-position of the styryl ring of (E)-8-styrylcaffeine analogues and MAO-B inhibition activity. In order to quantify the apparent relationships of the present study, a Hansch type SAR study was carried out by stepwise multiple linear regressions.

Six parameters were used to define the different physiochemical properties of the substituents. All of the physiochemical values of the substituents were obtained from standard compilations (Hansch & Leo, 1995; Hansch & Leo, 1979). To describe bulkiness the Van der Waals volume (V_w) (Bondi, 1964) and the Taft steric parameter (E_s) (Hansch *et al.*, 1995) were used. The lipophylicity of the substituents were described by the Hansch constant (π) (Fujita *et al.*, 1964). For electronic parameters the classical Hammet (σ_p) and Swain-Lupton (F) (Swain & Lupton, 1968) constants were used.The values for the substituent parameters σ_p, F, π, and E_s were obtained from the publication of Hansch & Leo (1995) and those for the Van der Waals volume (V_w) from Hansch & Leo (1979). Using the Statistica software package (StatSoft Inc.) a stepwise multiple regression analysis of the logK_i values as a function of the substituent parameter values were carried out. In order to estimate the significance of the regression equations the F statistic was employed. An F value higher than the critical F value indicated that the correlation was significant. The critical F values were calculated by a method described recently (Livingstone & Salt, 1995). The critical F value (F_{max}) for 95% significance for models constructed from 7 logK_i values (table 2) and which contains one parameter out of the possible six (σ_p, F, π, E_s ,V_w, MR) was calculated to be 25.32 .

Table 4: The values of the selected physiochemical parameters used in the SAR study (Hansch & Leo, 1995; Hansch & Leo, 1979)

	K_i	log K_i	V_w	σ_p	F	π	MR	E_s
H	12.43	1.094471	0.08	0	0	0	0.1	0
Cl	2.83	0.451786	1.07	0.23	0.42	0.71	0.6	-0.97
Br	2.54	0.404834	1.32	0.23	0.45	0.86	0.89	-1.16
F	14.95	1.174641	0.36	0.06	0.45	0.14	0.1	-0.46
CF_3	0.43	-0.36653	1.11	0.54	0.38	1.55	0.5	-2.4
CH_3	5.52	0.741939	1.01	-0.17	0.01	0.56	0.57	-1.24
OCH_3	5.82	0.764923	1.49	-0.27	0.29	-0.02	0.79	-0.55

Values obtained from Hansch & Leo (1979) and Hansch & Leo (1995).

The analogues were all analyzed as a single group since they all bear substituents at C-4 of the styrylring. The results of the statistical analysis of the group of (E)-2-styryl-1-methylbenzimidazole analogues are shown in table 5. For analogues substituted at C-4 of the phenyl ring the single substituent parameters that showed a meaningful correlation with the logarithm of the K_i values (expressed in µM) were the Taft steric parameter (E_s) and the Hansch constant (π) which

describes lipophilicity. Regression analysis of logK_i with E_s and π exhibited moderate correlations with R^2 values of 0.90 and 0.88, respectively. The statistical F values were found to be 46.65 and 38.22 for the two correlations (a higher F value indicates a better fit) (Livingstone & Salt, 2005).

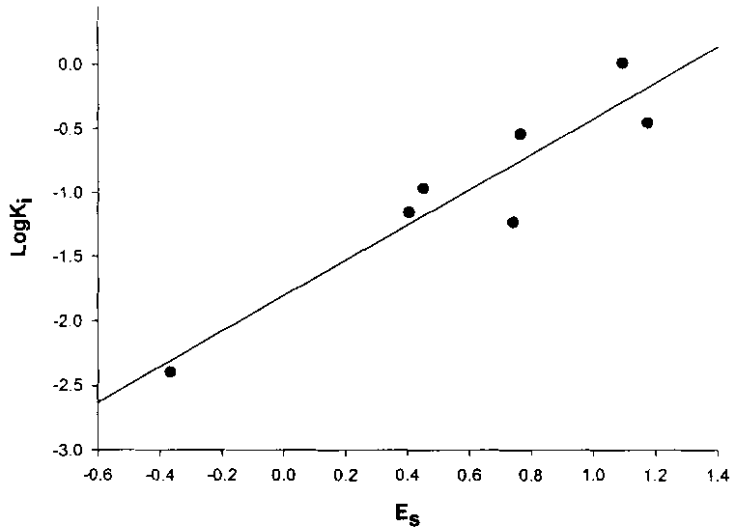

Figure 36: Graphical illustration of the correlation between the LogK_i values of the (E)-2-styryl-1-methylbenzimidazole analogues and the Taft steric parameter E_s. The correlation coefficient (R^2) was found to be 0.90.

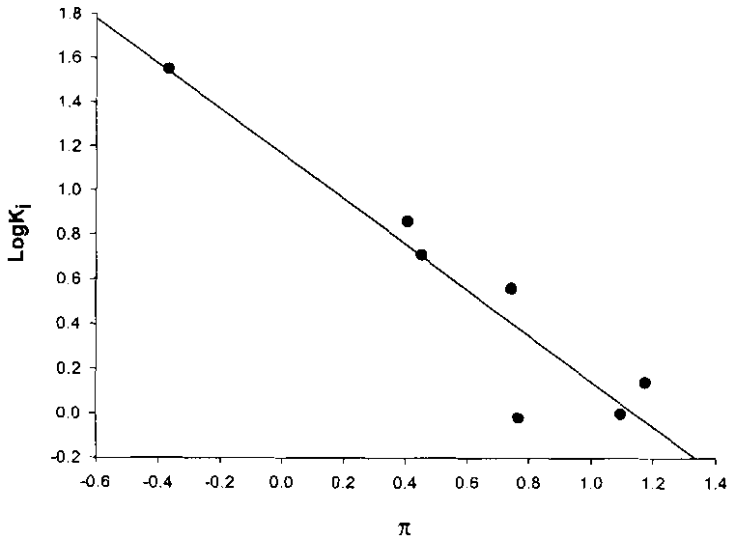

Figure 37: Illustration of the correlation between the LogK_i values of the (E)-2-styryl-1-methylbenzimidazole analogues and the Hansch constant (π). The correlation coefficient (R^2) was found to be 0.88.

All other single-parameter correlations with the logK_i values exhibited poorer statistical correlations. Therefore, the best mathematical description of binding affinity (logK_i) of C-4 substituted (*E*)-2-styryl-methylbenzimidazole analogues to MAO-B with a one parameter fit is:

$$\text{Log}K_i = 0.67(\pm 0.09)E_s + 1.27(\pm 0.11)$$

Because a small E_s value is an indication of a large steric substituent, the positive correlation of the Taft steric parameter (E_s) (0.67 ± 0.09) is an indication that a larger steric substituent enhances inhibition potency. Since the Hansch constant (π) is negatively correlated (–0.899 ± 0.15; Table 5) with logK_i, lipophylic C-4 substituents will lead to enhanced MAO-B inhibition potency.

Table 5: Correlations of the MAO-B inhibition constants (logK_i) of the (E)-2-styryl-1-methylbenzimidazole analogues bearing substituents on the C-4 of the styryl ring (**23a-g**) with steric, electronic and hydrophobic substituent parameters.

Parameter	Correlation (slope)	y-intercept	Coefficient of determination	F[a]	Significance[b]
σ_p	-1.43 ± 0.61	0.75 ± 0.16	0.52	5.50	0.066
F	-1.07 ± 1.11	0.93 ± 0.38	0.16	0.92	0.38
π	-0.899 ± 0.15	1.11 ± 0.11	0.88	38.22	0.0016
E_s	0.67 ± 0.09	1.27 ± 0.11	0.90	46.65	0.0010
V_w	-0.66 ± 0.37	1.23 ± 0.38	0.39	3.15	0.14
MR	-0.91 ± 0.67	1.08 ± 0.39	0.27	1.84	0.23

The logK_i values (expressed in μM) obtained with MMTP were used in linear regression analysis; [a] The F test statistic relates the mean squares due to regression to the error variance. Higher F values indicate a better fit and a regression equation with a F value higher than the critical F value may be deemed significant. [b]The significance is the fractional probability that the coefficient of the added variable is zero.

3.7 Summary and conclusion.

All of the (E)-2-styryl-1-methylbenzimidazole analogues (**23a-g**) tested were found to be inhibitors of MAO-B. As illustrated by the Linweaver–Burke plots (figure 24-31) all the lines have a common intercept indicating that the mode of inhibition was competitive. The K_i values for the inhibition of MAO-B calculated from the Lineweaver-Burke plots are presented in tables 2 and 3. The inhibitors were all found to be moderately potent with (E)-2-(4-trifluoromethylstyryl)-1-methylbenzimidazole proving to be the most potent with a Ki value of 0.56 μM. 1-Methylbenzimidazole had the largest K_i value of 2084 μM. This is an indication that the styryl functional group plays an important role in the interaction of the inhibitor with the enzyme active site.

After the determination of the K_i values, a Hansch type SAR study was performed in order to determine whether there are possible relationships between the substituents on C-4 of the styryl ring and their inhibition potency. The results of the study indicated that the MAO-B inhibition potency of the (E)-2-styryl-1-methylbenzimidazole analogues bearing C-4 substituents are dependant upon steric properties defined by the Taft steric parameter. For these substituents, sterically large substituents appear to enhance the inhibition potency. A moderate correlation was also found between the lipophylicity of the substituents and the $LogK_i$ values. Increased lipophylicity of the substituents at the C-4 of the styryl ring leads to enhanced MAO-B inhibition potency.

Chapter 4

DISCUSSION AND CONCLUSION

4.1 Parkinson's disease

PD is a slowly, progressive, degenerative CNS disorder which leads to the loss of dopaminergic neurons. The disease is of growing concern because it affects millions of people. The neurodegeneration caused by the disease results in muscle rigidity, bradykinesia, resting tremor and loss of postural reflex. The etiology of PD has not been established, although it is believed to be the result of endogenous toxins such as hydrogen peroxide or possibly a result of genetic mutations.

At present the treatment of PD is mainly based on dopamine replacement which is achieved with the dopamine precursor L-dopa. The results of the therapy are however overshadowed by development of drug induced dyskinesia, psychiatric complications and other side effects. Therefore, MAO-B inhibitors emerged as a promising drug target. The inhibitors currently used in the treatment of PD are irreversible mechanism based inactivators of the MAO-B. An example is (R)-deprenyl which binds covalently to the FAD-cofactor of the enzyme, rendering the enzyme permanently inactive. Enzyme activity can only be regained after *de novo* synthesis of new MAO-B proteins. Although the inhibitors temporarily ameliorate the symptoms of the disease they are irreversible and may lead to severe side effects. This led to the decision to develop new inhibitors of MAO-B which are reversible while retaining their selectivity towards MAO-B.

4.2 Aim

In this study a series of (E)-2-styryl-1-methylbenzimidazole analogues were synthesized and evaluated as competitive inhibitors of MAO-B. The one aim of the study was to further investigate benzimidazole analogues as competitive inhibitors after a small series of benzimidazole analogues were recently found to exhibit moderate inhibition potency of MAO-B. The series prepared in this study were substituted with both electron withdrawing and electron donating substituents at the 4-position of the styryl ring. The principle aim was to investigate the influence that the various substituents may have on the inhibition potency of the different analogues.

Also included in the study was 1-methylbenzimidazole which lacks the styryl functional group. The reason for inclusion of this analogue was to determine the importance of the styryl functional group for MAO-B inhibition potency. This may shed light on the importance of a styryl ring for interaction of the inhibitors with the active site of the enzyme.

After determination of the K_i values a Hansch type SAR study was performed in order to determine a possible correlation between the $\log K_i$ values of the inhibitors and the physiochemical properties of the substituents at C-4 of the styryl ring.

4.3 Summary of the study

4.3.1 Synthesis

Preparation of the (E)-2-styryl-1-methylbenzimidazole analogues was successfully achieved by acylation of commercially available o-phenylenediamine with an appropriate substituted trans-cinnamic acid in the presence of a carbodiimide reagent (EDAC). The resulting amides were cyclisized when heated with hydrochloric acid to give the corresponding aromatic intermediates. Treatment with iodomethane afforded the desired N-methylated analogues This procedure was similar to that used to prepare (E)-8-styrylcaffeines (Jacobson *et al.*, 1993) and benzimidazole analogues (Petzer *et al.*, 2003). The target compounds were purified via crystallization and silica gel column chromatography. The procedure followed for the successful synthesis of 1-methylbenzimidazole was described by Gazit *et al.*, (2003). Eight compounds and their intermediates were successfully synthesized and characterized by HRMS, ^{1}H-NMR and ^{13}C-NMR (Refer to appendix A).

4.3.2 Enzymology and biological activity

The K_i values for the competitive inhibition of MAO-B by the target compounds were estimated by measuring the extent by which various concentrations of the test inhibitors slowed the rate of the oxidation of 1-methyl-4-(1-methylpyrrol-2-yl)-1,2,3,6-tetrahydropyridine (MMTP) to the corresponding dihydropyridinium metabolite ($MMDP^+$). $MMDP^+$ production was measured spectrophotometrically at 420 nm, a wavelength at which neither the substrate not the test inhibitors absorbs light (Inoue *et al.*, 1999). Because of the favorable chromophoric characteristics and *in vitro* chemical stability of $MMDP^+$, this assay is frequently used to estimate K_i values for the inhibition of both MAO-A and –B (Castagnoli *et al.*, 1997; Petzer *et al.*, 2003) The Lineweaver-Burke plots with increasing concentrations of the test inhibitor were constructed and the K_i values were estimated from a secondary plot in which the values of the slopes obtained from the

Lineweaver-Burke plots were graphed as a function of the concentration of the test compound (Segel, 1993). The K_i values for the entire range of target compounds were obtained and the (E)-2-styryl-1-methylbenzimidazole analogues were found to have moderate inhibition activity of MAO-B. From the results of the inhibition study it became clear that there was a correlation between the different types of subtituents and the inhibition potency. This apparent correlation was futher quantified with a Hansch type SAR study. 1-Methylbenzimidazole, included in the study, was found to be a very weak inhibitor of MAO-B with a K_i value of 2084 μM. From this result it appears that the styryl functional group plays an important role in the interaction between the inhibitors and the enzyme..

4.3.3 Structureactivity relationship study

In order to quantify relationships between inhibitor activity and the physiochemical properties of the substituents attached at C-4 of the styryl ring, a Hansch-type (Hansch & Leo, 1995) SAR study was carried out by stepwise multiple linear regression. Six parameters were used to describe each substituent. The Van der Waals volume (V_w), molecular refractivity (MR) and Taft steric parameter (E_s) were used as descriptors of bulkiness while the lipophylicity of the substituents was described by the Hansch constant (π). The classical Hammett (σ_p) and Swain–Lupton (F) constants served as electronic parameters. All physiochemical values of the substituents were obtained from standard compilations (Hansch & Leo, 1995).

For the substitution at the C-4 position of the styryl ring, the best correlation was found with the Taft steric parameter, indicating that a sterically large substituent increases inhibitor potency. The parameter for lipophylicity also showed a moderate correlation indicating that more lipophylic substituents could lead to an increase in MAO-B inhibition potency.

4.4 Conclusion

From the results of this study it is evident that the (E)-2-styryl-1-methylbenzimidazole analogues are moderate inhibitors of MAO-B. The most potent analogue was found to be (E)-(4-trifluoromethylstyryl)-1-methylbenzimidazole with a K_i value of 0.56 μM. This compound is the most potent benzimidazole analogue MAO-B inhibitor yet reported. The potency of the analogues was found to correlate with the degree of steric hinderance and lipophylicity of the substituents at C-4 of the styryl ring. 1-Methylbenzimidazole, which lacks the styryl functional group, was a very weak inhibitor of MAO-B with a K_i value of 2084 μM. It can now be speculated that the styryl functional group is of importance for potent MAO-B inhibition. This

could be explained by dual mode interaction of the (E)-2-styryl-1-methylbenzimidazole inhibitors with the active site of the enzyme.

BIBLIOGRAPHY

1. **Arnold, J., Gasser, T., Storch, A., Lipp, A., Kupsch, A., Hundemer, H. and Schwarz, D.J.** 2005. High doses of pergolide improve clinical global impression in advanced Parkinson's disease- A preliminary open label study. *Archives of gerontology and geriatrics*, 41:293-253.

2. **Bach, A.W.J., Lan, N.C., Johnson, D.L., Abell, C.W., Bembenek, M.E., Kwan, S.W., Seeburg, P.H. and Shih, J.C.** 1988. cDNA cloning of human liver monoamine oxidase A and B: Molecular basis of differences in enzymatic properties. *Proceeding of the national academy of sciences of the United States of America*, 85:4934-4938.

3. **Blum, D., Torch, S., Lambeng, N., Nissou, M., Benabid, A., Sadoul, R. and Verna, J.** 2001. Molecular pathways involved in the neurotoxicity of 6-OHDA, dopamine and MPTP: contribution to the apoptotic theory in Parkinson's disease. *Progress in neurobiology*, 65:135-172.

4. **Bondi, A.** 1964. Van der Waals Volumes and Radii. *Journal of physical chemistry*, 68:441-451.

5. **Bradford, M.M.** 1976. A rapid and sensitive method for the quantitation of microgram quantities of protein utilizing the principle of protein-dye binding. *Analytical biochemistry*, 72:247-254.

6. **Cano, J., Dela Cruz, C.P., Machado, A., Revilla, E., Rodriguez-Gomez, J.A. and Steffen, V.** 1996. Protection of the aged substantia nigra of the rat against oxidative damage by (-)-deprenyl. *British journal of pharmacology*, 117:1756-1760.

7. **Castagnoli, K., Palmer, S., Anderson, A., Bueters, T. and Castagnoli, N., Jr.** 1997. The neuronal nitric oxide synthase inhibitor 7-nitroindazole also inhibits the monoamine oxidase-B catalyzed oxidation of 1-methyl-4-phenyl-1,2,3,6-tetrahydropyridine. *Chemical research in toxicology*, 10:364-368.

8. **Castagnoli, N., Jr., Rimoldi, J.M., Bloomquist, J. and Castagnoli, K.P.** 1997. Potential metabolic bioactivation pathways involving cyclic tertiary amines and azaarenes. *Chemical research in toxicology*, 10:924-940.

9. **Chen, J.F., Steyn, S., Staal, R., Petzer, J.P., Xu, K., Van Der Schyf, C.J., Castagnoli, K., Sonsalla, P.K., Castagnoli, N., Jr. and Schwarzschild, M.A.** 2002. 8-(3-Chlorostyryl) caffeine may attenuate MPTP neurotoxicity through dual

actions of monoamine oxidase inhibition and A_{2A} receptor antagonism. *Journal of biological chemistry*, 277:36040-36044.

10. **Chiba, K., Trevor, A.J. and Castagnoli, N. Jr.** 1985. Active uptake of MPP^+, a metabolite of MPTP, by brain synaptosomes. *Biochemical and biophysical research communications*, 128:1228-1232.

11. **Chiba, K., Trevor, A.J. and Castagnoli, N., Jr.** 1984. Metabolism of the neurotoxic tertiary amine, MPTP, by brain monoamine oxidase. *Biochemical and biophysical research communications*, 120:574-578.

12. **Dubey, P.K., Eswara Rao, D., Ramanatham, J., Kumar, R. and Grossert, J.S.** 1998. Studies on the preparation of 2-styrylbenzimidazole. *Journal of the Indian chemical society*, 75:460-464.

13. **Fowler, C.J., Callingham, B.A., Mantle, T.J. and Tipton, K.F.** 1980. The effect of lipoohilic compounds upon the activity of rat liver mitochondrial monoamine oxidase-A and –B. *Biochemical pharmacology*, 29:1177-1183.

14. **Fujita, T., Iwasa, J. and Hansch, C.** 1964. A new substituent constant, π, derived from partition coefficients. *Journal of the American chemical society*, 86: 5175-5180.

15. **Gaal, J. and Hermecz, I.** Medical chemistry of present and future MAO-B inhibitors. Inhibitors of monoamine oxidase B. Pharmacology and clinical use in neurodegenerative disorders, Basel: *Birkhauser*, pp. 75-108.

16. **Gazit, A., Yee, K., Uecker, A., Böhmer, F., Sjöblom, T., Östman, A., Waltenberger, J., Golomb, G., Banai, S., Heinrich, M.C. and Levitzki, A.** 2003. Tricyclic Quinoxalines as potent kinase inhibitors of PDGFR kinase, Flt3 and Kit. *Bioorganic & medicinal chemistry*, 11:2007-2018.

17. **Gerlach, M. and Riederer, P.** 1996. Animal models of Parkinson's disease: an empirical comparison with the phenomenology of the disease in man. *Journal of neural transmission.* 103:987-1041.

18. **Gnerre, C., Catto, M., Leonetti, F., Weber, P., Carrupt, P.-A., Altomare, C., Carotti, A. and Testa, B.** 2000. Inhibition of monoamine oxidases by functionalized coumarin derivatives: biological activities, QSARs, and 3D-QSARs. *Journal of medicinal chemistry*, 43:4747-4758.

19. **Grimsby, J., Lan, N. C., Neve, R., Chen, K. and Shih, J. C.** 1990. Tissue distribution of human monoamine oxidase A and B mRNA. *Journal of*

neurochemistry, 55:1166-1169.

20. **Hansch, C. and Leo, A.** 1979. Substituent constants for correlation analysis in chemistry and biology. New York: *John Wiley and Sons.* pp. 352-352.

21. **Hansch, C. and Leo, A.** 1995. Exploring QSAR. Fundamentals and applications in chemistry and biology. *American Chemical Society*, pp 557.

22. **Hansch, C. Leo, A. and Hoekman, D.** 1995. Exploring QSAR. Hydrophobic, electronic and steric constants. Washington, DC: *American Chemical Society*, pp557.

23. **Heikkila, R.E., Manzino, L., Cabbat, F.S. and Duvoison, R.C.** 1984. Protection against the dopaminergic neurotoxicity of 1-methyl-4-phenyl-1,2,5,6-tetrahydropyridine by monoamine oxidase inhibitors. *Journal of biological chemistry*, 280:15761-15766.

24. **Heinonen, E.H., Anttila, M.I. and Lammintausta, R.A.** 1994. Pharmacokinetic aspects of L-deprenyl (Selegiline) and its metabolites. *Clinical pharmacological therapy*, 56:742-749.

25. **Houslay, M.D., Garrett, N.J. and Tipton, K.F.** 1974. Mixed substrate experiments with human brain monoamine oxidase. *Biochemical pharmacology*, 23:1937-1944.

26. **Hubalek, F., Binda, C., Khalil, A., Li, M., Mattevi, A., Casatagnoli, N. and Edmondson, D.E.** 2005. Demonstration of isoleucine 199 as astructural determinant for the selective inhibition of human monoamine oxidase B by specific reversible inhibitors. *Journal of biological chemistry*, 280:15761-15766.

27. **Inoue, H., Castagnoli, K., Van der Schyf, C., Mabic, S., Igarashi, K., and Castagnoli, N., Jr.** 1999. Species dependent differences in the monoamine oxidase A and B catalyzed oxidation of various C-4 substituted 1-methyl-4-phenyl-1,2,3,6-tetrahydropyridinyl derivatives. *Journal of pharmacology and experimental therapeutics*, 291:856-864.

28. **Jacobson, K.A., Gallo-Rodriguez, C., Melman, N., Fischer, B., Maillard, M., Van Bergen, A., Van Galen, P.J.M. and Karton, Y.** 1993. Structure–activity relationships of 8-styrylxanthines as A_2-selective adenosine antagonists. *Journal of medicinal chemistry*, 36:1333-1342.

29. **Jankovic, J. and Marsden, C.D.** 1993. Therapeutic strategies in Parkinson's disease. Parkinson's disease and movements disorders. Baltimore: *Williams & Wilkins*. pp. 115-144.

30. **Javitch, J.A., D'Amat, R.J., Strittmatter, S.J. and Snyder, S.H.** 1985. Parkinsonism-inducing neurotoxin 1-methyl-4-phenyl-1,2,3,6-tetrahydropyridine: uptake of the metabolite N-methyl-4-phenylpyridine by dopamine neurons explains selective toxicity. *Proceedings of the national academy of sciences of the United States of America*, 82:2173-2177.

31. **Kakkar, T., Boxenbaum, H. and Mayersohn, M.** 1999. Estimation of Ki in a competitive enzyme-inhibition model: comarisons among three methods of data analysis. *Drug metabolism and disposition*, 27:756-762.

32. **Kalgutkar, A.S., Castagnoli, K., Hall, A. and Castagnoli, N., Jr.** 1994. Novel 4-(aryloxy)tetrahydropyridine analogs of MPTP as monoamine oxidase A and B substrates. *Journal of medicinal chemistry*, 37:944-949.

33. **Kalir, A., Sabbagh, A. and Youdim, M.B.H.** 1981. Selected acetylenic suicide and reversible inhibitors of monoamine oxidase types A and B. *British journal of pharmacology*, 73:55-64.

34. **Knoll, J.** 2000. (-) Deprenyl (Selegiline): past, present future. *Neurobiology*, 8:179-190.

35. **Langston, J.W., Ballard, P., Tetrud, J.W. and Irwin, I.** 1983. Chronic Parkinsonism in human due to a product of meperidine-analog synthesis. *Science*, 219:979-980.

36. **Livingstone, D.J. and Salt, D.W.** 2005. Judging the significance of multiple linear regression models. *Journal of medicinal chemistry*, 48:661-663.

37. **Nicotra, A. and Parvez, S.H.** 2000. Cell death induced by MPTP, a substrate for monoamine oxidase B. *Toxicology*, 153:157-166.

38. **Nimkar, S. K., Anderson, A., Rimoldi, J. M., Stanton, J. M., Castagnoli, K. P., Mabic, S., Wang, Y. –X. and Castagnoli, N., Jr.** 1996. Synthesis and monoamine oxidase-B catalyzed oxidation of C-4 heteroaromatic substituted 1,2,3,6-tetrahydropyridine derivatives. *Chemical research in toxicology*, 9:1013-1022.

39. **Oh, C., Murray, B., Bhattacharya, N., Holland, D. and Tatton, W.G.** 1994. (-)-Deprenyl alters the survival of adult murine facial motorneurons after axotomy: increases in vulnerable C57BL strain but decreases in motor neuron degeneration

mutants. *Journal of neuroscientific research*, 38:64-74.

40. **Parkinson Study Group.** 1989. Effects of deprenyl on the progression of disability in early Parkinso's disease. *New England journal of medicine*, 321:1364-1371.

41. **Parkinson Study Group**. 1993. Effect of tocopherol and deprenyl on the progression of disability in early Parkinson's disease. *New England journal of medicine*, 328:176-183.

42. **Petzer, J.P., Steyn, S., Castagnoli, K.P., Chen, J.F., Schwarzschild, M.A., Van der Schyf, C.J. and Castagnoli, N., Jr.** 2003. Inhibition of monoamine oxidase B by selective adenosineA_{2A} receptor antagonists. *Bioorganic & medicinal chemistry*, 11:1299-1310.

43. **Rabey, J. M., Sagi, L., Huberman, M., Melamed, E., Korezyn, A., Giladi, M., Inzelberg, R., Djaldetti, R., Klein, C. and Berecz, G.** 2000. Rasagiline mesylate, a new MAO-B inhibitor for the treatment of Parkinson's disease: a double-blind study as adjunctive therapy to levodopa. *Clinical neuropharmacology*, 23:324-330.

44. **Riederer, P., Lachenmayer, L. and Laux, G.** 2004. Clinical applications of MAO-inhibitors. *Current medicinal chemistry*, 11:2033-2043.

45. **Riederer, P., Sofic, E., Rausch, W.D., Schnidt, B., Reynolds, G.P., Jellinger, K. and Youdim, M.B.**1989. Transition metals, ferritin, gluthione, and ascorbic acid in parkinsonian brains. *Journal of neurochemistry*, 52:515-520.

46. **Rodwell, V.W.** 1993. Enzymes: kinetics. ***Harper's Biochemistry***, 23rd ed, Connecticut: *Appleton and Lange*. pp. 71-85.

47. **Salach, J. and Weyler, J.** 1987. Preparation of the flavin-containing aromatic amine oxidase of human placenta and beef liver. *Methods in enzymology*, 142:627-637.

48. **Saura, J., Luque, J.M., Cesura, A.M., Da Prada, M., Chan-Palay, V., Huber, G., Loffler, J. and Richards, J.G.** 1994. Increased monoamine oxidase B activity in plaque-associated astrocytes of Alzheimer brain revealed by quantitative enzyme autoradiography. *Neuroscience*, 62:15-30.

49. **Segel, I. H.** 1993. Enzyme kinetics, New York: *Wiley*. pp 100-125.

50. **Shih, J.C., Chen,K. and Geha, R.M.** 1998. Determination of regions of important for monoamine oxidase (Mao) A and B substrate and inhibitor sensitivities. *Journal of neural transmission*, 52:1-8.

51. **Shimada, J., Koike, N., Nonaka, H., Shiozaki, S.,Yanagawa, K., Kanada, T., Kobayashi, H. and Fumio, S.** 1997. Adenosine A_{2A} antagonists with potent anti-cataleptic activity. *Bioorganic & medicinal chemistry letters*, 7:2349-2352.

52. **Suzuki, F., Shimada, J., Shiozaki, S., Ichikawa, S., Ishii, A., Nakamura, J., Nonaka, H., Kobayashi, H. and Fuse, E.** 1993. Adenosine A_1 antagonists. 3. Structure-activity relationships on amelioration against scopolamine- or N^6 –((R)-phenylisopropyl)adenosine-induced cognitive disturbance. *Journal of medicinal chemistry*, 36: 2508-2518.

53. **Swain, C.G. and Lupton, E.C., Jr.** 1968. Field and resonance components of substituent effects. *Journal of the american chemical society*, 90:4328-4337.

54. **Takeda, M., Li, Z.K. and Hattori, T.** 1990. Astroglial ablation prevents MPTP-induced nigrostriatal neuronal death. *Brain research*, 509:55-61.

55. **Tatton, W,G.** 1993. Selegiline can mediate neuronal rescue rather than neuronal protection. *Movement disorders*, 8:20-30.

56. **Tatton, W.G. and Greenwood, C.E.** 1991. Rescue of dying neurons a new action for deprenyl in MPTP parkinsonism. *Journal of neuroscience research*, 30:666-667.

57. **Tipton. K.F. and Fowler. C.J.** 1984. The kinetics of monoamine oxidase inhibitors in relation to their clinical behaviour. Monoamine oxidase and disease. Prospects for therapy with reversible inhibitors. London: *Academic Press.* pp. 27-40.

58. **Vlok, N., Malan, S.F., Castagnoli, N.Jr., Bergh, J.J. and Petzer, J.P.** 2006. Inhibition of monoamine oxidase B by analogues of the adenosine A_{2A} receptor antagonist (E)-8-(3-chlorostyryl)caffeine (CSC). *Bioorganic & medicinal chemistry*, 14:3512-3521.

59. **Volz, H.P. and Gleiter, C.H.** 1998. Monoamine oxidase inhibitors: a perspective on their use in the elderly. *Drugs in the aging*, 13:341-355.

60. **Waldmeier, P. C.** 1987. Amine oxidases and their endogenous substrates. *Journal of neural transmission*, 23:55-72.

61. **Weyler, W., Hsu, Y.P. and Breakefield, X.O.** 1990. Biochemistry and genetics of monoamine oxidase. *Pharmacology and therapeutics*, 47:391-417.

62. **Wu, E.Y., Langston, J.W.E. and Di Monte, D.A.J.** 1992. Toxicity of the 1-methyl-4-phenyl-2,3-dihydropyridinium and 1-methyl-4-phenylpyridinium species in primary cultures of mouse astrocytes. *Pharmacological experimental therapy*, 262:225-234.

63. **Yoshinga, N., Murayama, T.E. and Nomura, Y.** 2000. Apoptosis induction by a dopaminergic neurotoxin, 1-methyl-4-phenylpyridiniumion (MPP^+), and inhibition by epidermal growth factor in GH3 cells. *Biochemistry and pharmacology*, 60:111-116.

64. **Youdim, M.B. and Riederer, P.F.** 2004. A review of the mechanisms and role of monoamine oxidase inhibitors in Parkinson,s disease. *Neurology*, 63:32-35.

65. **Youdim, M.B., Fridkin, M. and Zheng, H.** 1995. Bifunctional drug derivatives of MAO-B inhibitor rasagiline and iron chelator VK-28 as a more effective approach to treatment of brain ageing and ageing neurodegenerative diseases. *Mechanisms of ageing and development*, 126:317-326.

66. **Youdim, M.B.H. and Bakhle, Y.S.** 2006. Monoamine oxidase: isoforms and inhibitors in Parkinson's disease and depressive illness. *British journal of pharmacology*, 147:287-296.

67. **Zang, L. E. and Misra, H.P.** 1992. EPR kinetic studies of superoxide radicals generated during the autoxidation of 1-methyl-4-phenyl-2,3-dihydropyridinium, a bioactivated intermediate of parkinsonian-inducing neurotoxin 1-methyl-4-phenyl-1,2,3,6-tetrahydropyridine. *Journal of biological chemistry*, 267:23601.

APPENDIX A

MS, ^{1}H-NMR, ^{13}C-NMR Spectra

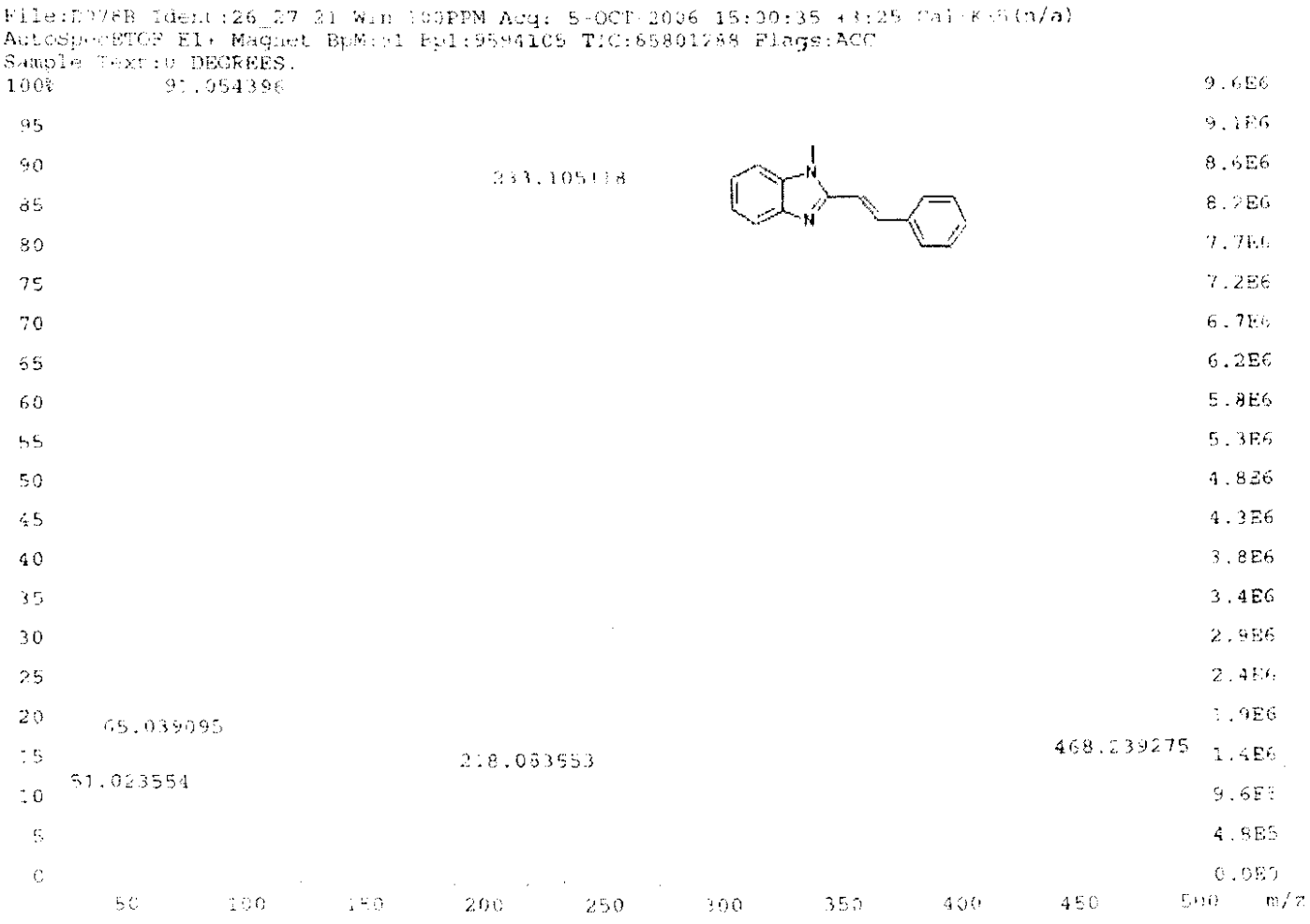
File:D978B Ident:26_27_31 Win:100PPM Acq: 5-OCT-2006 15:30:35 +3:25 Cal:K5(n/a)
AutoSpec6TOF EI+ Magnet BpM:31 Bpl:9594105 TIC:65801288 Flags:ACC
Sample Text:0 DEGREES.
100%
95
90
85
80
75
70
65
60
55
50
45
40
35
30
25
20
15
10
5
0
91.054396
233.105118
65.039095
51.023554
218.083553
468.239275
9.6E6
9.1E6
8.6E6
8.2E6
7.7E6
7.2E6
6.7E6
6.2E6
5.8E6
5.3E6
4.8E6
4.3E6
3.8E6
3.4E6
2.9E6
2.4E6
1.9E6
1.4E6
9.6E5
4.8E5
0.0E0
50
100
150
200
250
300
350
400
450
500
m/z

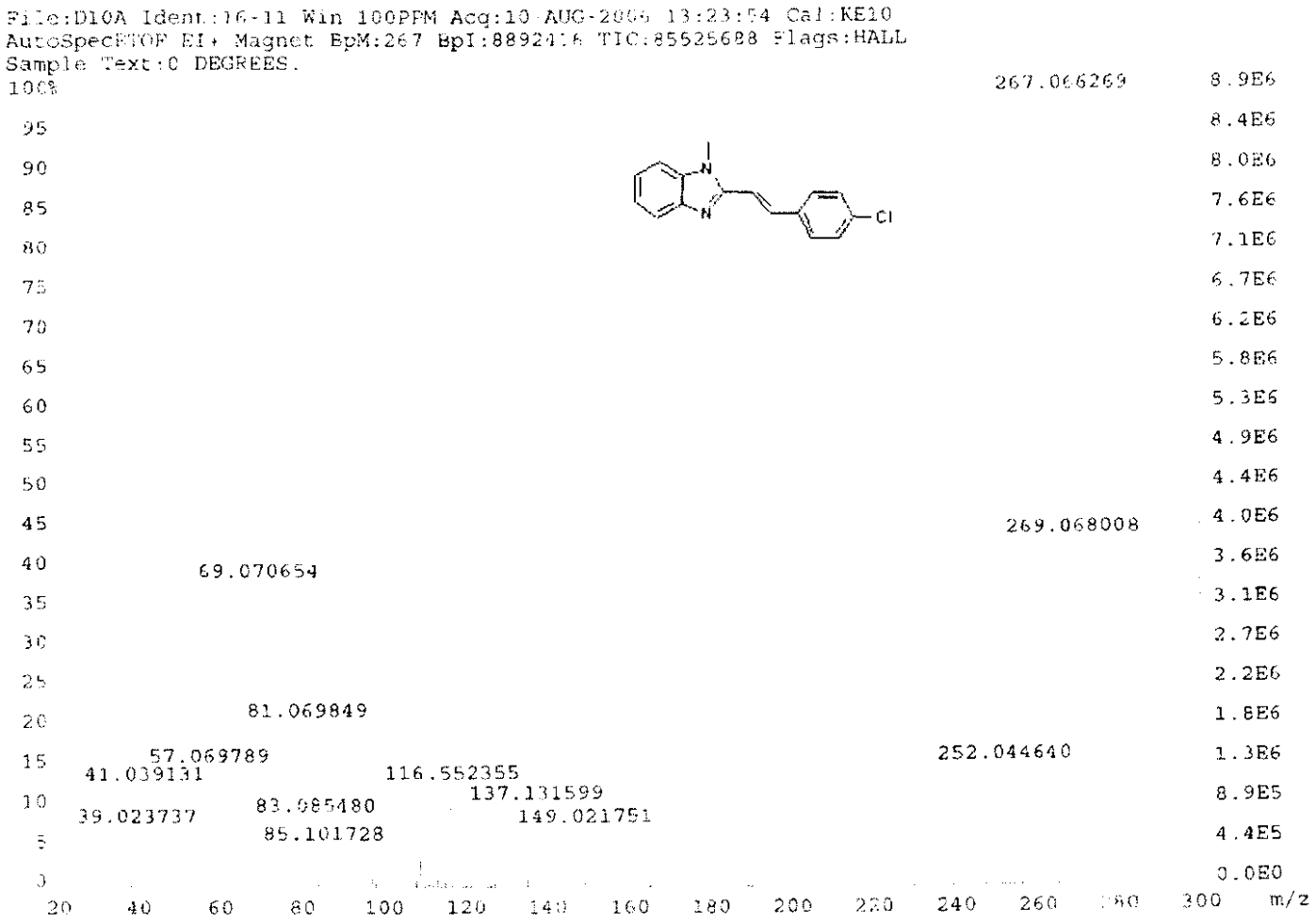
File:D10A Ident:16-11 Win 100PPM Acq:10 AUG-2006 13:23:54 Cal:KE10
AutoSpecETOF EI+ Magnet BpM:267 BpI:8892416 TIC:85525688 Flags:HALL
Sample Text:0 DEGREES.
100%
95
90
85
80
75
70
65
60
55
50
45
40
35
30
25
20
15
10
5
0
267.066269
8.9E6
8.4E6
8.0E6
7.6E6
7.1E6
6.7E6
6.2E6
5.8E6
5.3E6
4.9E6
4.4E6
269.068008
4.0E6
3.6E6
3.1E6
2.7E6
2.2E6
1.8E6
252.044640
1.3E6
8.9E5
4.4E5
0.0E0
69.070654
81.069849
57.069789
41.039131
116.552355
137.131599
39.023737
83.085480
149.021751
85.101728
Cl
20
40
60
80
100
120
140
160
180
200
220
240
260
280
300
m/z

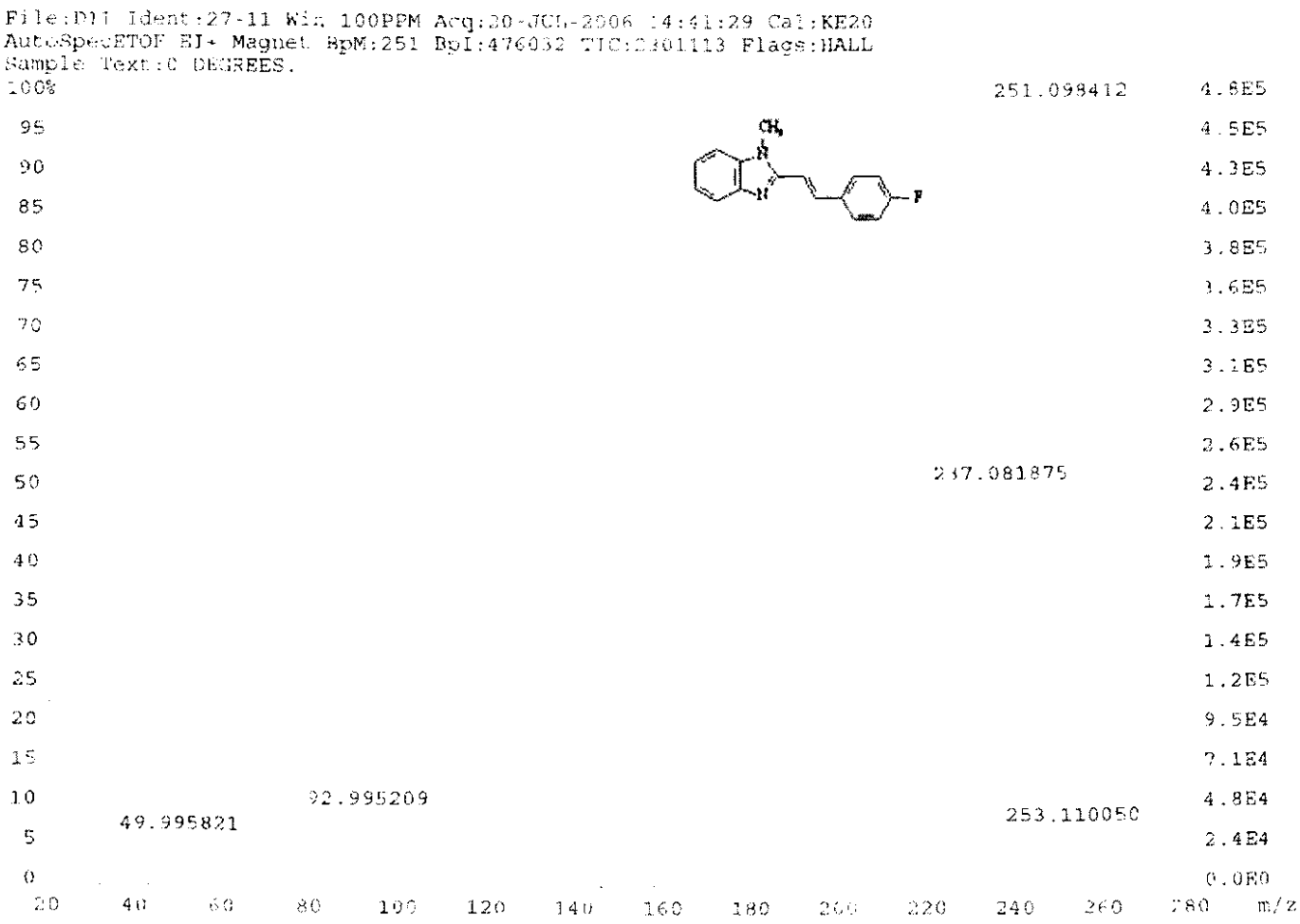
File:D11 Ident:27-11 Wk 100PPM Acq:20-JUL-2006 14:41:29 Cal:KE20
AutoSpecETOF EI+ Magnet BpM:251 BpI:476032 TIC:3301113 Flags:HALL
Sample Text:0 DEGREES.
100%
95
90
85
80
75
70
65
60
55
50
45
40
35
30
25
20
15
10
5
0
251.098412
4.8E5
4.5E5
4.3E5
4.0E5
3.8E5
3.6E5
3.3E5
3.1E5
2.9E5
2.6E5
237.081875
2.4E5
2.1E5
1.9E5
1.7E5
1.4E5
1.2E5
9.5E4
7.1E4
4.8E4
2.4E4
0.0E0
92.995209
49.995821
253.110050
20
40
60
80
100
120
140
160
180
200
220
240
260
280
m/z

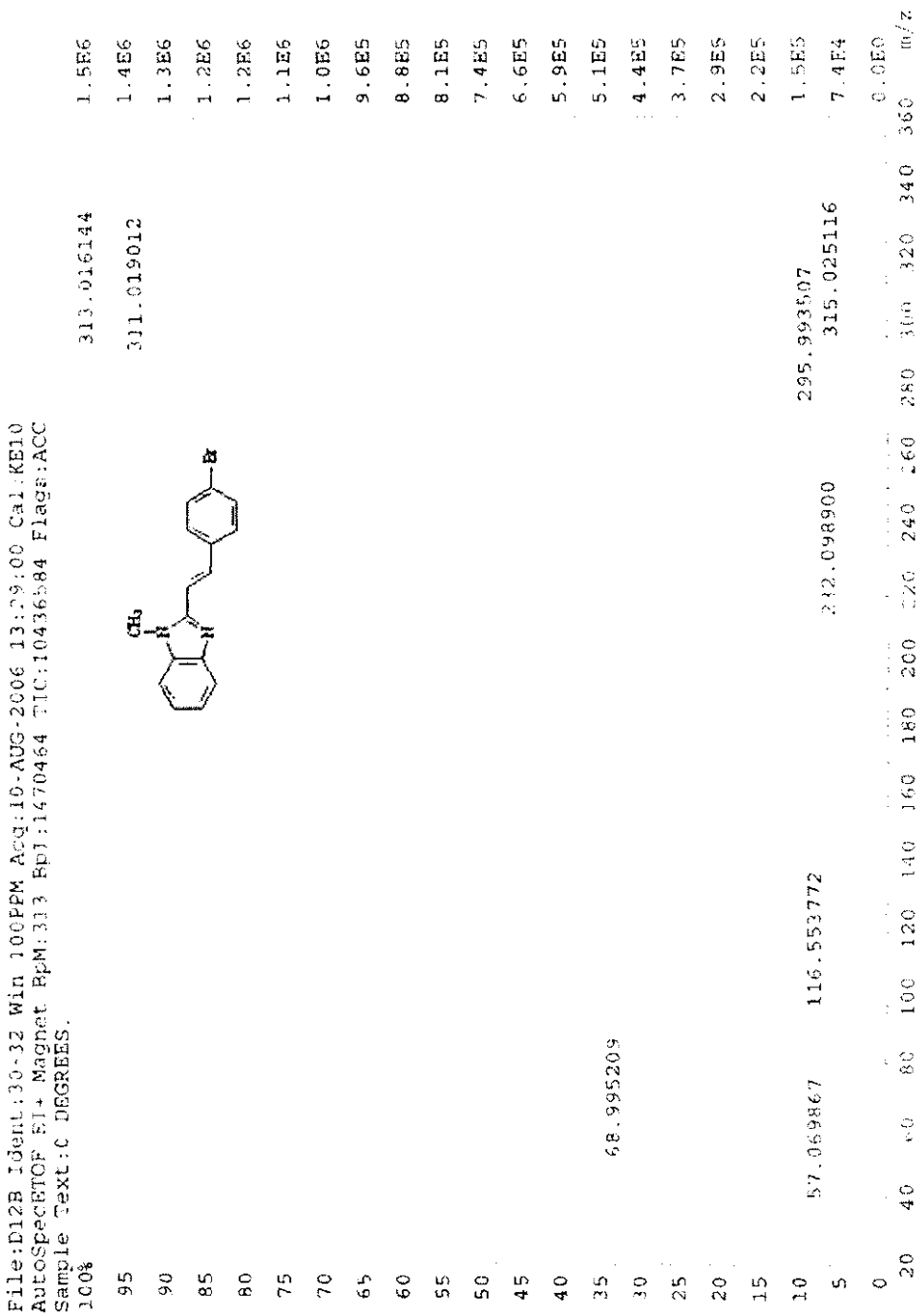
File:D12B IDent:30-32 Win 100PPM Acq:10-AUG-2006 13:29:00 Cal:KE10
AutoSpecGTOF EI+ Magnet BpM:313 BpI:1470464 TIC:10436584 Flags:ACC
Sample Text:C DEGREES.
100%
95
90
85
80
75
70
65
60
55
50
45
40
35
30
25
20
15
10
5
0
68.995209
57.069867
116.553772
282.098900
295.993607
311.019012
313.016144
315.025116
1.5E6
1.4E6
1.3E6
1.2E6
1.2E6
1.1E6
1.0E6
9.6E5
8.8E5
8.1E5
7.4E5
6.6E5
5.9E5
5.1E5
4.4E5
3.7E5
2.9E5
2.2E5
1.5E5
7.4E4
0.0E0
20
40
60
100
120
140
160
180
200
220
240
260
280
300
320
340
360
m/z

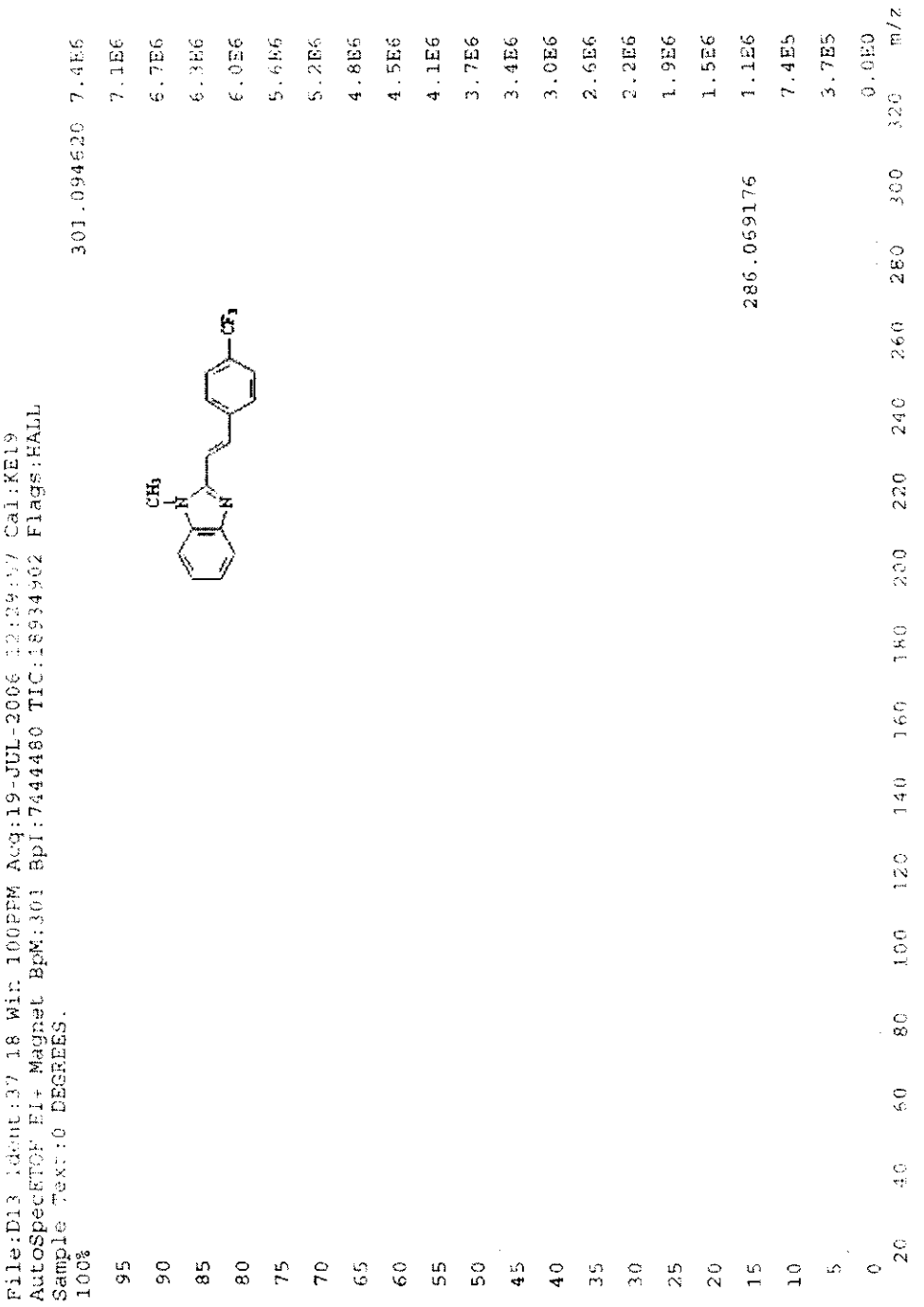
File:D13 Count:37 18 Win 100PPM Acq:19-JUL-2006 12:39:07 Cal:KE19
AutoSpecRTOF EI+ Magnet BpM:301 Bpf:7444480 TIC:18934902 Flags:HALL
Sample Text:0 DEGREES.
100%
95
90
85
80
75
70
65
60
55
50
45
40
35
30
25
20
15
10
5
0
301.094620 7.4E6
7.1E6
6.7E6
6.3E6
6.0E6
5.6E6
5.2E6
4.8E5
4.5E6
4.1E6
3.7E6
3.4E6
3.0E6
2.6E6
2.2E6
1.9E6
1.5E6
286.069176 1.1E6
7.4E5
3.7E5
0.0E0
20 40 60 80 100 120 140 160 180 200 220 240 260 280 300 320 m/z
CH3
N
H
N
CF3

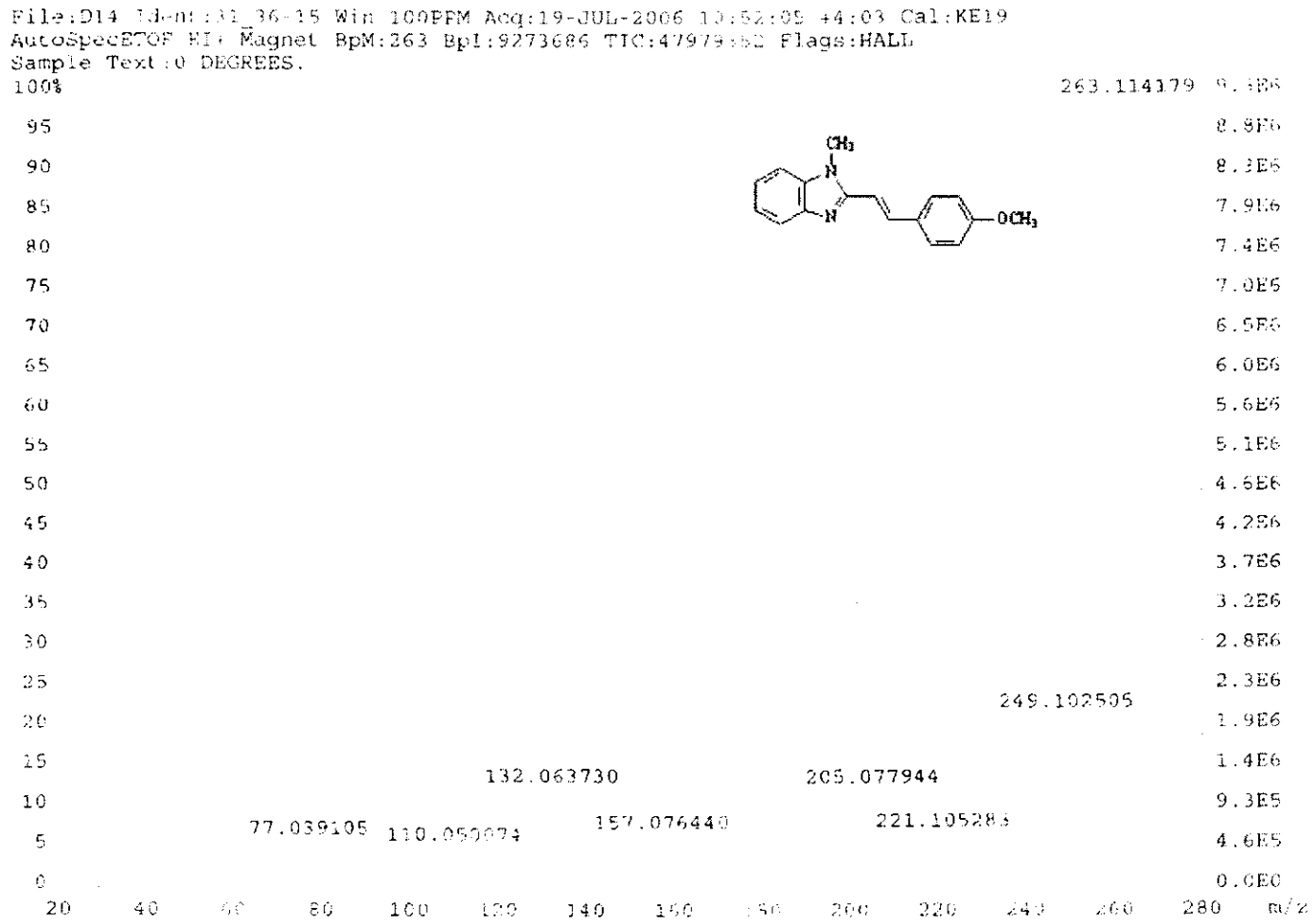
File:D14 Ident:31_36-15 Win 100PPM Acq:19-JUL-2006 13:52:05 +4:03 Cal:KE19
AutoSpecETOF HI: Magnet BpM:363 Bpl:9273686 TIC:47979:52 Flags:HALL
Sample Text:0 DEGREES.
100%
95
90
85
80
75
70
65
60
55
50
45
40
35
30
25
20
15
10
5
0
263.114179
249.102505
205.077944
221.105283
132.063730
157.076440
77.039105
110.059074
20
40
60
80
100
120
140
160
180
200
220
240
260
280
m/z

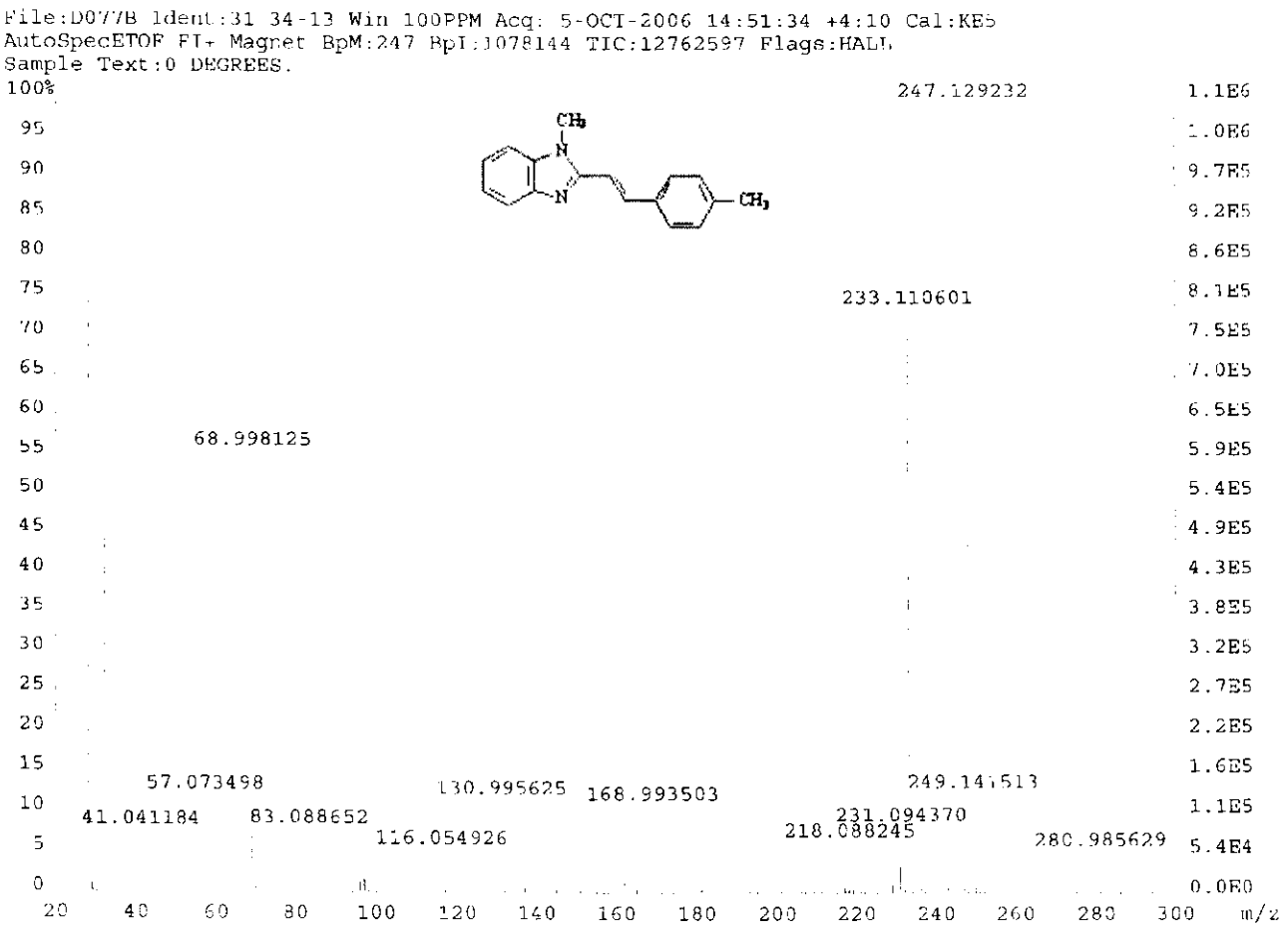
File:D077B Ident:31 34-13 Win 100PPM Acq: 5-OCT-2006 14:51:34 +4:10 Cal:KE5
AutoSpecETOF FI+ Magnet BpM:247 BpI:1078144 TIC:12762597 Flags:HALF
Sample Text:0 DEGREES.
100%
247.129232
233.110601
68.998125
57.073498
130.995625
168.993503
249.141513
41.041184
83.088652
231.094370
116.054926
218.088245
280.985629
1.1E6
1.0E6
9.7E5
9.2E5
8.6E5
8.1E5
7.5E5
7.0E5
6.5E5
5.9E5
5.4E5
4.9E5
4.3E5
3.8E5
3.2E5
2.7E5
2.2E5
1.6E5
1.1E5
5.4E4
0.0E0
m/z

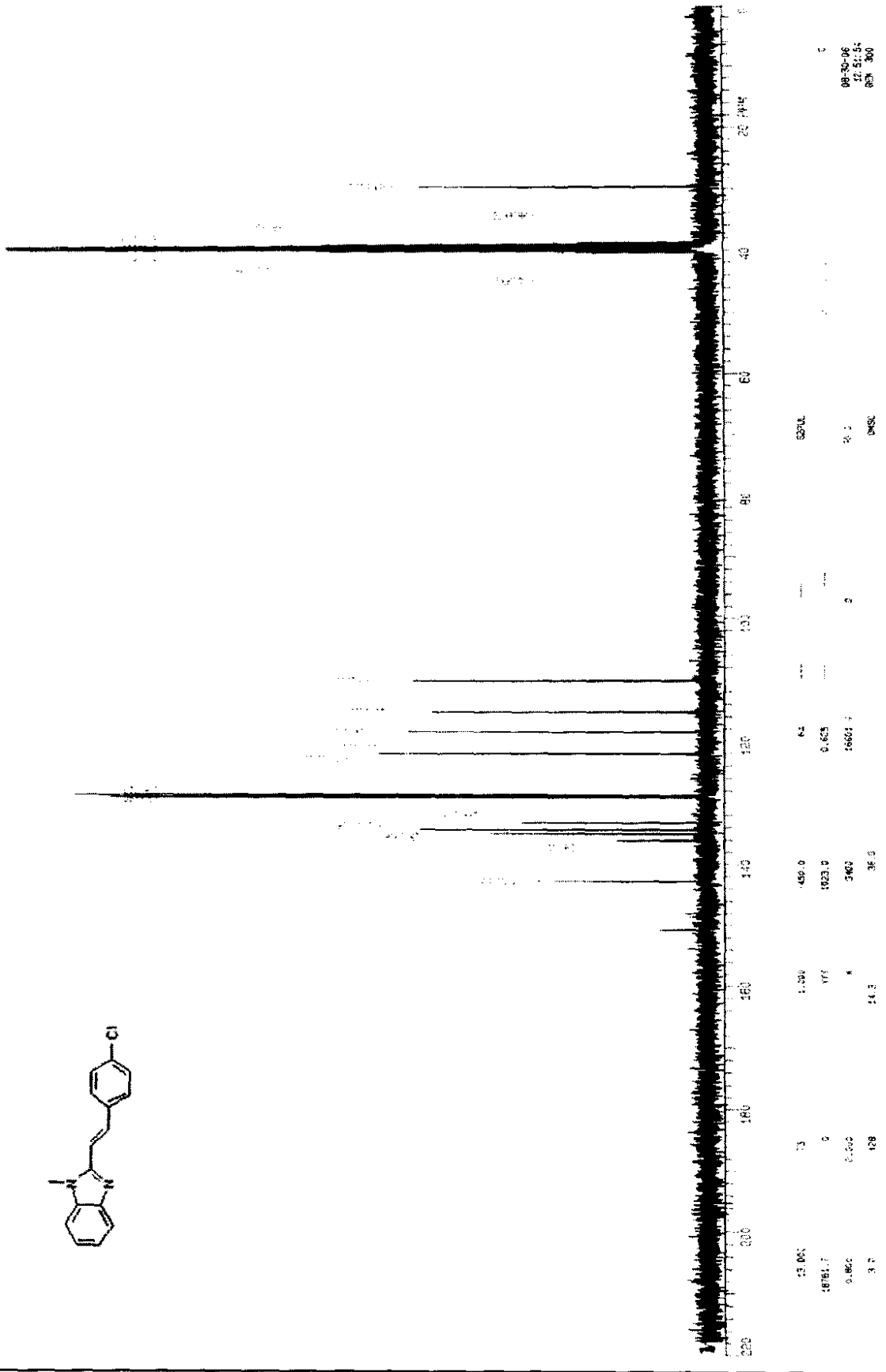

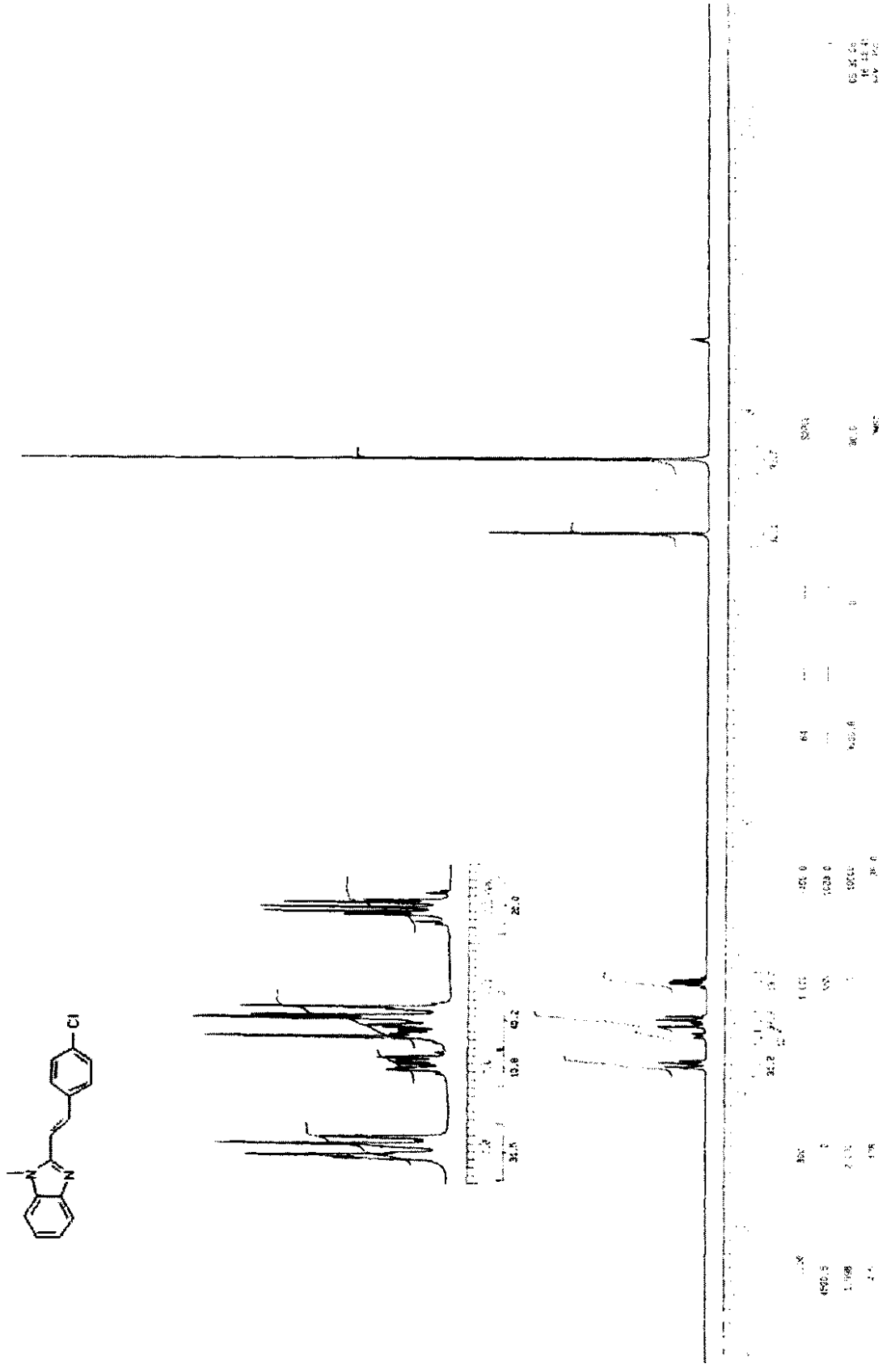
Cl
N
N

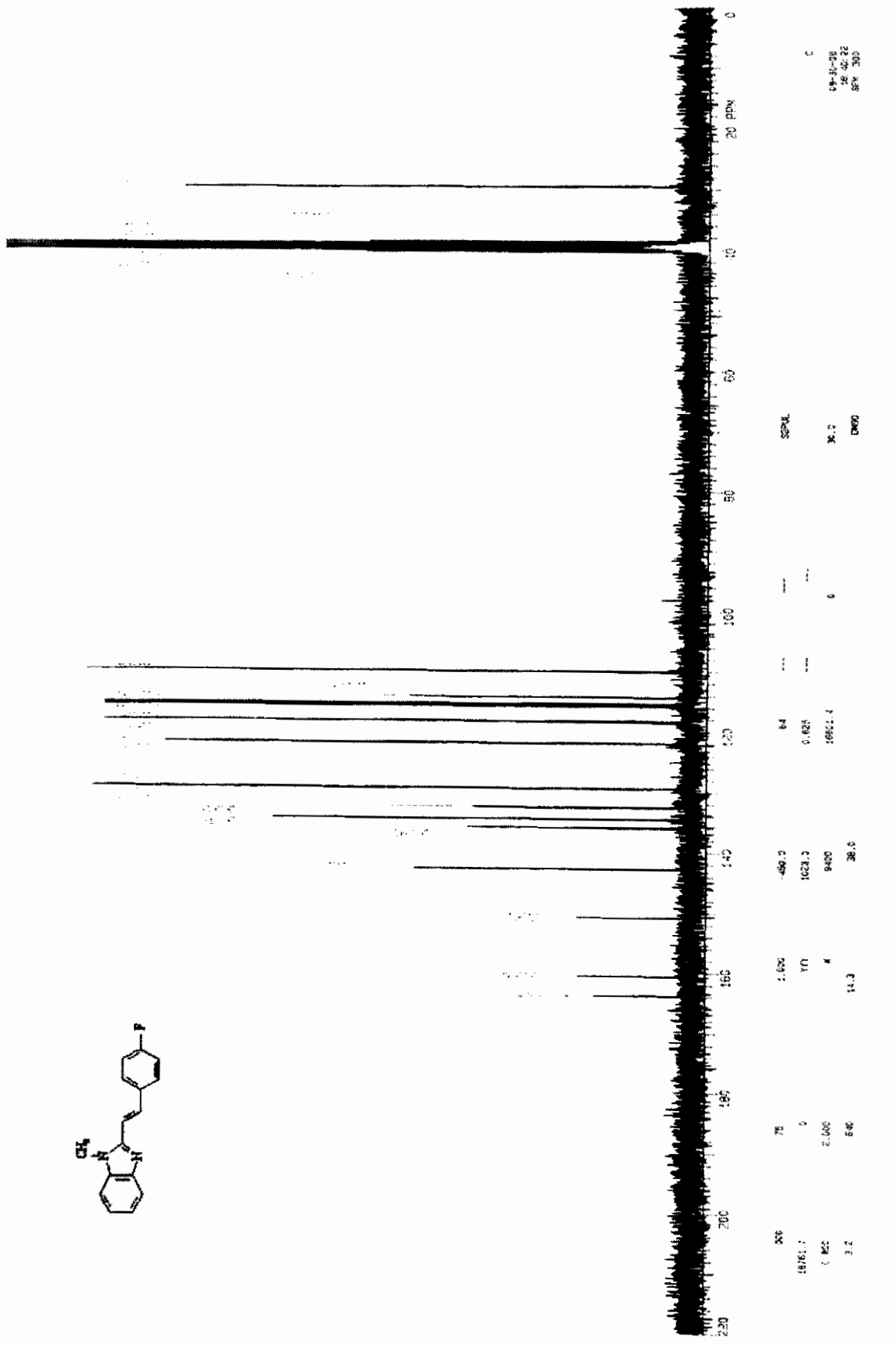

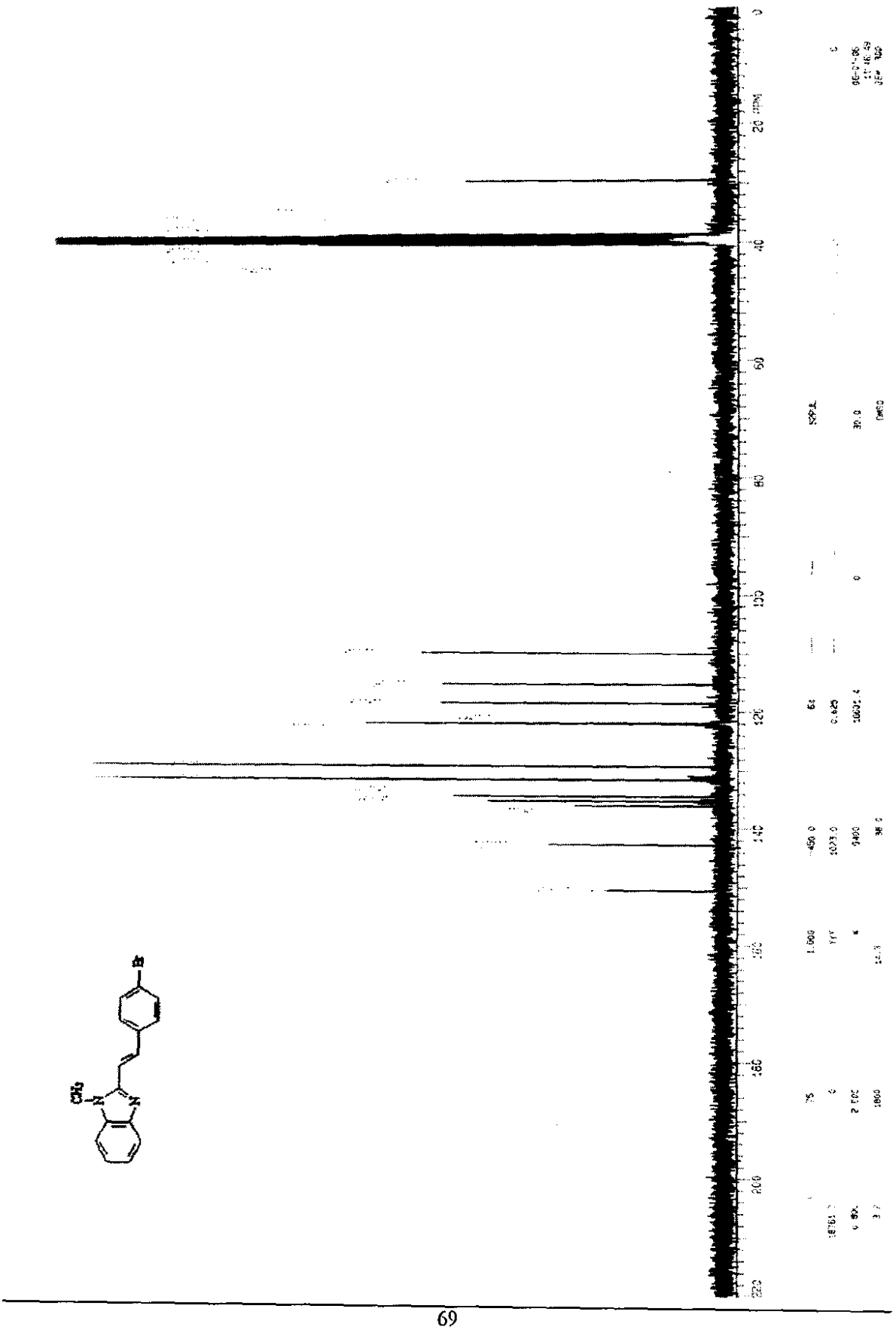

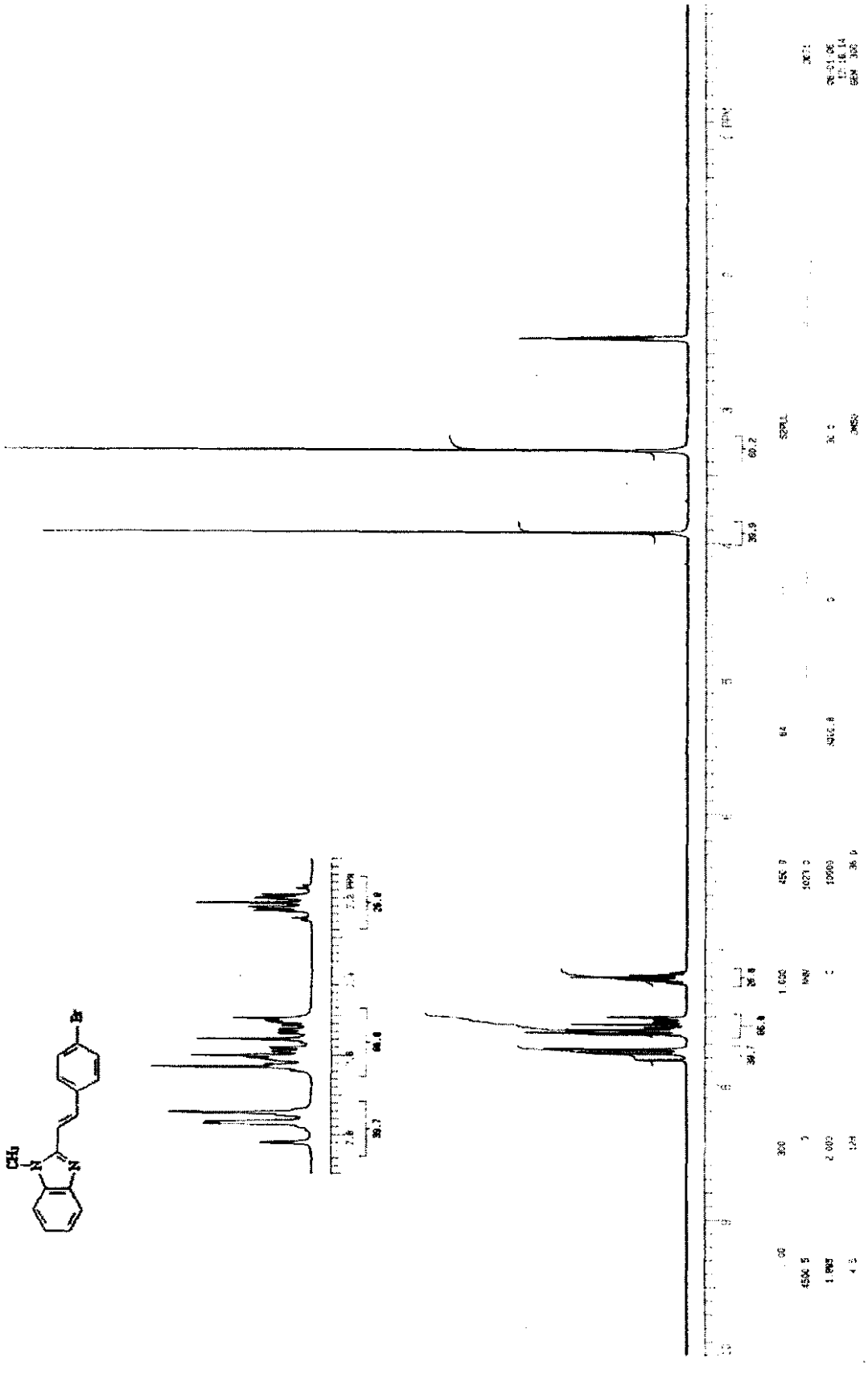

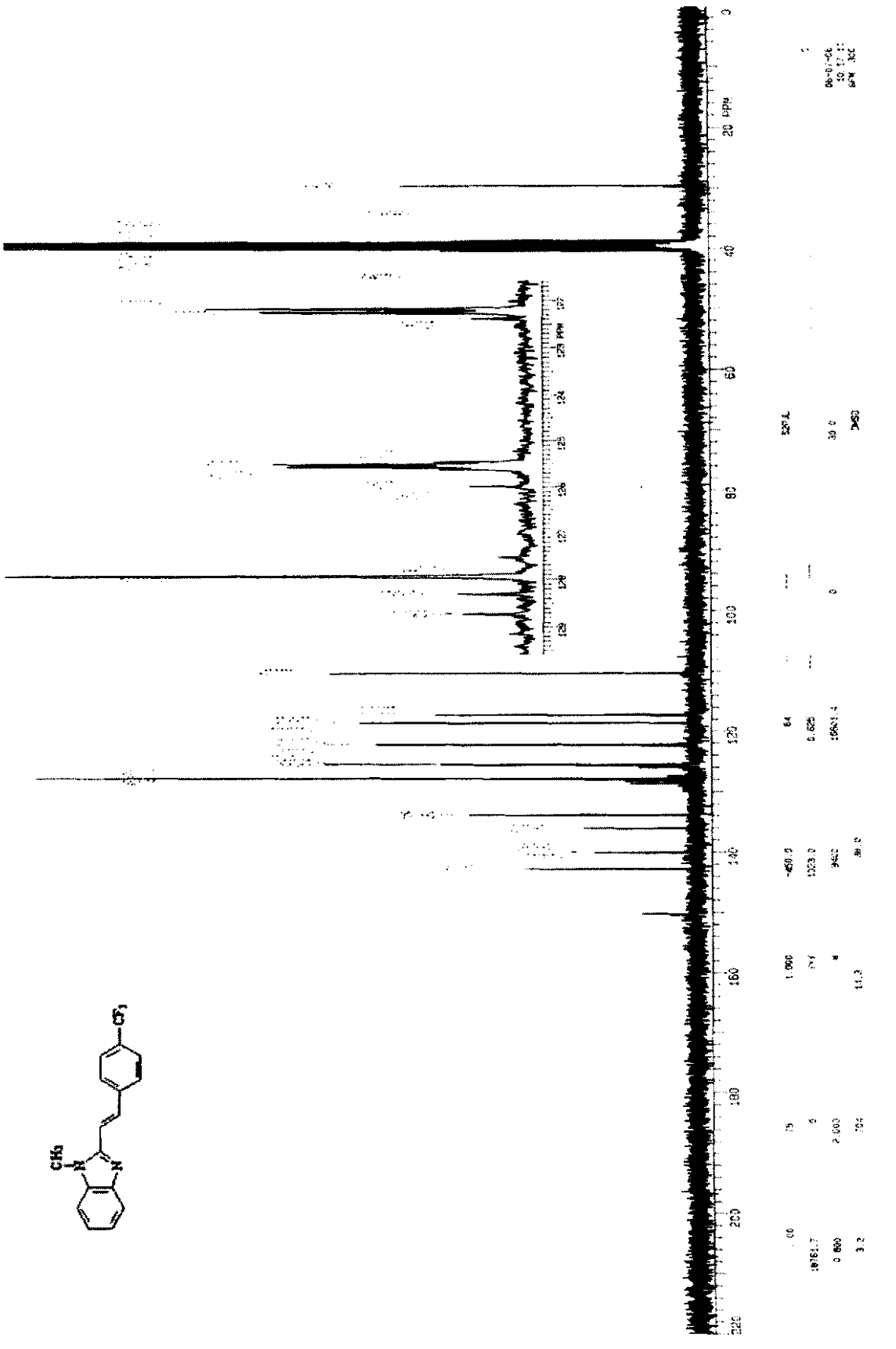

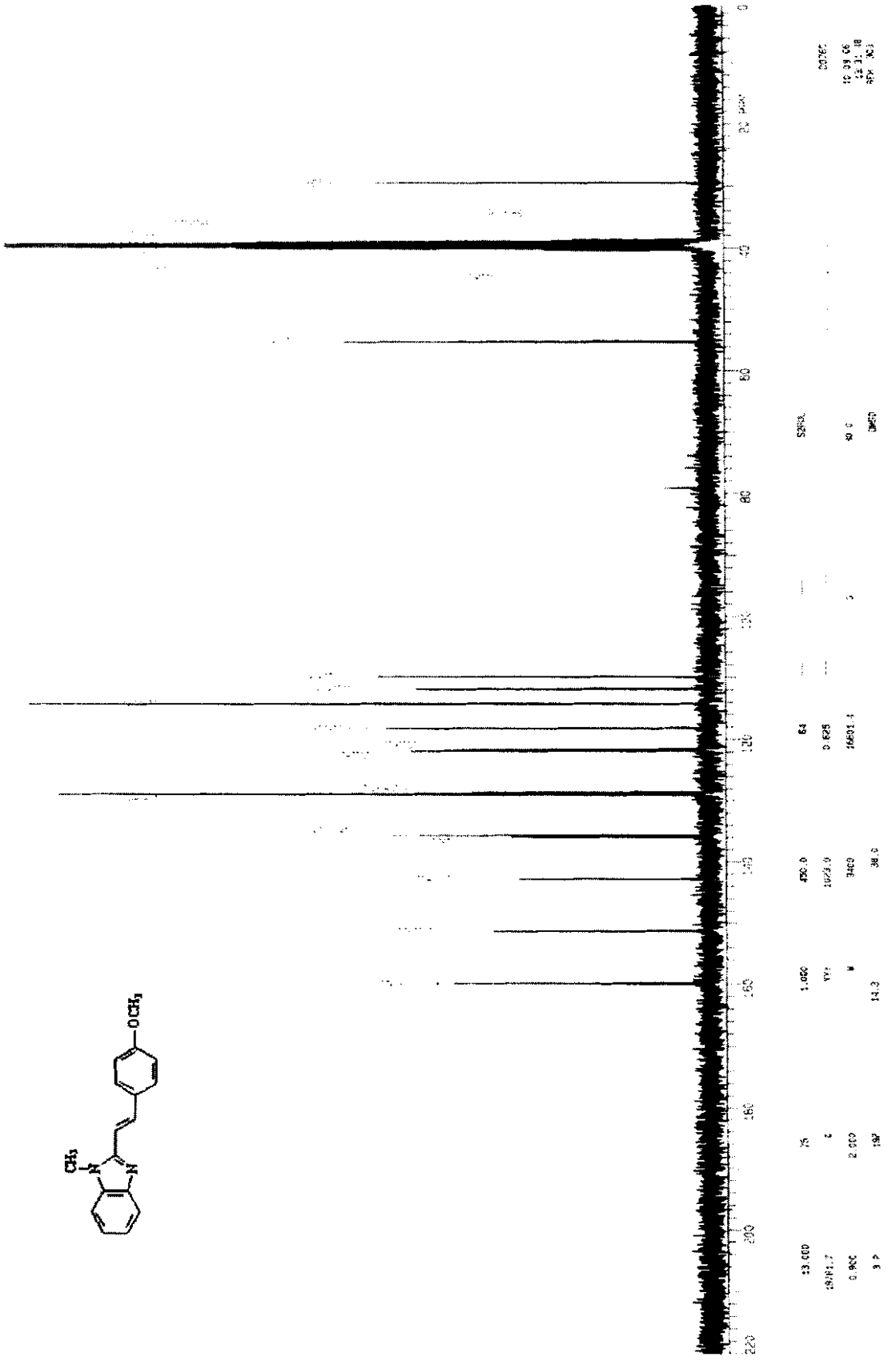

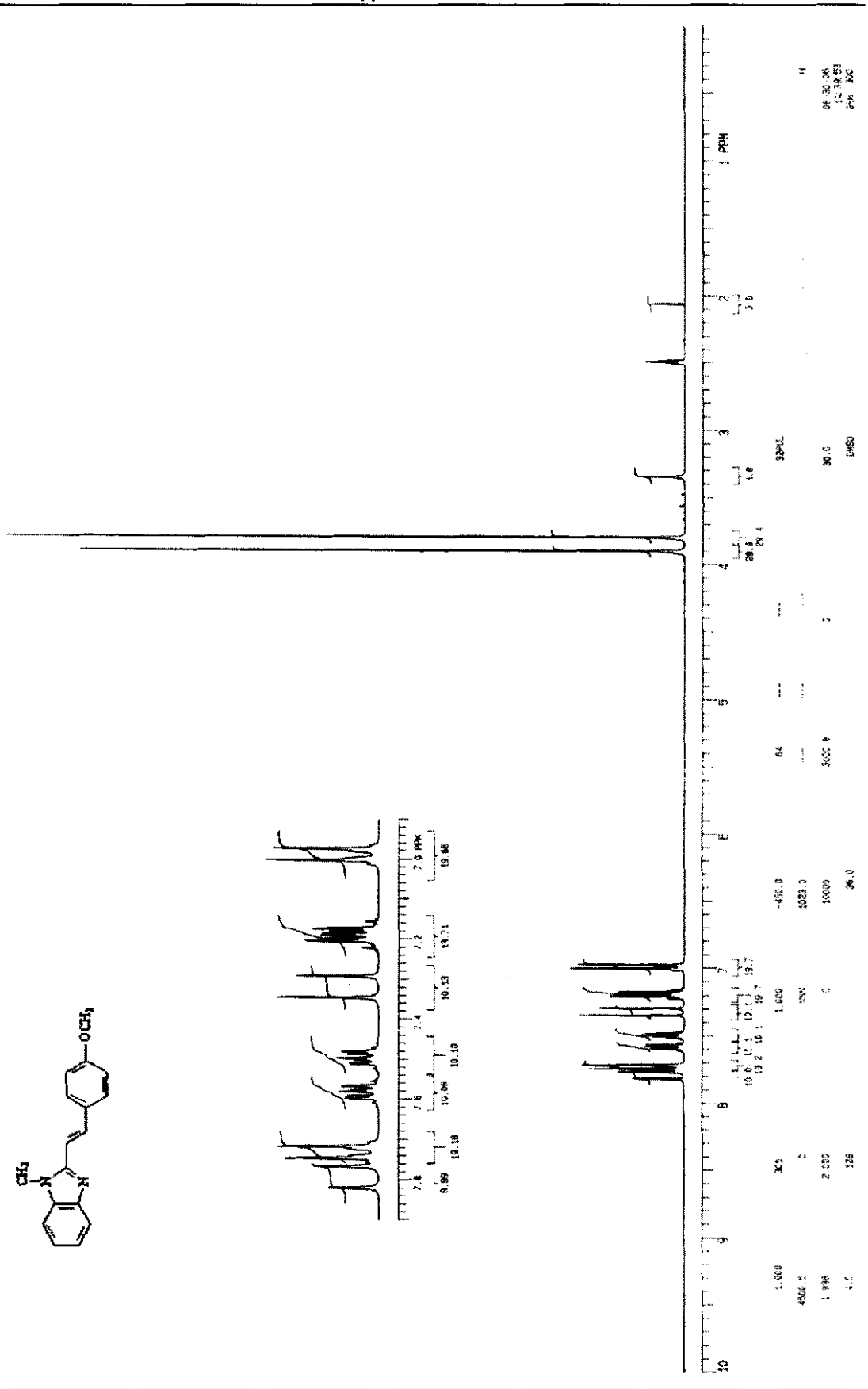

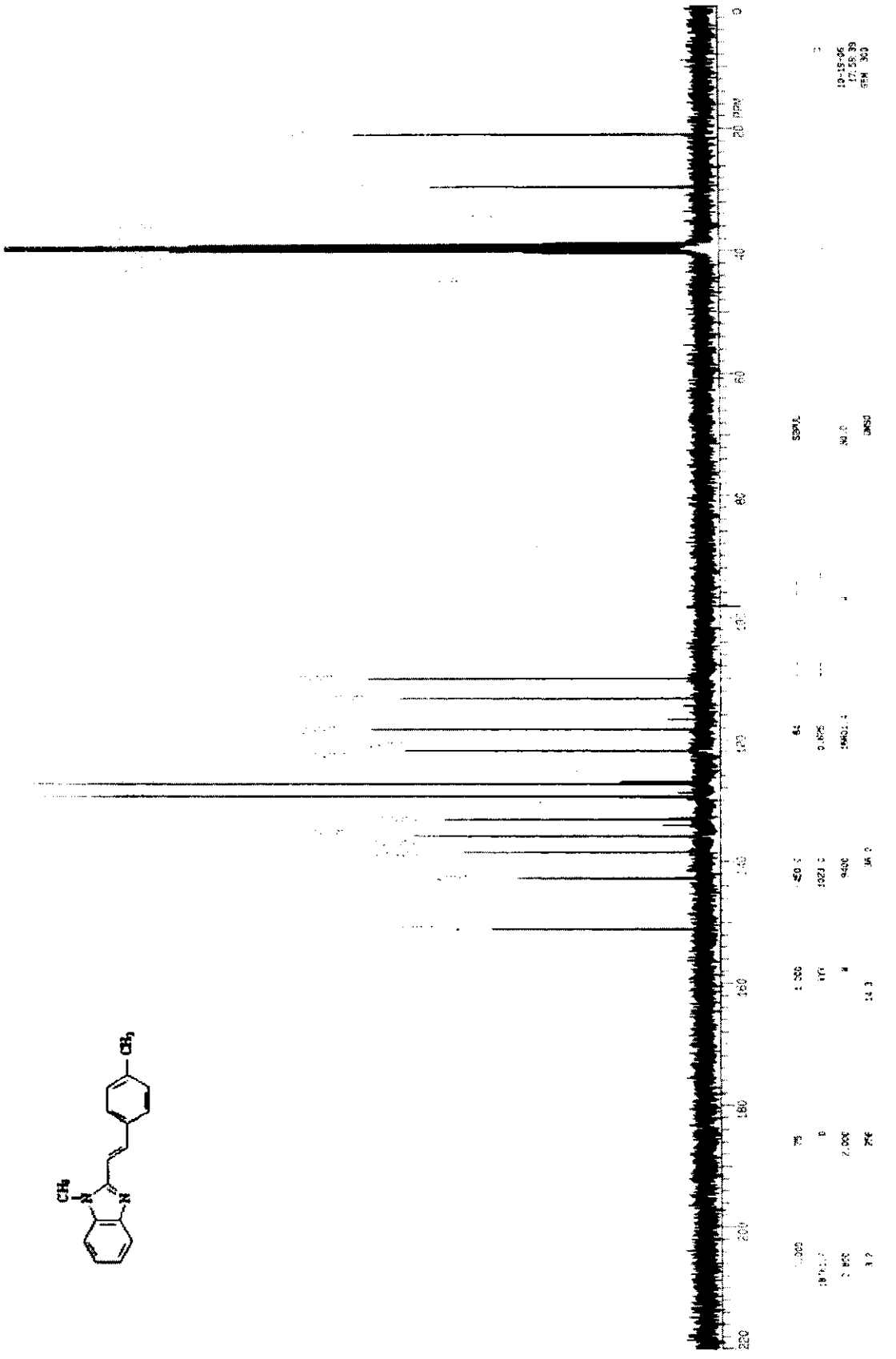

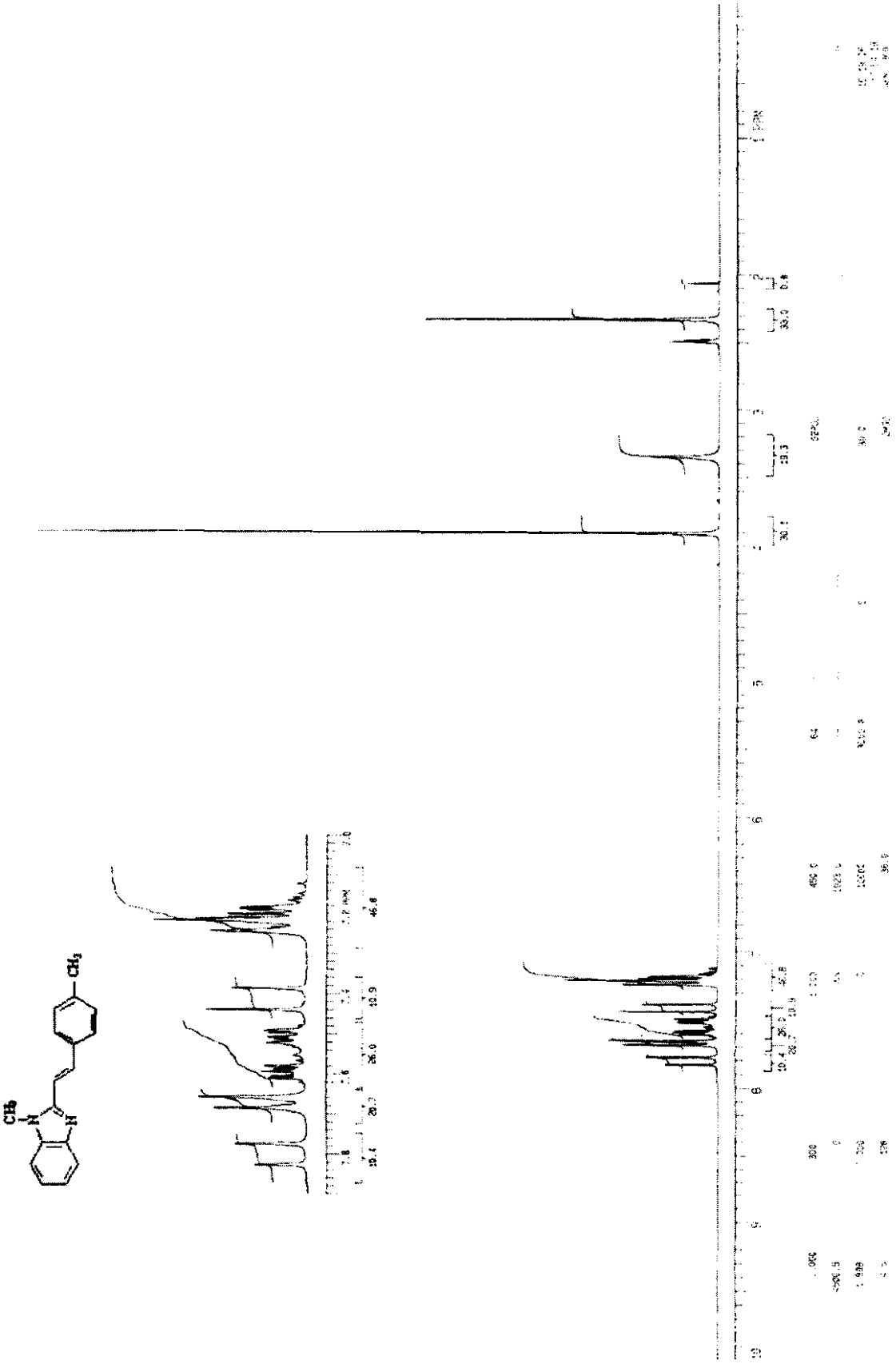

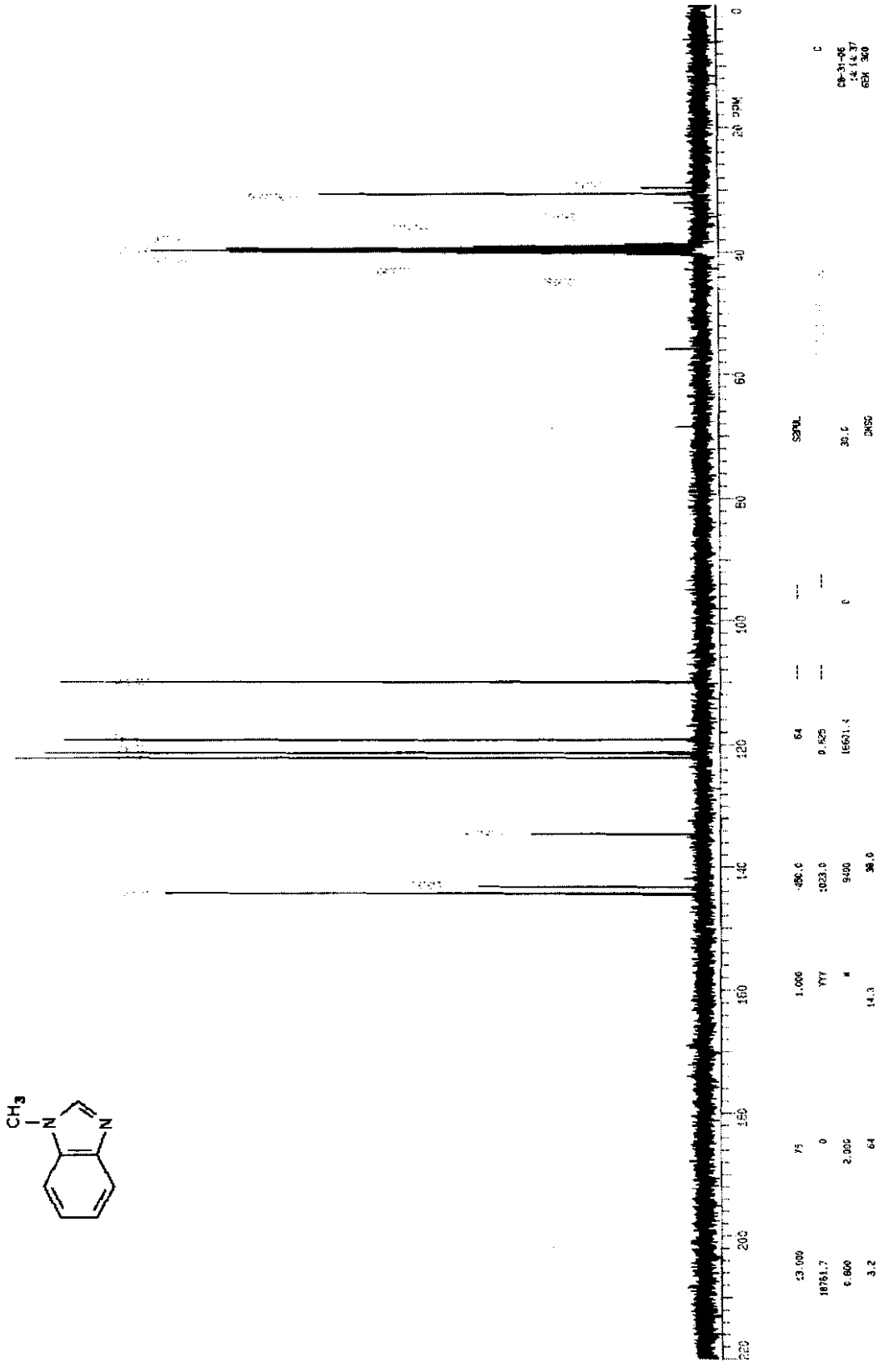

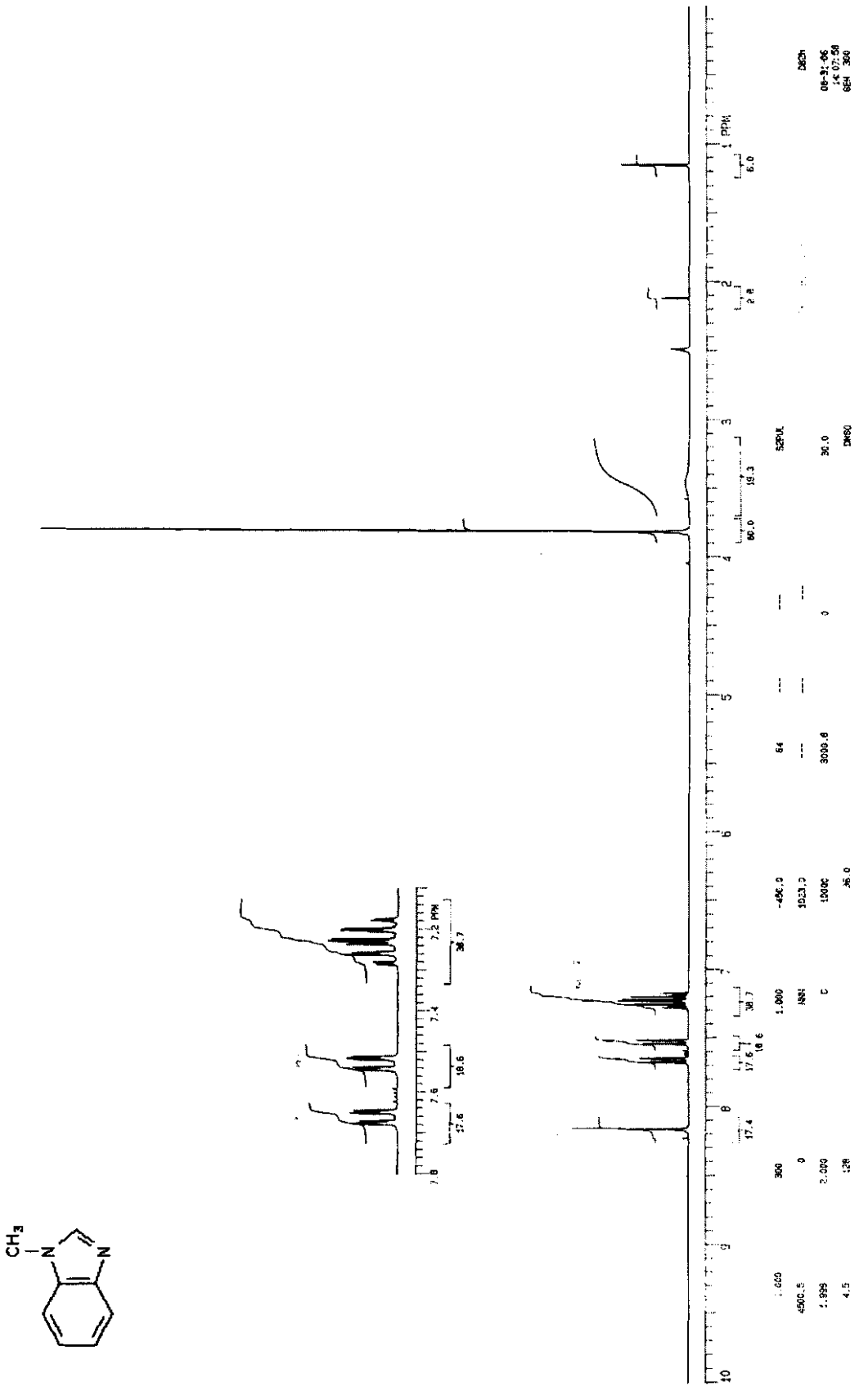

ACKNOWLEDGMENTS

- Firstly I want to thank my parents and brothers for all their love and support.
- Dr. J.P. Petzer, thank you for your guidance and inspiration. I greatly appreciate every thing you have taught me.
- Prof. S.F. Malan and Prof. J.J. Bergh, thank you for you insight and guidance.
- Jerry-man thank you for everything.
- To all my friends, thank you for all the coffee and motivation.
- And finally I want to thank almighty God for the amazing opportunities and success that I have been blessed with.